

AD-A052 422

BOEING COMMERCIAL AIRPLANE CO SEATTLE WASH

F/G 1/3

APPLICATION OF LAMINAR FLOW CONTROL TO LARGE SUBSONIC MILITARY --ETC(U)

JUL 77 R M KULFAN, J D VACHAL

F33615-76-C-3035

UNCLASSIFIED

D6-45148

AFFDL-TR-77-65

NL

1 OF 2

AD
A052422



AD A052422

DDC FILE COPY

AFFDL-TR-77-65

2

APPLICATION OF LAMINAR FLOW CONTROL TO LARGE SUBSONIC MILITARY TRANSPORT AIRPLANES

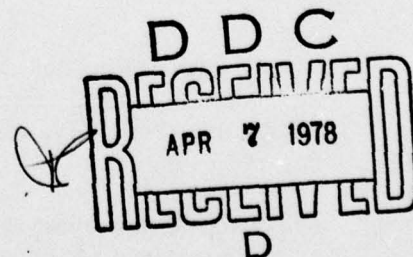
*Boeing Commercial Airplane Company
P.O. Box 3707
Seattle, Washington 98124*

July 1977

TECHNICAL REPORT AFFDL-TR-77-65

Final Technical Report for Period March 1976 through February 1977

Approved for public release; distribution unlimited



AIR FORCE FLIGHT DYNAMICS LABORATORY
AIR FORCE WRIGHT AERONAUTICAL LABORATORIES
AIR FORCE SYSTEMS COMMAND
WRIGHT-PATTERSON AIR FORCE BASE, OHIO 45433

NOTICE

When Government drawings, specifications, or other data are used for any purpose other than in connection with a definitely related Government procurement operation, the United States Government thereby incurs no responsibility nor any obligation whatsoever; and the fact that the government may have formulated, furnished, or in any way supplied the said drawings, specifications, or other data, is not to be regarded by implication or otherwise as in any manner licensing the holder or any other person or corporation, or conveying any rights or permission to manufacture, use, or sell any patented invention that may in any way be related thereto.

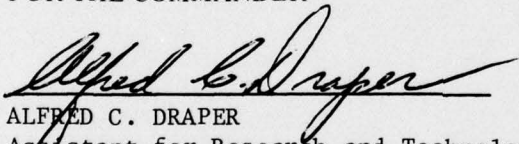
This report has been reviewed by the Information Office (OI) and is releasable to the National Technical Information Service (NTIS). At NTIS, it will be available to the general public, including foreign nations.

This technical report has been reviewed and is approved for publication.



Charles E. Jobe
Project Engineer

FOR THE COMMANDER



ALFRED C. DRAPER
Assistant for Research and Technology
Aeromechanics Division

"If your address has changed, if you wish to be removed from our mailing list, or if the addressee is no longer employed by your organization please notify AFFDL/FXM, W-PAFB, OH 45433 to help us maintain a current mailing list."

Copies of this report should not be returned unless return is required by security considerations, contractual obligations, or notice on a specific document.

SECURITY CLASSIFICATION OF THIS PAGE (When Data Entered)

19 REPORT DOCUMENTATION PAGE		READ INSTRUCTIONS BEFORE COMPLETING FORM
1. REPORT NUMBER AFFDL TR-77-65	2. GOVT ACCESSION NO.	3. RECIPIENT'S CATALOG NUMBER
4. TITLE (and Subtitle) APPLICATION OF LAMINAR FLOW CONTROL TO LARGE SUBSONIC MILITARY TRANSPORT AIRPLANES	5. TYPE OF REPORT & PERIOD COVERED Final Technical Report. March 1976 - March 1977	
7. AUTHOR(s) Robert M. Kulfan John D. Vachal	6. PERFORMING ORG. REPORT NUMBER D6-45148	
9. PERFORMING ORGANIZATION NAME AND ADDRESS Boeing Commercial Airplane Company P. O. Box 3707 Seattle, Washington 98124	8. CONTRACT OR GRANT NUMBER(s) F33615-76-C-3035	
11. CONTROLLING OFFICE NAME AND ADDRESS Air Force Flight Dynamics Laboratory/FXM Air Force Systems Command Wright-Patterson Air Force Base, Ohio 45433	10. PROGRAM ELEMENT, PROJECT, TASK AREA & WORK UNIT NUMBERS Program Element 62201F Project 1476 Task 01 Work Unit 41	
14. MONITORING AGENCY NAME & ADDRESS (if different from Controlling Office)	12. REPORT DATE Jul 77	
	13. NUMBER OF PAGES	
	15. SECURITY CLASS. (of this report) Unclassified	
16. DISTRIBUTION STATEMENT (of this Report) Approved for Public Release, Distribution Unlimited		
17. DISTRIBUTION STATEMENT (of the abstract entered in Block 20, if different from Report)		
18. SUPPLEMENTARY NOTES		
19. KEY WORDS (Continue on reverse side if necessary and identify by block number) Laminar Flow Control Military Aircraft Subsonic Transports Boundary Layer Control		
20. ABSTRACT (Continue on reverse side if necessary and identify by block number) A Preliminary Design study has been made to investigate the impact of the application of laminar flow control on the performance, weight, fuel consumption, and economics of a large transport airplane designed to carry a heavy payload (350,000 lb) for a long range (10,000 nmi). The study was conducted in three phases. In the first phase, conceptual design investigations were conducted to identify the features of an LFC airplane optimized to accomplish the mission objectives. A reference turbulent airplane also was developed in this phase. Design and analysis studies		

DD FORM 1 JAN 73 1473

EDITION OF 1 NOV 65 IS OBSOLETE

SECURITY CLASSIFICATION OF THIS PAGE (When Data Entered)

390 145

were made to develop the final LFC configuration. This configuration was sized to determine the gross weight, engine size, wing area, and fuel requirements necessary to achieve the design mission. Various performance trade and sensitivity studies were conducted for the turbulent and LFC airplanes in the third phase. Life-cycle and operating cost evaluations were also made. A valid assessment of an LFC airplane must be preceded by an extensive design, development, and flight test program. Consequently, this study focused on identifying the relative benefits from applying LFC, and on the sensitivities of these relative benefits to the current major LFC uncertainty items.

The optimum LFC wing planform is shown to have a high aspect ratio, low thickness/chord ratio and low sweep. This planform minimized both fuel and gross weight, and maximized productivity. The same planform geometry results in low chord Reynolds numbers, low cross-flow and low attachment line Reynolds number and thereby eases the task of laminarization.

Normal military reserves were found adequate to meet the mission objectives with reasonable losses in LFC. The reserves allow the LFC airplane to fly 2000 nmi or 5 hours with full loss of laminar flow and it can then achieve the mission range by establishing the design laminarization for the remainder of the flight.

Results of an extent of laminarization study suggest the following order for achieving maximum LFC benefits with minimum technical risks. First, laminarize the wing back to the trailing-edge control surfaces. Second, laminarize the empennage back to the trailing-edge controls. Then conduct the necessary trade and detailed design studies to identify the practical benefits and technical risks of full chord laminarization.

The fuselage drag of an LFC airplane is a significant drag item. A 25% drag reduction in the body drag of an LFC airplane results in additional fuel (8%) and gross weight (4%) savings.

Results indicate that LFC can provide large reductions in fuel usage (27 to 30%). The gross weights are also reduced (7 to 10%); however, the gross weights are very dependent upon the total LFC structural and systems weight increment. Operating costs for a 60-day surge condition are lower (10 to 15%) but depend on the required maintenance costs. The life-cycle costs were found to be higher for the LFC airplane because the low peacetime airplane usage rates do not reflect the large fuel savings as a significant cost item.

Recommendations are given for additional system studies, and for more detailed design and development work to fully establish the potential performance and economic benefits for application of LFC to very large transport aircraft.

FOREWARD

This is the final technical report on the application of laminar flow control to large military transport airplanes. This report, which has been assigned Boeing document number D6-45418 for internal use, covers work performed by the Boeing Commercial Airplane Company, Seattle, Washington. This work was under the technical direction of Dr. Charles E. Jobe, Air Force Flight Dynamics Laboratory/FXM, Air Force Systems Command Wright-Patterson Air Force Base, Ohio.

J. D. Vachal was the program manager, and R. M. Kulfan was the technical integrator and principal investigator. Others supporting the effort were R. D. Anderson, V. D. Bess, P. W. Brubaker, S. L. Bryant, L. A. DeCan, H. J. Funk, W. N. Holmquist, W. R. Lambert, J. L. Mark, R. N. McGuire, W. F. Minkler, R. L. Sullivan, F. J. Traeger, J. H. Ward, and L. L. Wright.

The work was performed under Contract F33615-76-C-3035, Project 1476, Task 01. The study period included March 1976–March 1977. The final report was submitted in July 1976.

ACCESSION for	
NTIS	White Section <input checked="" type="checkbox"/>
DDC	Buff Section <input type="checkbox"/>
UNANNOUNCED	<input type="checkbox"/>
JUSTIFICATION.....	
BY.....	
DISTRIBUTION/AVAILABILITY CODES	
Dist.	AVAIL. and/or SPECIAL
A	

DDC
RECEIVED
APR 7 1978
D

TABLE OF CONTENTS

	Page
1.0 INTRODUCTION	1
2.0 APPROACH	2
2.1 Design Development Method.	2
2.2 Study Plan.	5
3.0 CONFIGURATION DESCRIPTIONS	8
3.1 Reference Turbulent Flow Configuration, Model 767-768	8
3.2 Laminar Flow Control Configuration, Model 767-773	13
3.3 Configuration Comparisons.	13
4.0 CONFIGURATION PERFORMANCE AND ECONOMICS	20
4.1 Mission Rules and Performance Objectives	20
4.2 Engine-Airframe Matching.	22
4.3 LFC Fuel and Weight Savings	27
4.4 Payload-Range Capability	30
4.5 Impact of Design Takeoff Field Length.	30
4.6 In-flight Loss of LFC.	30
4.7 Extent of Laminarization	36
4.8 Potential Benefits of Body Drag Reduction.	40
4.9 Life-Cycle and Operating Cost Comparisons	43
4.10 Total LFC Fuel Savings.	46
5.0 LFC DESIGN CONSIDERATIONS	49
5.1 Factors Affecting Laminarization	49
5.2 Laminarized Flow Areas	49
5.3 Suction Surfaces	49
5.4 Structural Concepts.	52
5.5 Suction System	54
5.6 LFC Thrust-Drag-Weight Bookkeeping System	56
5.7 Takeoff-Climb-Cruise Thrust Matching	61
6.0 LFC CONFIGURATION EVOLUTION	63
6.1 Initial Baseline LFC Configuration	63
6.2 LFC Braced-Wing Study	63
6.3 LFC Wing Geometry/Cruise Speed Optimization Study	67
6.3.1 Performance Optimization	73
6.3.2 Ease of Laminarization	83
6.4 Final LFC Configuration Selection	86

TABLE OF CONTENTS (Concluded)

	Page
7.0 CONFIGURATION ANALYSIS AND METHODS	88
7.1 Aerodynamics	88
7.1.1 Aerodynamics Technology	88
7.1.2 Cruise Aerodynamic Analyses	90
7.1.3 Low-Speed Aerodynamic Analyses	93
7.1.4 Laminar Boundary Layer Analyses	95
7.2 Flight Controls	100
7.2.1 Flight Control Technology	100
7.2.2 Airplane Balance and Tail Sizing	103
7.3 Propulsion and Noise	103
7.3.1 Propulsion Technology	106
7.3.2 Engine Cycle Selection	106
7.3.3 Suction Engine/Compressor Design	110
7.3.4 Acoustical Treatment	110
7.4 Systems	111
7.4.1 Suction System Analysis	111
7.4.2 Ice Protection	111
7.4.3 Lightning Protection	115
7.4.4 Integrated Systems	115
7.5 Weight and Balance	115
7.5.1 Advanced Technology Weight Benefits	116
7.5.2 Weight Analysis Approach	116
7.5.3 LFC Systems and Structural Weight Estimation	116
7.6 Cost and Economics	118
7.6.1 Cost Estimation Ground Rules	118
7.6.2 Cost Analysis Approach	119
7.6.3 LFC Cost Factors	119
8.0 RECOMMENDED RESEARCH AND DEVELOPMENT	123
8.1 General LFC R&D Items	123
8.2 Specific R&D Items for Large Military Transport Airplanes	125
9.0 CONCLUSIONS	127
REFERENCES	129

LIST OF ILLUSTRATIONS

No.		Page
1	Study Technology Levels	2
2	Boundary Layer Control Study Data Base.	3
3	Design Development Method.	4
4	USAF Boundary Layer Control Study	6
5	Reference Turbulent Airplane, Model 767-768.	9
6	Fuselage Design Development Considerations.	10
7	Aerodynamic Effects of Forebody Cab Design	11
8	Advanced One-Piece Windshield	12
9	Final Laminar Flow Control Airplane, Model 767-773	14
10	Cruise Drag Polar Comparison.	18
11	Gross Weight Comparison	19
12	Flight Profile and Mission Rules	21
13	Engine/Airframe Matching for the Reference Turbulent Airplane.	23
14	Reference Turbulent Airplane Design Selection	24
15	Engine/Airframe Matching for the Final Laminar Flow Control Airplane	25
16	Final Laminar Flow Control Airplane Design Selection.	26
17	Laminar Flow Control Fuel and Weight Savings	29
18	Payload-Range Capability	31
19	Effect of Design Takeoff Field Length on Fuel and Weight.	32
20	Effect of Loss of LFC on Mission Range.	33
21	Performance Capability with Loss of Laminar Flow Control.	34
22	Allowable Cruise Time and Distance with Loss of Laminar Flow Control.	35
23	Effect of Extent of Laminarization on Cruise Drag and Suction Engine Fuel	37
24	Effect of Extent of Laminarization on Suction Mass Flow Requirements.	38
25	Effect of Extent of Laminarization on Fuel and Weight	39
26	Body Drag Reduction Study	41
27	Potential Benefits of Body Drag Reduction.	42
28	Twenty-Year Life-Cycle Cost Elements.	44
29	Sixty-Day Surge Condition Cost Elements	44
30	Laminar Flow Control Cost Comparisons	45
31	Life-Cycle and Operating Cost Sensitivities for LFC Configuration, Model 767-773	47
32	Effect of Technology Complexity on Relative Laminar Flow Control Life-Cycle Costs.	47
33	Laminar Flow Control Fuel Savings	48
34	Factors Affecting Laminar Flow	50
35	Laminarized Flow Areas	51
36	Laminar Flow Control Structural Concept Considerations	53
37	Wing Suction Duct Characteristics.	55
38	Baseline LFC Airplane Collector Duct Sizes	57
39	Suction Pump Drive System Selection.	58
40	Compressor/Suction Engine Design.	59
41	LFC System Bookkeeping Method	60
42	Takeoff, Climb, and Cruise Thrust Match Considerations	62

LIST OF ILLUSTRATIONS (Concluded)

No.		Page
43	Uncycled Initial Baseline Laminar Flow Control Airplane, Model 767-769	64
44	Baseline Laminar Flow Control Airplane Design Selection	65
45	Initial Baseline Laminar Flow Control Airplane Structural and System Weight Sensitivity Study	66
46	Laminar Flow Control Braced-Wing Design Considerations	68
47	Uncycled Braced-Wing Laminar Flow Control Airplane, Model 767-767	69
48	Laminar Flow Control Braced-Wing Study Results	70
49	Laminar Flow Control Wing Parametric Optimization Study	71
50	Design Selection for AR=8 Laminar Flow Control Configurations	74
51	Design Selection for AR=10 Laminar Flow Control Configurations	75
52	Design Selection for AR=12 Laminar Flow Control Configurations	76
53	Design Selection for AR=14 Laminar Flow Control Configurations	77
54	Effect of Wing Planform Geometry on Cruise Mach	78
55	Effect of Wing Planform Geometry on Fuel	79
56	Effect of Wing Planform Geometry on Weight	80
57	Effect of Wing Planform Geometry on Productivity	81
58	Laminar Flow Control Wing Optimization Study Results	82
59	Effect of Wing Planform Geometry on Ease of Laminarization	84
60	Effect of Wing Planform Geometry on Ease of Laminarization (Cont.)	85
61	Desirable Laminar Flow Control Wing Planform Characteristics	87
62	Advanced Aerodynamic Technology	89
63	Laminar Flow Control Profile Drag Calculation Procedure	91
64	Friction, Wake, and Suction Drag	92
65	Profile Drag Factor for Transition Location	92
66	Laminar Flow Control and Turbulent Configurations Cruise Aerodynamic Data	94
67	Low-Speed Aerodynamic Data for Turbulent Airplane, Model 767-768	96
68	Low-Speed Aerodynamic Data for the LFC Airplane, Model 767-773	97
69	Suction Flow Calculation Method	98
70	Model 767-773 Wing Suction Distribution and Boundary Layer Stability Evaluation	101
71	Advanced Flight Control Technology	102
72	Horizontal Tail Sizing	105
73	Potential Turbofan Fuel Consumption TSFC Improvement	107
74	STF482 Installed Engine Performance, TSLS=60,000 Pounds	109
75	Model 767-773 Wing Slot Geometry and Spacing	113
76	Suction System Calculation Procedure	114
77	Weight Reduction Due to Advanced Materials	117

LIST OF TABLES

No.		Page
1	Configuration Design Characteristics	15
2	Configuration Weight Comparisons	16
3	Airplane Performance Characteristics Summary	28
4	Active Control Technology Usage	104
5	Suction Flow Requirements for Model 767-773 (0 to 70 Percent of Chord)	112
6	Airplane Cost Estimating Input Requirements	120
7	Airplane Cost Estimating Elements	121

LIST OF ABBREVIATIONS AND SYMBOLS

A	Boundary layer disturbance amplification rate
ACEE	Aircraft Energy Efficient
ACT	Active control technology
AFFDL	Air Force Flight Dynamic Laboratory
Alt	Altitude, ft
A/P	Airplane
AR	Aspect ratio = b^2/s
AS	Augmented stability
ATT	Advanced Technology Transport
b	Span, ft
BL	Boundary layer, buttock line
BLC	Boundary layer control
C	Chord, constants, ft
\bar{c}	Mean aerodynamic chord
C_D	Drag coefficient = D/q_s
C_{D_F}	Friction drag coefficient
C_{D_I}	Induced drag coefficient = $C_L^2/\pi AR_e$
C_{D_M}	Drag coefficient due to compressibility
C_{D_P}	Profile drag coefficient
C_f	Local friction coefficient
C_F	Average friction coefficient; flap chord
C_{F_T}	Turbulent flow friction coefficient
cg	Center of gravity
c_l	Section lift coefficient

C_L	Lift coefficient = L/q_s
C_{LR}	Ratio of cruise C_L to C_L for maximum lift/drag ratio
C_{LP}	Lift coefficient at $C_{DP_{MIN}}$
C_{MO}	Zero lift pitching moment coefficient
Coeff	Coefficients
Const	Constant
C_p	Pressure coefficient
C_Q	Suction flow coefficient
CS	Command support
c	Expanded flap chord due to Fowler action, ft
C_{N_β}	Static directional stability coefficient
D	Drag, diameter
deg	Degrees
D_{Fi}	Friction force due to viscous deceleration of suction flow, lb
D_i	Induced drag, lb
DIA	Diameter, in
D_w	Wake drag, lb
e	Oswald efficiency factor
e.g.	For example
EQUIP	Equipment
f	Braced wing cutout thickness near the brace intersection, in.
$^{\circ}F$	Degrees Fahrenheit
FBW	Fly-by-wire control system
FMC	Flutter mode control
F_n	Net thrust, lb

FO*	Suction mass flow parameter = $\frac{\rho_s V_s}{\rho_\infty V_\infty} \sqrt{Re_c}$
fpm	Feet per minute
FPR	Fan pressure ratio
fps	Feet per second
ft	Feet
f()	Function of ()
g	Acceleration due to gravity, ft/sec ²
gal	Gallons
GLA	Gust load alleviation
GLE	Equivalent leading edge geometry factor = $\sqrt{\frac{(RO/C) \perp}{1 + \tau_e}}$
h	Height, ft
H	Plenum depth, boundary layer shape factor
H/C	Honeycomb
HP	High pressure compressor
HPX	Horse power extraction
hr	Hour
ICAC	Initial cruise altitude capability, ft
INBD	Inboard
keas	Equivalent air speed, kts
K _F	Profile drag factor due to thickness and sweep
K _L	Profile drag factor due to lift effects
ktas	True air speed, kts
kts	knots
K _{X_T}	Profile drag factor due to transition location
L	Lift, lb; length, ft

lb	Pounds
L/D	Lift/drag ratio
LE	Leading edge
LFC	Laminar flow control
LP	Low-pressure compressor
M	Mach number
MAC	Mean aerodynamic chord, ft
MAX	Maximum
M _{CRIT}	Critical Mach number for drag rise
M _{DD}	Drag divergence Mach number
M.E.	Main engines
mil	Military
MIN	Minimum
misc	Miscellaneous
MLC	Maneuver load control
MTW	Maximum taxi weight, lb
NASA	National Aeronautics and Space Administration
nmi	Nautical miles
NON REC	Nonrecurring cost item
N _{ZZ}	Nondimensional second derivative of the crossflow velocity profile at the surface
OEW	Operational empty weight, lb
OPR	Overall pressure ratio
OUTBD	Outboard
P	Pressure, psi; power
Pi	Isentropic power requirements

PL, P/L	Payload, lb
psi	Pounds per square inch
P_t	Total pressure, psi
P&WA	Pratt and Whitney Aircraft Co.
q	Dynamic pressure, psi = $\frac{1}{2} \rho V^2$
Q	Volume flow rate, ft ³ /sec
R	Range, nmi
R&D	Research and development
REC	Recurring cost item
Re_c	Chord Reynolds number = $\frac{\rho VC}{\mu}$
ref	Reference
Re_s	Slot Reynolds number = $\frac{\rho V_s W_s}{\mu}$
$Re_{\eta 0.1}$	Crossflow Reynolds number = $\frac{\rho W_{MAX} \delta 0.1}{\mu}$
Re_N/ft	Unit Reynolds number, $\frac{\rho V}{\mu}$
Ro	Leading-edge radius, in.
$Re_{0.7C}$	Reynolds number based on 0.7 chord length
R_{δ^*}	Displacement thickness Reynolds number
$R_{\theta AL}$	Momentum thickness Reynolds number
S	Wing area, ft ² ; bleed hole spacing, in.
SAS	Stability augmentation system
S.E.	Suction engine
sec	Seconds
SFC	Specific fuel consumption
SLST	Sea level static thrust
SNP	Static neutral point
STA	Station

STD	Standard
t	thickness, in.
T	Thrust, lb; skin thickness, in; temperature, deg
t/c	thickness/chord ratio
TE	Trailing edge
T.O.	Takeoff
TOGW	Takeoff gross weight, lb
TSF	Thrust scaling factor
TSFC	Thrust specific fuel consumption
TSLS	Sea level static thrust
turb	Turbulent
T/W	Thrust/weight ratio
t ₂	time to double amplitude, sec
UE	Unit equipped
V	Velocity, ft/sec
V _{APP}	Approach velocity, ft/sec
V _{bal}	Asymmetric thrust moment balance speed, ft/sec
V _{mc} _{GROUND}	Ground minimum control speed, ft/sec
Vol	Volume, ft ³
V _R	Rotation speed, ft/sec
V _S	Slot velocity; stall speed, ft/sec
\bar{V}	Tail volume coefficient
V ₂	Second segment climb speed, ft/sec
W	Crossflow velocity, ft/sec
W/b ²	Span loading, lb/ft ²
WL	Waterline

W_S	Slot width, in
W/S	Wing loading, lb/ft ²
\ddot{W}	Second derivative of the crossflow velocity
X	Streamwise distance
X/C	Chord fraction
X_{EFF}	Effective origin of the turbulent boundary layer
X_g	Landing gear location as a fraction of the wing MAC
X_{TRANS}	Transition location
$X_{T/l}$	Transition location as a fraction of total length

SYMBOLS

α	Angle of attack
β	Falkner-Skan parameter
δ	Boundary layer thickness, in.
δ^*	Displacement thickness
$\delta_{0.1}$	Boundary layer thickness at which one-tenth the maximum crossflow velocity occurs
Δ	Incremental amount
$(\Delta W_T)_{LFC}$	Total LFC structural plus systems weight penalty, lb/ft ² of the treated laminarized area
$\Delta C_{D_{ITE}}$	Induced drag increment due to flap span loading
ΔX_S	Slot-spacing distance, in.
η	Semispan fraction
λ	Taper ratio
Λ	Sweep angle
π	Pi=3.1416; empennage arrangement
ρ	Density
θ	Momentum thickness, in.

$\ddot{\theta}$	Pitching moment rate acceleration
τ_e	Equivalent leading-edge ellipse semiminor/semimajor axes ratio
ψ_{CRIT}	Crosstflow minimum stability limit Reynolds number

SUBSCRIPTS

app	Approach
AVE	Average
CL	Climb
CR, CRU	Cruise
C/4	Quarter chord
F	Flap
FS	Falkner-Skan
H	Horizontal
INC	Incompressible
J	Jet
L, LOC	Local
Max	Maximum
Min	Minimum
N	Normal to leading edge
O	Free-stream condition, wall value
OPT	Optimum
ref	Reference
S	Suction; surface; slot
SOB	Side of body
St	Strut

TE	Trailing edge
T/O	Takeoff
TRANS	Transition
Turb	Turbulent
V	Vertical
WET	Wetted
W	Wing; wake
∞	Free stream
\perp	Perpendicular to the LE

1.0 INTRODUCTION

Increased concern about the cost and availability of aviation fuel in addition to the possible requirements for global-range movement of large payloads suggested the need for efficient military transport aircraft designs that conserve fuel.

The recently completed AFFDL/Boeing Boundary Layer Control Technology Application study⁽¹⁾ evaluated large military transport designs that incorporated various advanced aerodynamic concepts. Study results identified laminar flow control (LFC) as the aerodynamic concept offering the greatest potential for conserving fuel.

The Northrop X-21 Flight Test program⁽²⁾ demonstrated the technical feasibility of LFC in the 1960s. The economic and practical feasibility of LFC remained to be proven. The aforementioned fuel concerns, together with projected new technology developments, may have a large favorable impact on the practical feasibility of LFC.

The purpose of this study was to conduct a preliminary design investigation of a large subsonic military transport aircraft to assess the economic application of LFC. Technology developments, wind tunnel tests, and flight test verification, necessary to reduce the risk associated with the application of LFC, also were to be identified. The study consisted of three phases:

- Phase 1—Initial LFC conceptual design investigations were conducted to identify features of an LFC airplane optimized to accomplish mission objectives. A reference fully turbulent airplane also was developed in this phase.
- Phase 2—Design and analysis studies were made to develop the final LFC configuration. The final LFC configuration was sized to determine the gross weight, engine size, wing area, and fuel requirements necessary to achieve the design mission.
- Phase 3—The preliminary design definitions of the LFC and reference turbulent airplanes were finalized. Performance trade and sensitivity studies were conducted for the LFC and turbulent airplanes. Life-cycle and operating cost evaluations were made for the LFC and turbulent configurations.

The approach and results are presented in Sections 2.0, 3.0, and 4.0. Sections 5.0 and 6.0 describe the evaluation of the LFC configuration. Section 7.0 describes how the study tasks were accomplished and the methods used. Remaining sections present the research and development recommendations and the main conclusions.

-
1. Kulfan, R. M. and Howard, W. M., *Application of Advanced Aerodynamic Concepts to Large Subsonic Transport Airplanes*, Tech. Report AFFDL-TR-75-112, Nov. 1975.
 2. Whites, R. C.; Sudderth, R. W.; and Wheldon, W. G., "Laminar Flow Control on the X-21," *Astronautics and Aeronautics*, July 1966, pp38-43.

2.0 APPROACH

Design mission objectives for the study configurations included:

- Range = 10,000 nmi
- Payload = 350,000 lb
- Takeoff field length = 9,000 ft
- Mach number: determined by tradeoff studies

Payload density limits were set by the requirement to carry either 75 military standard cargo containers or three M-60 tanks.

The general technology level assumed for the study configurations as shown in Figure 1 corresponds to projections that would allow start of prototype production in 1985. First flight would occur in 1988 or 1989 and airplane in service would be after 1990. Specific advanced technology assumptions are discussed in Section 7.0.

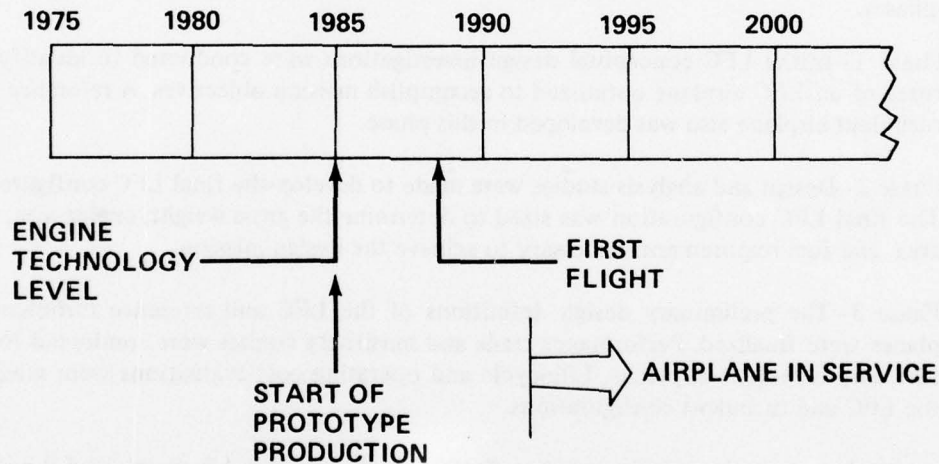


Figure 1 Study Technology Levels

This study used results of the substantial data base of past and present laminar flow control studies and Boeing in-house large freighter studies shown in Figure 2 to provide design ground rules and configuration development guidance.

2.1 DESIGN DEVELOPMENT METHOD

The design development method used to develop each of the aircraft configurations is illustrated in Figure 3.

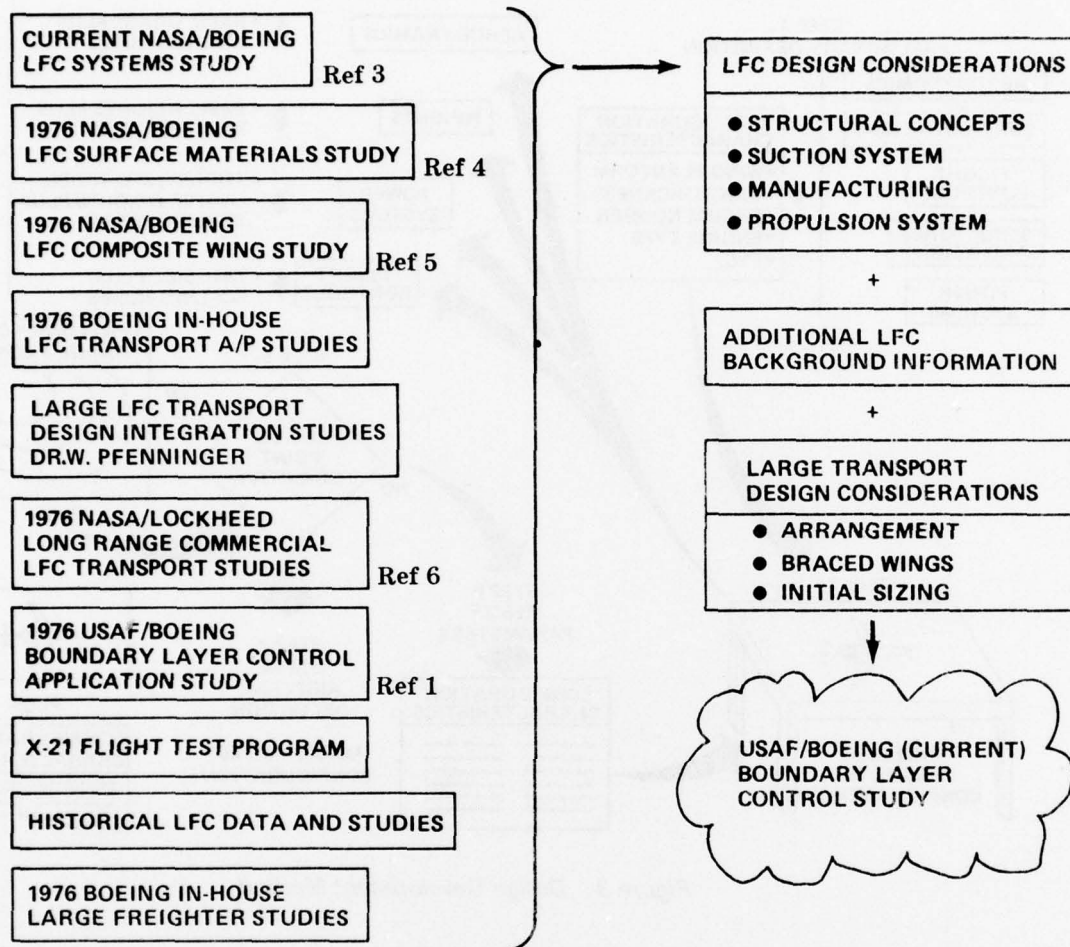


Figure 2 Boundary Layer Control Study Data Base

3. NASA Contract NAS1-14630, "Evaluation of Laminar Flow Control System for Subsonic Commercial Transport Aircraft," (study underway 1976).
4. Weiss, D. D. and Lindh, D. V., *Development of the Technology for the Fabrication of Reliable Laminar Flow Control Panels*, NASA CR-145124, Feb. 1976.
5. Swinford, G. R., *A Preliminary Design Study of a Laminar Flow Control Wing of Composite Materials for Long Range Transport Aircraft*, NASA CR-144950, April 1976.
6. Sturgeon, R. F., et al, *Study of the Application of Advanced Technologies to Laminar Flow Control Systems for Subsonic Transports*, NASA CR-133949, May 1976.

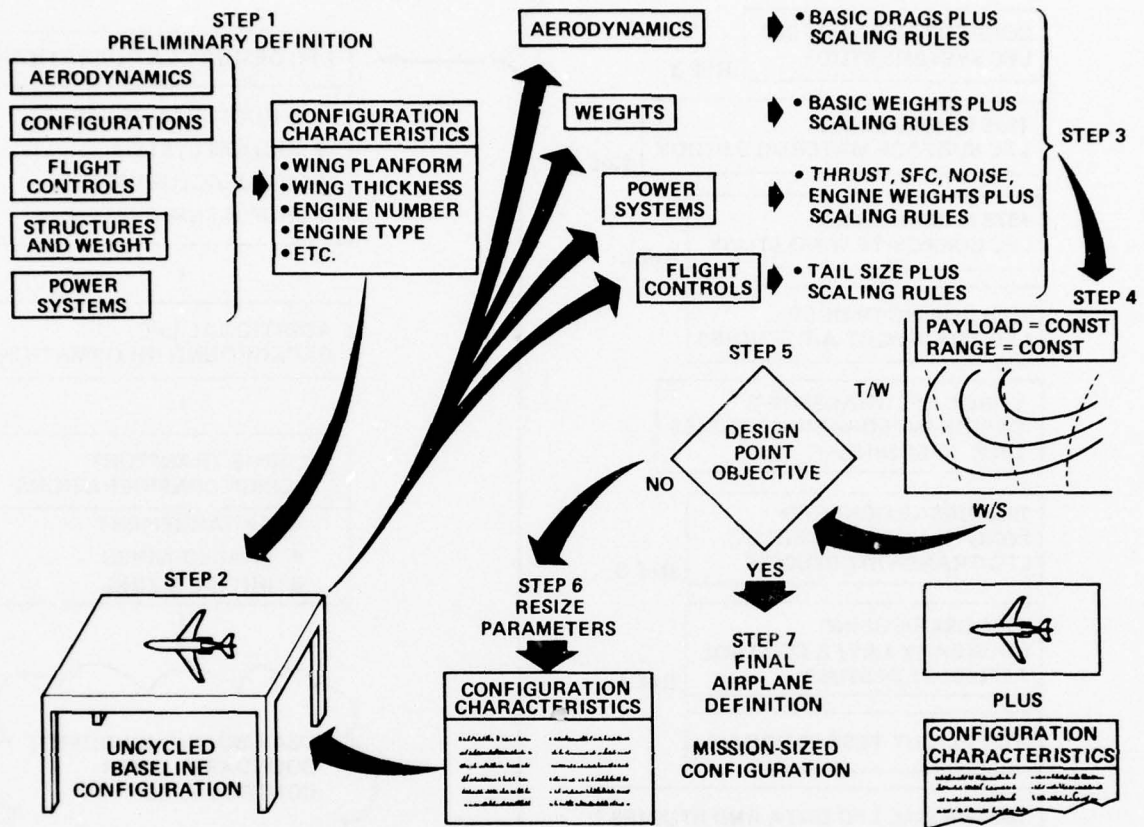


Figure 3 Design Development Method

The initial step was to define preliminary configuration characteristics, including such general items as:

- Wing planform, size, and thickness
- Number of engines, engine cycle, size, and location
- Tail planform, thickness, and size
- Estimated maximum takeoff gross weight

These characteristics were derived from results of past related studies or from specially conducted trade studies. These estimated configuration characteristics were used to develop preliminary configuration sketches. These sketches, along with supporting aerodynamic design optimization studies, weight and balance analyses, stability and control analyses, and structural layouts provided inputs for developing a detailed configuration layout (step 2).

The detailed design layout defined the uncycled baseline configuration. The baseline configuration then was analyzed in depth to determine basic weight, lift and drag, thrust, and noise characteristics. Additional analyses were made to determine the effects of varying gross weight, engine size, and wing area to establish scaling rules that account for these changes (step 3).

The results of the baseline configuration evaluation and the scaling rules form the inputs to a parametric performance analysis program that was used to size the airplane by determining the minimum gross weight, wing area, engine size, and tail size necessary to achieve the mission objective (step 4).

If the design objectives were not met, or if obvious deficiencies were identified, this process was repeated. The parametric trade, sensitivity, and optimization investigations required repeating this design development method a number of times for each particular study.

2.2 STUDY PLAN

The approach used to achieve study objectives is summarized in Figure 4. The initial task was to develop the reference turbulent airplane configuration. The baseline turbulent configuration, model 767-766a, arrangement was guided by results of Boeing in-house large freighter trade and optimization studies. The configuration features reflect the design mission objectives and the incorporation of the advanced technology concepts. The baseline turbulent configuration was sized to meet the mission objectives. The definition of the final sized turbulent airplane configuration model 767-768 was then completed.

The initial baseline LFC arrangement, model 767-769, was defined by modifying the reference turbulent airplane with the minimum changes necessary to incorporate the LFC systems. The LFC systems and structural concepts were derived from previous LFC studies, Boeing in-house LFC studies, and specially conducted LFC system design studies. The initial baseline LFC configuration was sized with different levels of LFC structural and system weight increments.

A braced-wing LFC configuration, model 767-767, was derived from the initial baseline LFC configuration model 767-769 that has a cantilever wing. The definition of the braced-wing geometry was guided by the results of Boeing large freighter braced-wing studies. The braced-wing LFC configuration was sized to meet mission objectives and was compared with the corresponding sized cantilever wing LFC configuration. Because of the large number of design variations that would be necessary to fully optimize a braced-wing configuration, the remainder of the study effort was concentrated on the development of the LFC cantilever wing configuration.

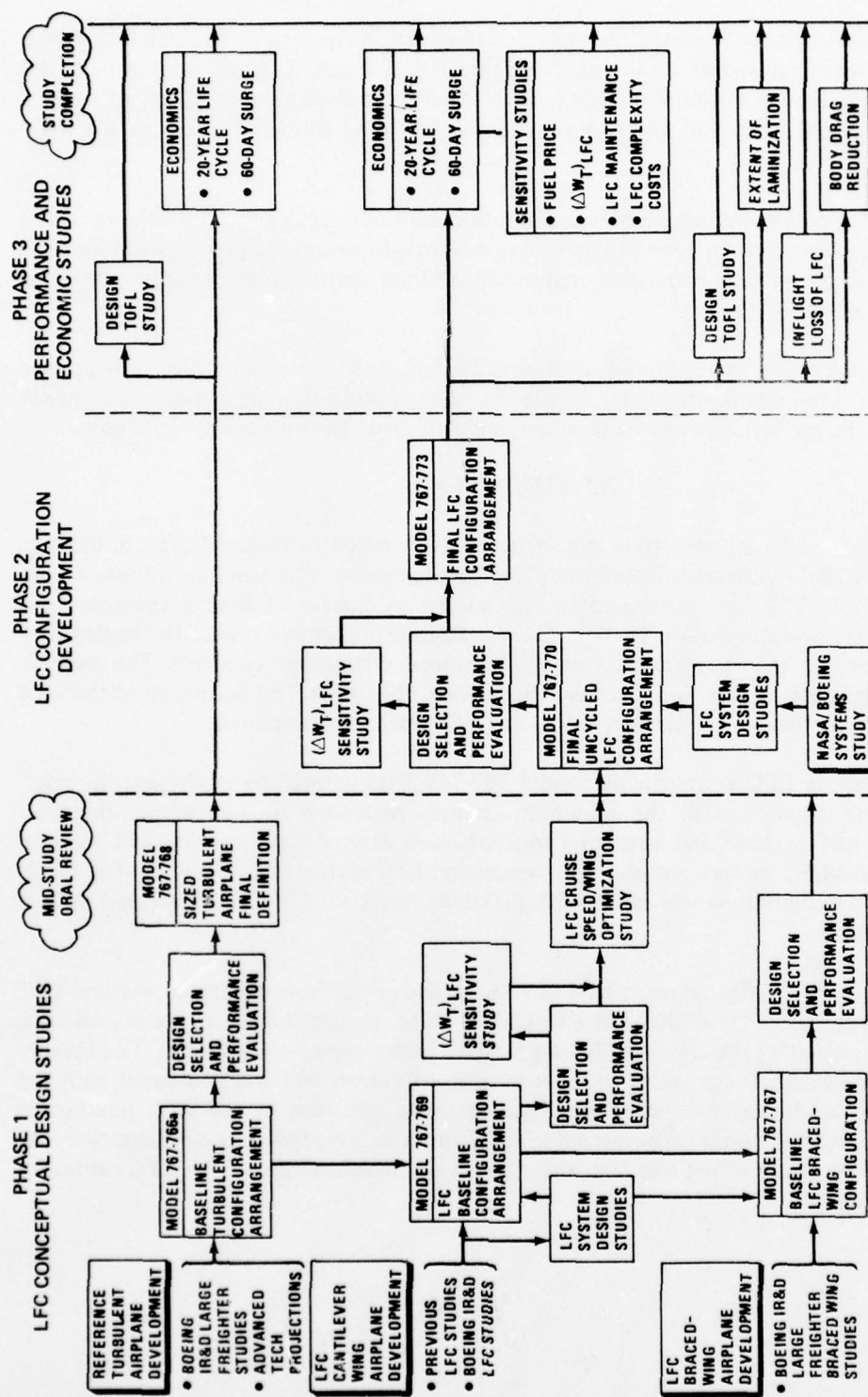


Figure 4 USAF Boundary Layer Control Study

A wing geometry/cruise speed parametric optimization study was conducted to optimize the LFC cantilever wing configuration. The final uncycled LFC configuration model 767-770 was developed using the best wing planform identified in the planform optimization study.

Model 767-770 then was sized to achieve the design mission objectives. The airplane was sized with different levels of LFC structural and system weight increments. The final LFC configuration arrangement definition then was completed.

The final turbulent airplane configuration, model 767-768, and the final LFC configuration, model 767-773, were used in design trade and sensitivity studies to determine the impact of the following on the fuel, weight, and cost of LFC and turbulent airplanes:

- Design takeoff field length
- Extent of laminarization
- Body drag reduction
- LFC maintenance costs
- LFC technology complexity costs
- Fuel prices

Additionally, the performance effects of in-flight loss of LFC were investigated.

Characteristics of the final LFC and turbulent configurations are discussed in Section 3.0.

3.0 CONFIGURATION DESCRIPTIONS

This section contains a description of the final LFC configuration and of the reference turbulent flow configuration. The reference turbulent flow configuration was developed from Boeing commercial large freighter study configurations that had approximately the same payload requirements but smaller design ranges. Considerations that led to the final configuration arrangements are discussed below. The performance and economic evaluations of the final configurations are discussed in Section 4.0.

3.1 REFERENCE TURBULENT FLOW CONFIGURATION, MODEL 767-768

The general arrangement of the reference turbulent flow configuration is shown in Figure 5.

Selection of a three-bay oval fuselage was strongly dictated by the design payload requirements. As shown in Figure 6, this configuration provides space for the required lower density payload of 75 military cargo containers without requiring excessive cargo floor length. The four-bay double-lobe body arrangement, also shown in Figure 6, would offer the advantage of an even shorter body length, and would require a lower pressurization weight penalty. Because the dense payload of three M-60 tanks would require substantially different loading in each of the lobes, this type of arrangement would have encountered a significant weight penalty. The kneeling landing gear results in a cargo floor loading height of 84 inches. The body has front and aft load capability for the cargo containers and for light vehicles. The tanks require front loading and unloading.

The design of the forebody cab can contribute significantly to the drag of a fuselage. Extensive investigations ⁽⁷⁾ of the aerodynamic effects of forebody cab design (Figure 7) indicate that sudden changes in curvature, particularly near the windshield, produce patches of supercritical flow, and areas of local flow separation that result in the formation of trailing vortices. Consequently, the fuselage of the turbulent airplane features an advanced one-piece windshield design shown conceptually in Figure 8. This design provides direct viewing and incorporates a conventional flight deck with state-of-the-art displays and controls for the 1985 time period. The seamless windshield assembly results in reduced body drag. This design is compatible and desirable for body drag reduction techniques such as boundary layer control (BLC), body LFC, or the use of compliant skins. This design requires the development of an optically corrected smooth structural windshield and a seamless seal assembly.

Wing planform characteristics were selected for efficient long-range cruise considerations incorporating the benefits of active controls and advanced composite structural materials. The high-lift system includes 747 SP-type single-slotted trailing-edge (TE) flaps and variable camber leading-edge (LE) flaps. The TE flap has a chord ratio (C_F/C) of 0.225 and a Fowler motion (C'_F/C) of 1.08.

The canted " π " tail empennage arrangement is a structurally efficient design that provides the desired drive-through and air-drop capability. The use of active controls, together with the double-hinge rudder, results in minimum tail areas.

7. George-Falvy, D., *An Investigation of the Flow Around the Cab of Boeing Jet Transports*, Boeing Document D6-15006, 1966.

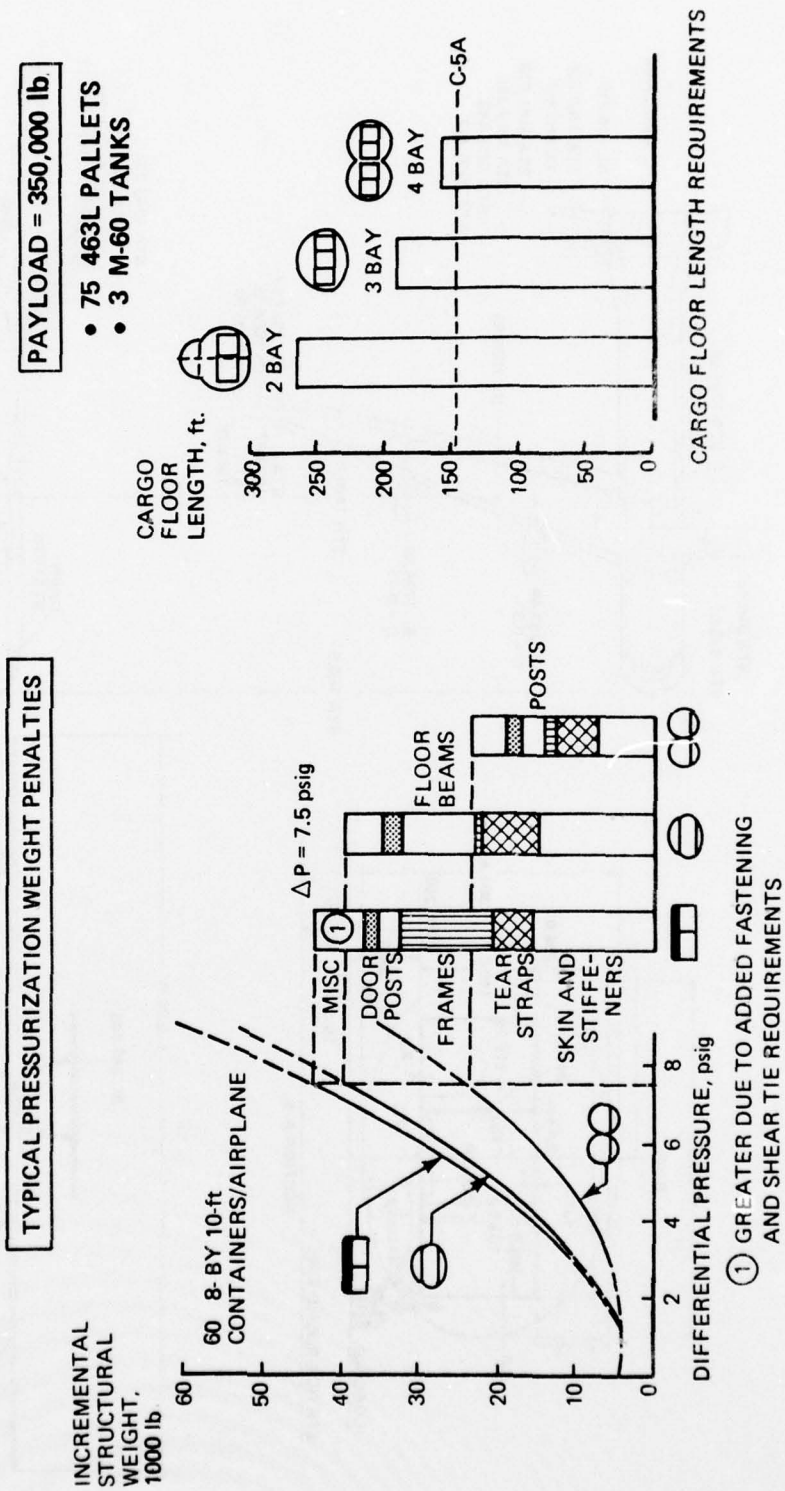
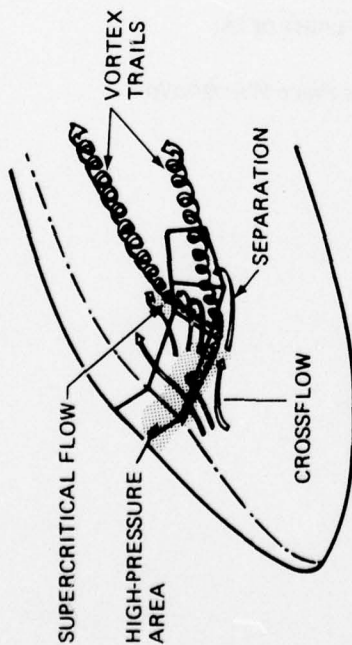
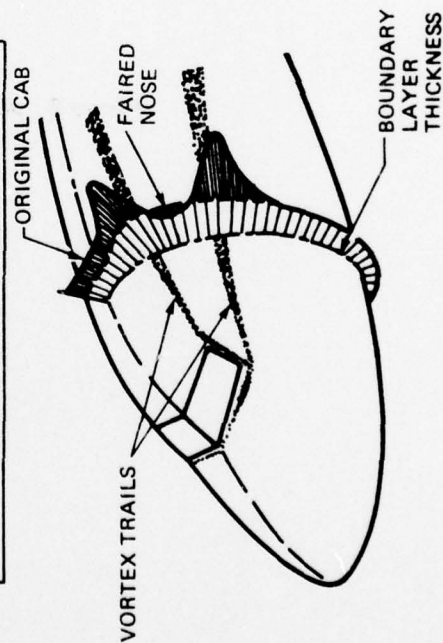


Figure 6 Fuselage Design Development Considerations

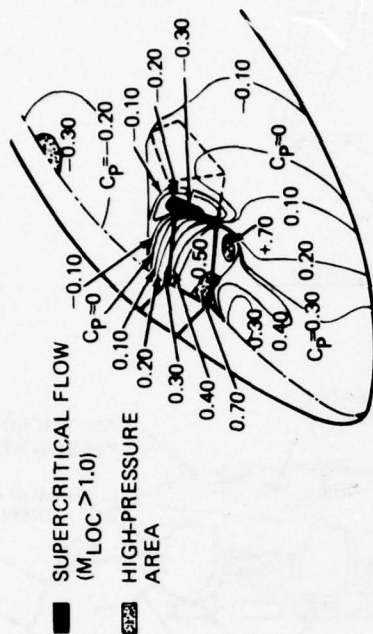
FLOW DISTURBANCES CAUSED BY THE CAB



EFFECT OF THE CAB ON THE BOUNDARY LAYER DEVELOPMENT



TYPICAL FOREBODY ISOBARS



DRAG INCREMENT DUE TO THE CAB

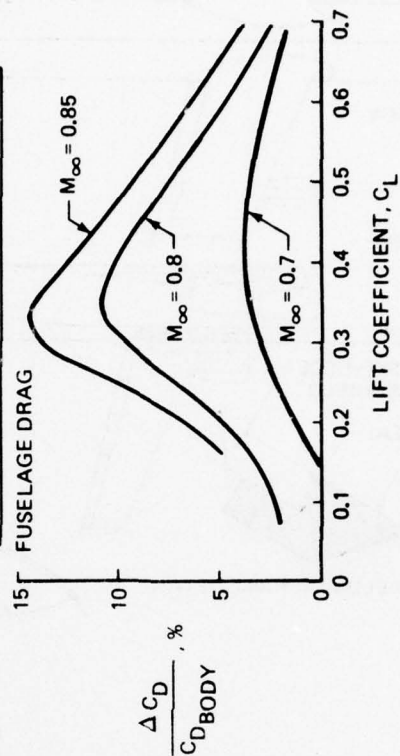


Figure 7 Aerodynamic Effects of Forebody Cab Design

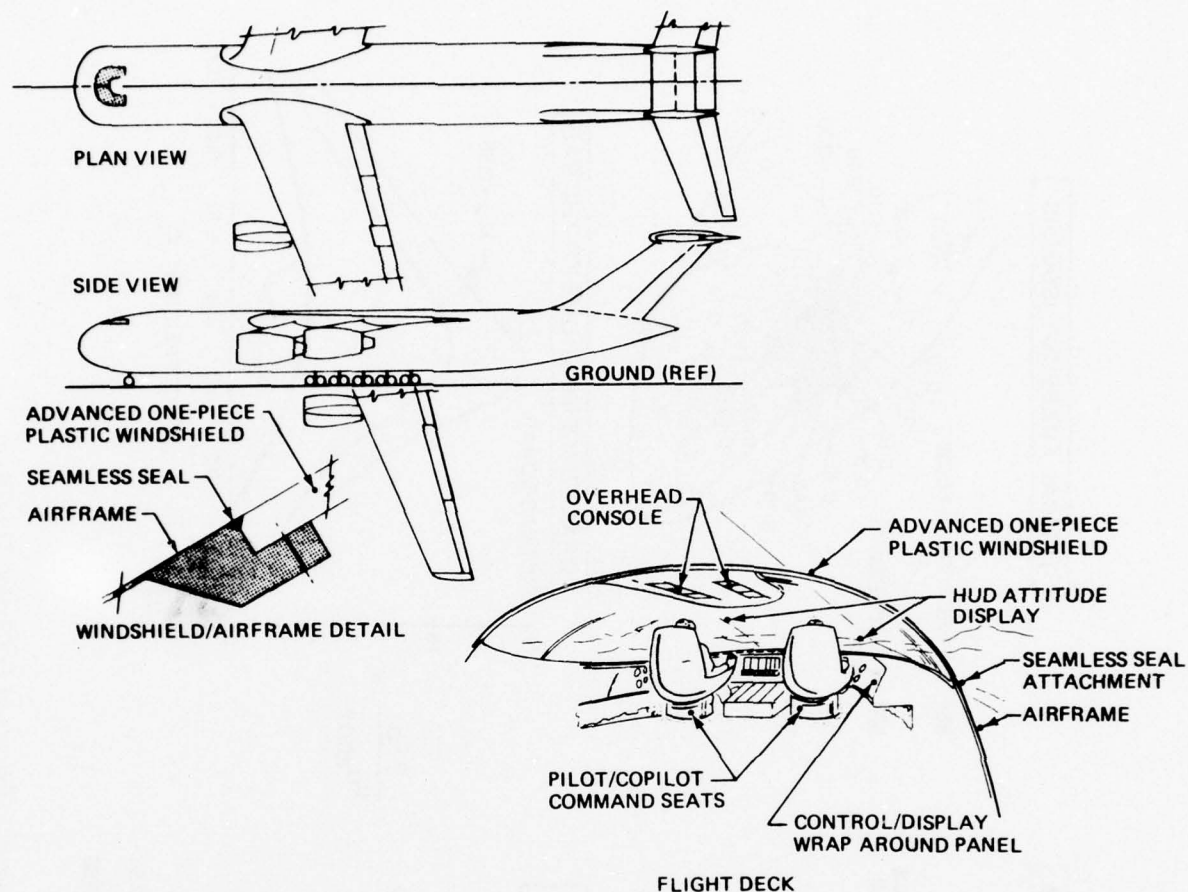


Figure 8 Advanced One-Piece Windshield

The propulsion system includes four 1985 technology high bypass ratio (BPR) engines. The engines are located on the wing primarily because of the airplane balance requirements and the engine design constraints (TSLs <90,000 lb) that require a minimum of four engines for the study airplanes. Airplane balance is the correct relationship of the center of gravity (cg) of the airplane to aerodynamic stability limits for different loading conditions. This relationship is more difficult to achieve when the engines are on the aft fuselage, especially for aircraft with heavy payloads and large high bypass ratio engines. Because of the difference between the position of the payload cg and the propulsion system cg, large shifts in the airplane cg would occur from one operating condition to the next. The spanwise locations were set by flutter considerations and provide wing bending relief.

3.2 LAMINAR FLOW CONTROL CONFIGURATION, MODEL 767-773

The general arrangement of the final laminar flow control configuration is shown in Figure 9.

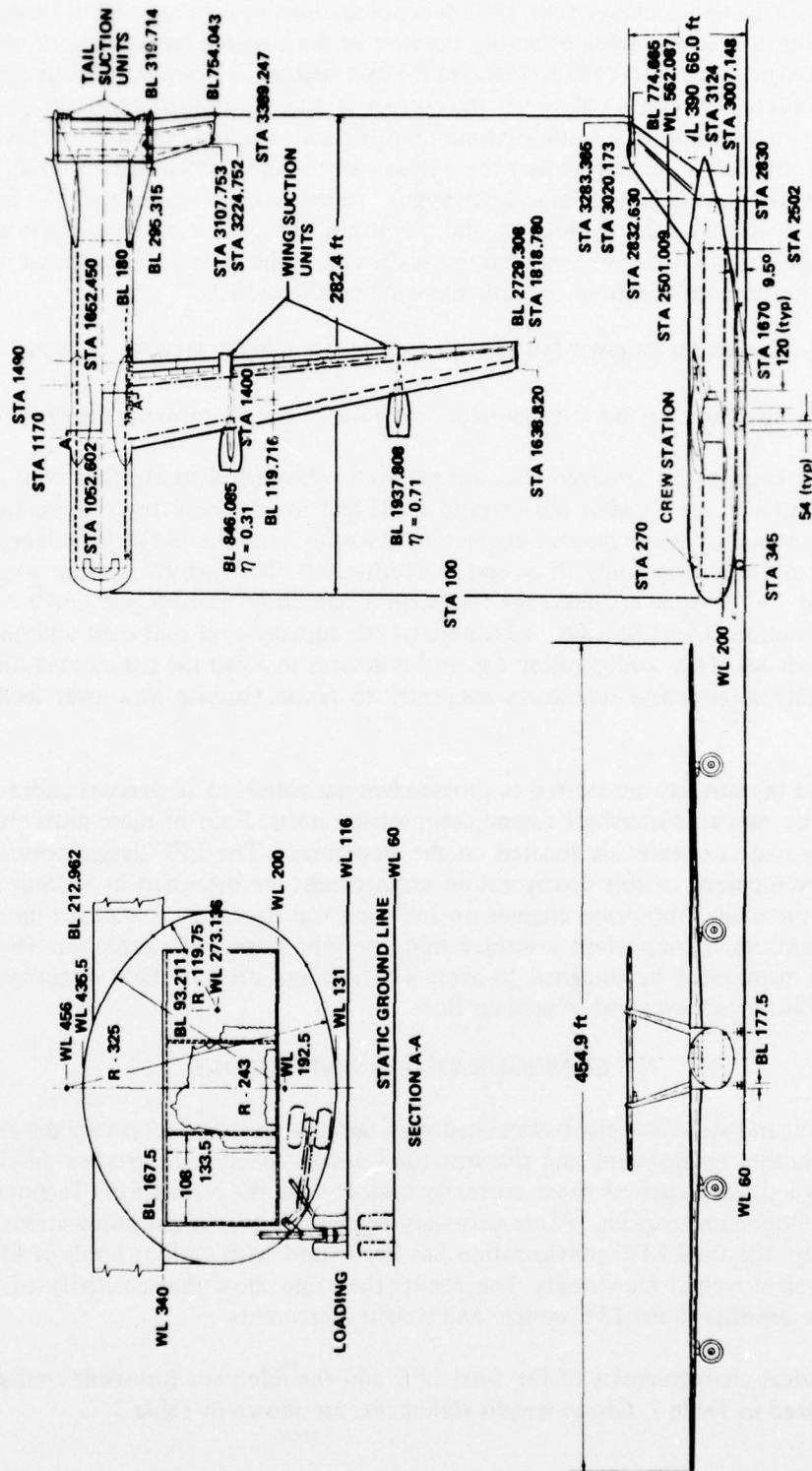
Fuselage and empennage arrangements are similar to the turbulent airplane configuration. The wing planform has a higher aspect ratio (AR) and lower sweep than the reference turbulent airplane wing. The geometry characteristics were determined by the wing geometry/cruise speed optimization study discussed in Section 6.0. The high-lift system consists of a single-slotted 747 SP-type trailing edge flap with a flap chord ratio (C_F/C) of 0.225 and a flap Fowler action (C'/C) of 1.08. Additionally, the inboard and outboard ailerons can be dropped to 10 deg. This configuration has no LE devices to avoid the anticipated difficulties of maintaining smoothness tolerances necessary to retain laminar flow over leading-edge junctions.

The wing and tail surfaces are slotted to provide laminarization to 70-percent chord. Suction is provided by ram-air turboshaft engine/compression units. Four of these units are located on the wing and two units are located on the empennage. The LFC design considerations affecting development of this configuration arrangement are discussed in Section 5.0. The location of the main propulsion engines on the wing was necessary to balance the airplane. This is an extremely important consideration for very large LFC airplanes. The engine, nacelle, and strut must be designed to avoid acoustic and pressure field disturbances that could prohibit the achievement of laminar flow.

3.3 CONFIGURATION COMPARISONS

The structural and systems weight associated with laminar flow control is very dependent on the configuration arrangement and the structural design concept. Innovative detailed LFC system design studies, such as those currently underway in the NASA LFC Technology and System Development program, ⁽³⁾ are necessary to identify the weight implications of LFC. Consequently, the final LFC configuration has been sized with various levels of LFC structural and system weight increments. The results therefore show the sensitivity of the LFC performance benefits to the LFC system and weight increments.

The geometrical characteristics of the final LFC and the reference turbulent configurations are summarized in Table 1. Group weight statements are shown in Table 2.



- WING AND TAILS ARE LAMINARIZED TO 70% CHORD
- $(\Delta W_T)_{LFC} = 2.25 \text{ lb/ft}^2$ LAMINAR WETTED AREA

Figure 9 Final Laminar Flow Control Airplane, Model 767-773

Table 1 Configuration Design Characteristics

DESIGN ITEM		TURBULENT CONFIGURA- TION MODEL 767-768	FINAL LFC CONFIGURATION		
			$(\Delta W_T)_{LFC} \text{ lb/ft}^2$		
			0.0	2.25	3.0
Major design parameters	Payload, lb	350,000			
	Range, nmi	10,000			
	Cruise Mach no.	0.78	0.79		
	TOFL, ft	9,000	8,650	8,950	9,050
	Turb. climb alt, ft		35,000		
	TOGW, lb	1,665,800	1,408,980	1,551,560	1,607,650
	OEW, lb	608,600	576,080		725,160
	Fuel, lb	668,600	455,960		502,650
	Reserves, lb	43,300	30,870		34,160
Fuselage	Length, ft	252			
	Max diameter, in.	426.5			
	Wetted area, ft ²	21,927			
Landing gear	Nose	4 (49 x 17)			
	Main	40 (49 x 17)			
	Area, ft ²	14,785	13,420		15,310
	Wetted area, ft ²	25,849	23,555	26,108	27,105
	Laminar treated area, ft ²		15,839	17,558	18,229
	AR	12			
	$\Lambda_{c/4}$, deg	20	10		
	Span, ft	421.2	433.4	454.8	463.0
	λ	0.30			
	MAC, ft	38.5	34.0	35.6	36.3
	t/c, root/tip	0.14/0.08			
Horizontal tail	Area, ft ²	2,562	2,290	2,460	2,510
	Wetted area, ft ²	5,118	4,574	4,914	5,014
	Laminar treated area, ft ²		3,013	3,237	3,303
	AR	5.07	6.42		
	$\Lambda_{c/4}$, deg, inbd/outbd	0.0/22.5			
	λ inbd/outbd	0.0/0.63			
	t/c	.11			
	MAC, ft	22.9	19.2	19.9	20.1
	Tail vol coeff	0.655	0.72	0.67	0.65
Vertical tail	Area, ft ² (2 tails)	2,392	1,820	2,055	2,150
	Wetted area, ft ²	4,784	3,640	4,110	4,300
	Laminar treated area, ft ²		2,237	2,526	2,643
	AR	1.00			
	$\Lambda_{c/4}$, deg	54			
	λ	0.52			
	t/c	0.12			
	MAC, ft	38.2	31.2	33.1	33.9
	Tail vol coeff	0.045	0.038	0.037	0.037
Propulsion	Type/BPR	STF 482/7.5			
	No./LOC	4/Wing mounted			
	SLST, lb	77,200	63,400	67,850	69,600
	Wetted area, ft ²	3,120	2,562	2,742	
Suction units	No./LOC		4/Wing mount + 2/Tail mount		

Table 2 Configuration Weight Comparisons

ITEM	TURBULENT CONFIGURATION MODEL 767-768 POUND	FINAL LFC CONFIGURATION		
		$(\Delta W_T)_{LFC}$ lb/ft ²		
		0.0	2.25	3.0
		POUND	POUND	POUND
Wing	211 000	211 860	289 180 (a)	320 140 (a)
Horizontal tail	11 900	10 730	19 620 (a)	22 830 (a)
Vertical tail	15 430	10 720	18 920 (a)	22 180 (a)
Body	186 630	180 910	183 890	185 060
Main gear	37 600	34 720	36 820	37 630
Nose gear	5 760	5 320	5 650	5 770
Nacelle and strut	23 800	19 550	20 920	21 460
Total structure	492 210	473 810	575 000	615 070
Engine	50 030	39 780	43 060	44 360
Engine accessories	1 330	1 330	1 330	1 330
Fuel system	6 740	5 980	6 400	6 570
Engine controls	320	320	320	320
Starting system	320	320	320	320
Thrust reverser	6 770	5 570	5 960	6 110
Total propulsion group	65 510	53 300	57 390	59 010
Auxiliary power unit	2 000	2 000	2 000	2 000
Instruments and nav equip	1 270	1 270	1 270	1 270
Surface controls	21 310	19 660	20 820	21 280
Hydraulic/pneumatic	4 680	4 420	4 770	4 910
Electrical	3 120	3 120	3 120	3 120
Avionics	3 140	3 140	3 140	3 140
Furnishings and equipment	6 710	6 710	6 710	6 710
Air cond and anti-icing	3 620	3 620	3 620	3 620
Auxiliary gear	270	270	270	270
Total fixed equipment	46 120	44 210	45 720	46 320
Manufacturer's empty weight	603 840	571 320	678 100	720 420
Crew	1 290	1 290	1 290	1 290
Crew provisions	320	320	320	320
Oil and trapped oil	600	600	600	600
Unavailable fuel	800	800	800	800
Payload provisions	1 750	1 750	1 750	1 750
Total non exp useful load	4760	4760	4760	4760
Operational empty weight	608 600	576 080	682 870	725 160
Payload	350 000	350 000	350 000	350 000
Fuel	668 600	455 960	489 640	502 650
Reserves	43 300	30 870	33 250	34 160
Takeoff gross weight	1 665 800	1 408 910	1 551 560	1 607 650
(a) Includes total LFC systems plus structural weight increment as $(\Delta W_T)_{LFC}$ x treated wetted area (defined in Table 1).				

Cruise drag comparisons of the turbulent flow and LFC configurations are shown in Figure 10. The reference turbulent airplane model 767-768 has a relatively high lift/drag ratio ($L/D = 27.9$). This is because of its large wing span/wetted area ratio. The profile drag of the wing and empennage is a large portion of the total cruise drag. Reduction of this drag element by LFC increased the cruise lift/drag ratio significantly ($L/D = 40.1$).

Gross weight comparisons of the study configurations are shown in Figure 11. The reference turbulent configuration is a large airplane (TOGW = 1,665,800 lb). The block fuel required to meet the mission objectives constitutes 40 percent of the gross weight. Hence, it might be expected that a large fuel savings by LFC would also reduce the takeoff gross weight (TOGW) if the associated system and structural weight increments are not significant. The relative fuel and gross weight savings with LFC are discussed in more detail in Section 4.0.

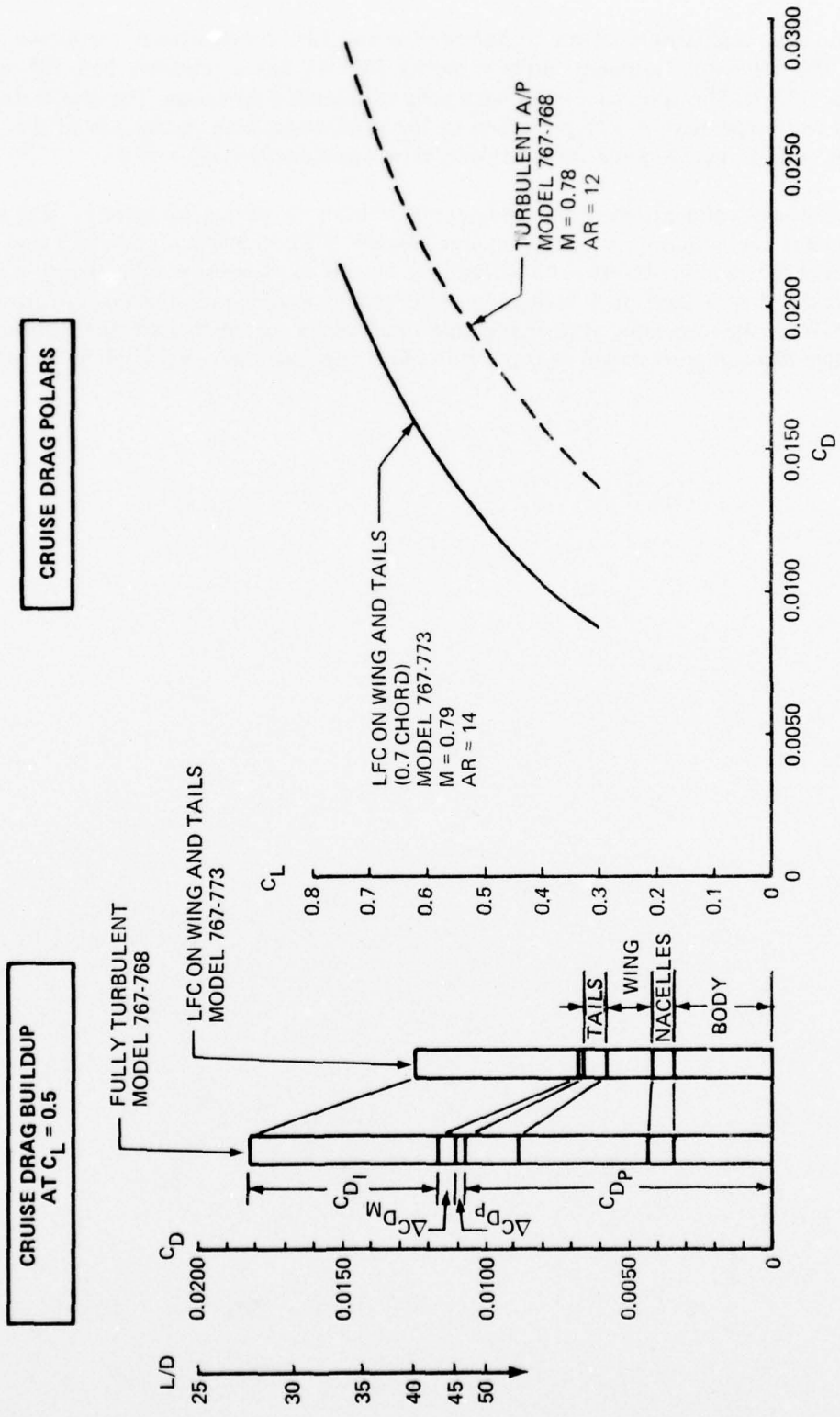


Figure 10 Cruise Drag Polar Comparison

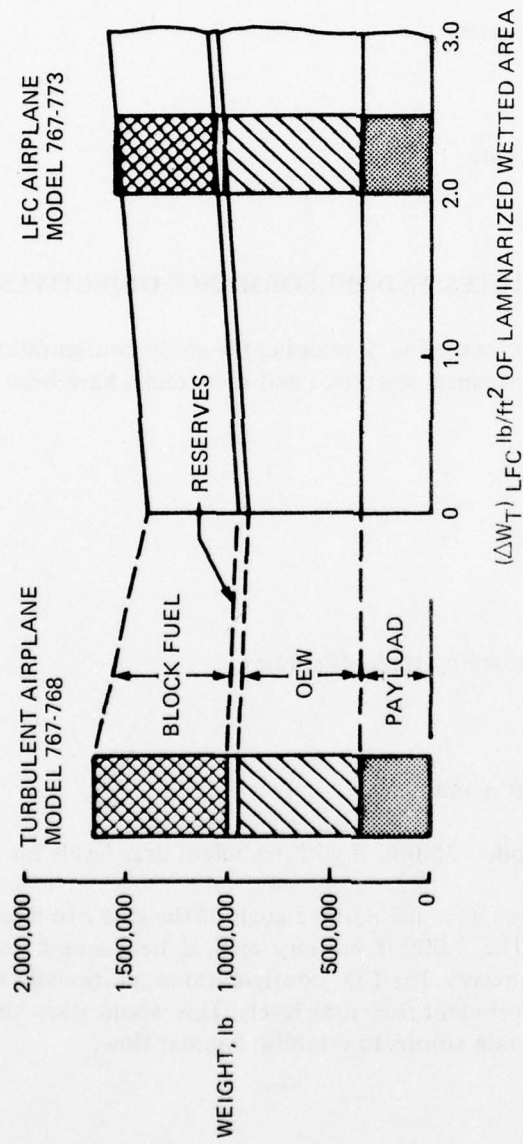


Figure 11 Gross Weight Comparison

4.0 CONFIGURATION PERFORMANCE AND ECONOMICS

The turbulent flow and laminar flow control configurations discussed in Section 3.0 were used to identify the potential impact on LFC on the fuel consumption, weight, life-cycle costs, and operating costs. Sensitivity studies also were conducted to determine the impact of the LFC weight increment, fuel price, LFC maintenance, and technology complexity costs. Additional performance and sensitivity studies included:

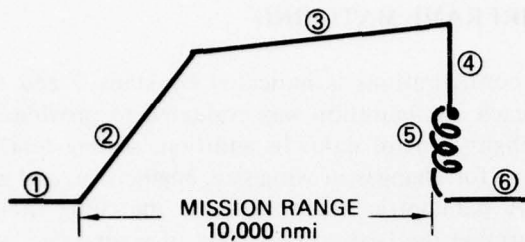
- Payload-range capability
- Design takeoff field length study
- Effect of loss of LFC
- Extent of laminarization study
- Body drag reduction study

4.1 MISSION RULES AND PERFORMANCE OBJECTIVES

The flight profile and mission rules used in developing the study configurations are shown in Figure 12. The following performance objectives and constraints have been used to size airplane configurations:

- Objectives:
 - Payload = 350,000 lb
 - Range = 10,000 nmi
 - Cruise Mach: determined by tradeoff studies
- Constraints:
 - Field length: 9,000 ft maximum
 - Minimum climb altitude: 35,000 ft with turbulent drag levels for LFC airplane

The range and payload objectives were the defined goals of the study to meet the long-range military airlift requirements. The 9,000-ft military critical field length requirements will allow operation off existing runways. The LFC configurations additionally were required to climb to 35,000 ft with fully turbulent flow drag levels. This would allow the LFC airplanes to climb above typical snow or rain storms to establish laminar flow.



● **PAYLOAD = 350,000 lb**
 75 463L CARGO CONTAINERS
 3 M-60 TANKS

MISSION ELEMENT	ALLOWANCES
① START, TAXI, TAKEOFF	<ul style="list-style-type: none"> • 5 MINUTES AT MAXIMUM CRUISE THRUST AT SEA LEVEL • 1 MINUTE AT MAXIMUM TAKEOFF THRUST AT SEA LEVEL
② CLIMB	<ul style="list-style-type: none"> • CLIMB FROM SEA LEVEL TO BEST CRUISE ALTITUDE AT MAXIMUM CLIMB POWER
③ CRUISE-CLIMB	<ul style="list-style-type: none"> • CRUISE-CLIMB AT BEST CRUISE ALTITUDE
④ DESCENT	<ul style="list-style-type: none"> • NO ALLOWANCE FOR FUEL, TIME, OR DISTANCE
RESERVES	
⑤ LOITER	<ul style="list-style-type: none"> • 30-MINUTE LOITER AT MAXIMUM ENDURANCE SPEED AT SEA LEVEL
⑥ LANDING	<ul style="list-style-type: none"> • LAND WITH 5% OF INITIAL MISSION FUEL

- NOTES:
- ① SFC IS INCREASED BY 5% THROUGHOUT THE MISSION
 - ② TAKEOFF DISTANCE IS BASED ON ALL ENGINES OPERATING
 - TAKEOFF SPEED $\geq 1.2 V_s$
 - DISTANCE TO 50 ft OBSTACLE ≤ 9000 ft, SEA LEVEL, $90^\circ F$
 - ONE ENGINE-OUT CLIMB REQUIREMENT ≥ 100 FPM
 - ③ INITIAL CRUISE ALTITUDE $\geq 30,000$ ft FOR TURBULENT AIRPLANE
 - ④ CLIMB TO 35,000 ft WITH TURBULENT DRAGS FOR LFC AIRPLANE
 - ⑤ ENROUTE CRUISE SPEED ≥ 300 KEAS

Figure 12 Flight Profile and Mission Rules

4.2 ENGINE-AIRFRAME MATCHING

The procedure used to size the airplane configurations is indicated by steps 3 and 4 of Figure 3. The detailed design layout of each configuration was evaluated to provide base point thrust, weight, aerodynamic, and flight control data. In addition, scaling relations were derived by further analyses to account for changes in wing size, engine size, and gross weight variations in the resizing cycle. A parametric engine-airframe matching method described in Reference 8 was used to determine the best combination of engine size, wing size, fuel requirements, and gross weight necessary to achieve the design mission objectives.

The design selection chart for the reference turbulent airplane is shown in Figure 13. This type of design chart parametrically shows the effect of thrust/weight ratio (T/W) and wing loading (W/S) on the airplane gross weight and block fuel requirements. Performance factors, such as takeoff field length (TOFL), initial cruise altitude capability (ICAC), and the ratio of the initial cruise lift coefficient capability to the lift coefficient for maximum lift/drag ratio (C_{L_R}) also are identified.

The minimum gross weight for the turbulent airplane requires a high wing loading of approximately 160 lb/ft^2 . With the high wing loading, the configuration could not meet the TOFL requirement. The minimum fuel burned arrangement requires a lower wing loading (110 lb/ft^2). This configuration does meet the takeoff field requirements of 9,000 ft. The final design for the turbulent airplane was selected by considering the trade between fuel burned and gross weight along the $\text{TOFL} = 9,000\text{-ft}$ constraint line (Figure 14). The selected design, which has a wing loading of 112.7 lb/ft^2 , has almost the minimum fuel requirements, and has a gross weight within approximately 2 percent of the minimum gross weight for this configuration. This selected wing loading corresponds to a span loading (W/b^2) of 9.3 lb/ft^2 .

The corresponding design selection chart for the LFC configuration is shown in Figure 15. The minimum gross weight configuration would require a wing loading in excess of 120 lb/ft^2 . The design wing loading for minimum fuel is approximately 95 lb/ft^2 .

The LFC configuration is required to climb to 35,000 ft with fully turbulent drag levels and also has the TOFL limit of 9,000 ft. The 35,000-ft turbulent climb altitude limit is equivalent to an initial climb altitude capability of 41,000 ft with the laminarized flow drag levels. These two design constraints limit the acceptable design region. Neither the minimum fuel nor the minimum TOGW configuration meets the design constraints.

The LFC configuration was sized with different levels of LFC system and structural weight penalties by considering the trade between gross weight and fuel burned as shown in Figure 16. The selected design has a wing loading of 105 lb/ft^2 . This corresponds to a span loading of 7.5 lb/ft^2 . Because of performance constraints, the selected designs for the LFC configuration have a gross weight approximately 7 percent greater than the minimum gross weight arrangement and require approximately 5 percent more fuel than the minimum fuel LFC configuration.

8. Wallace, R. E., *Parametric and Optimization Techniques for Airplane Design Synthesis*, Paper No. 7 in AGARD-LS-56, April 1972.

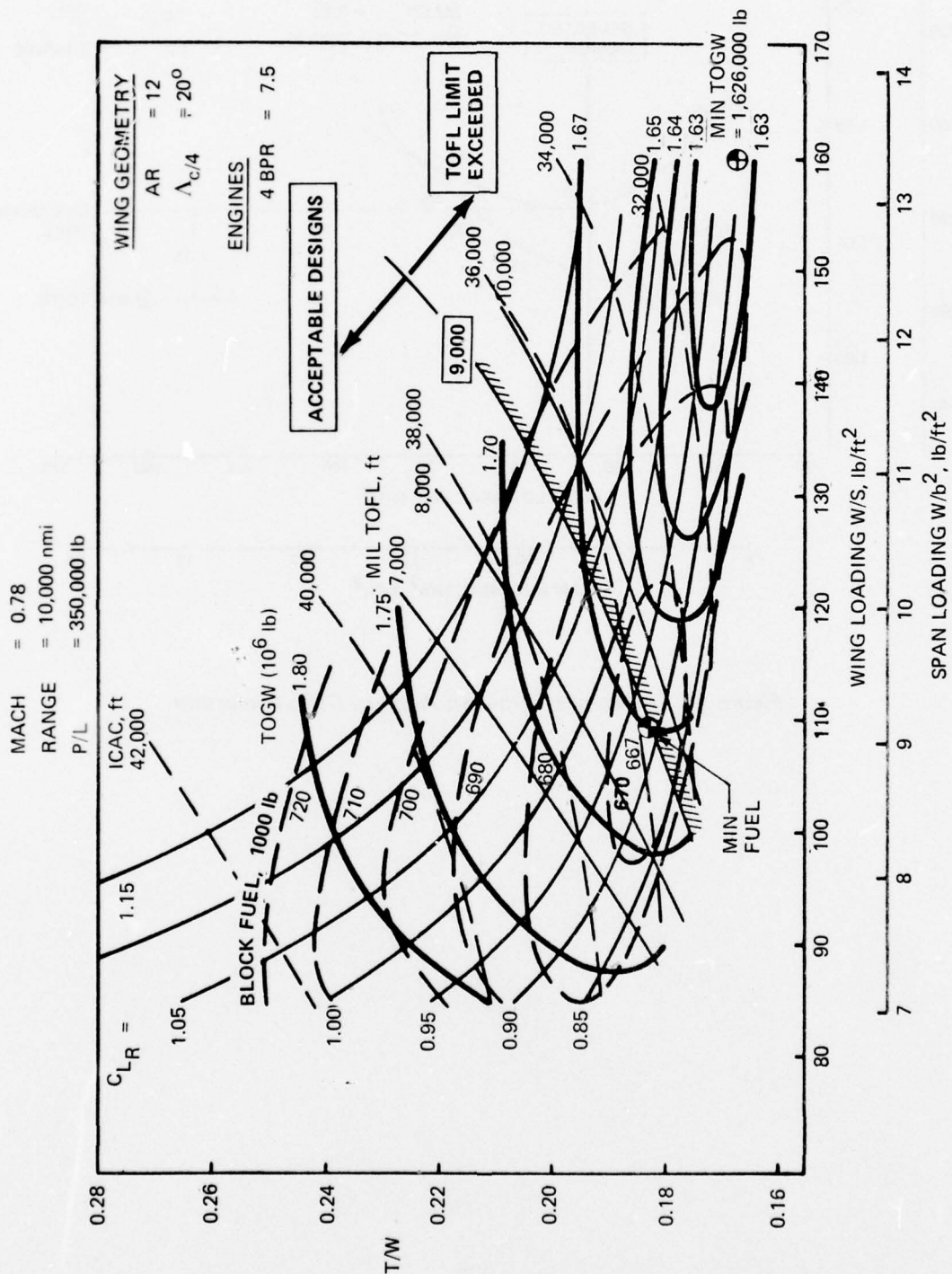


Figure 13 Engine Airframe Matching for the Reference Turbulent Airplane

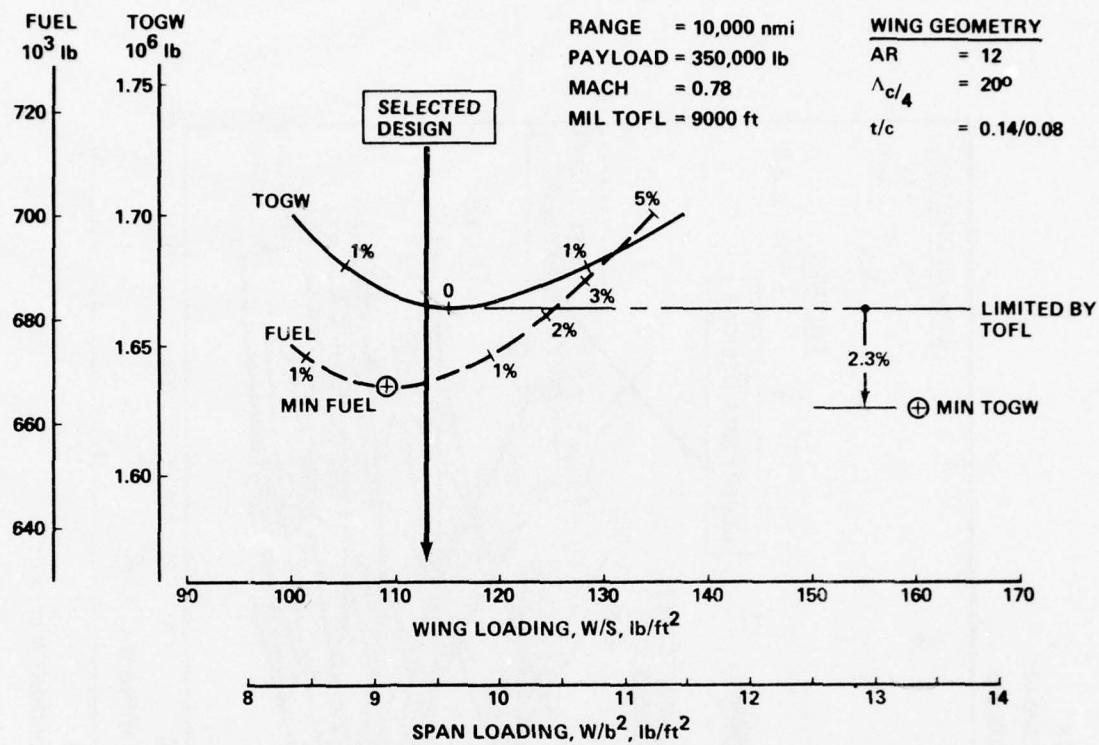


Figure 14 Reference Turbulent Airplane Design Selection

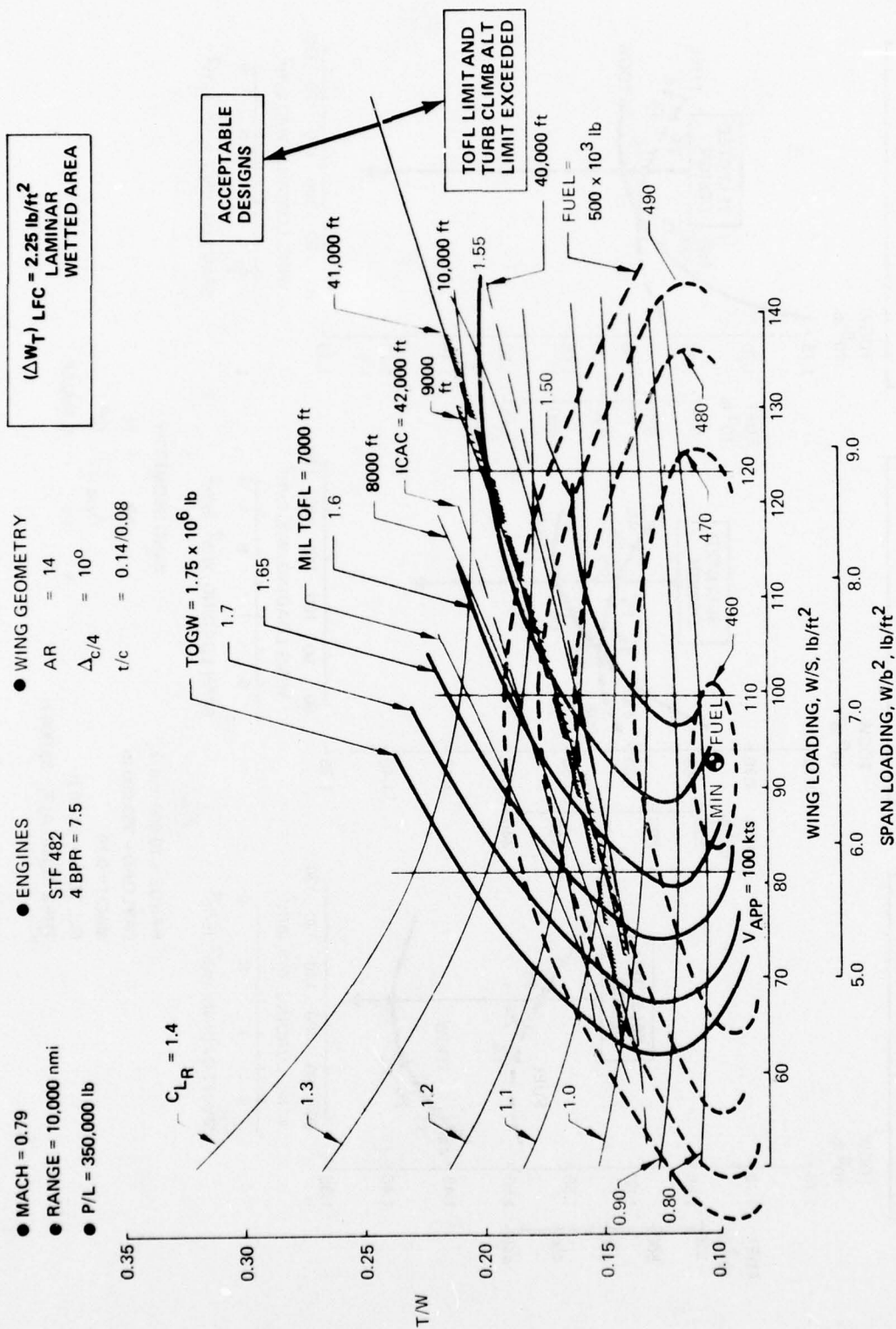
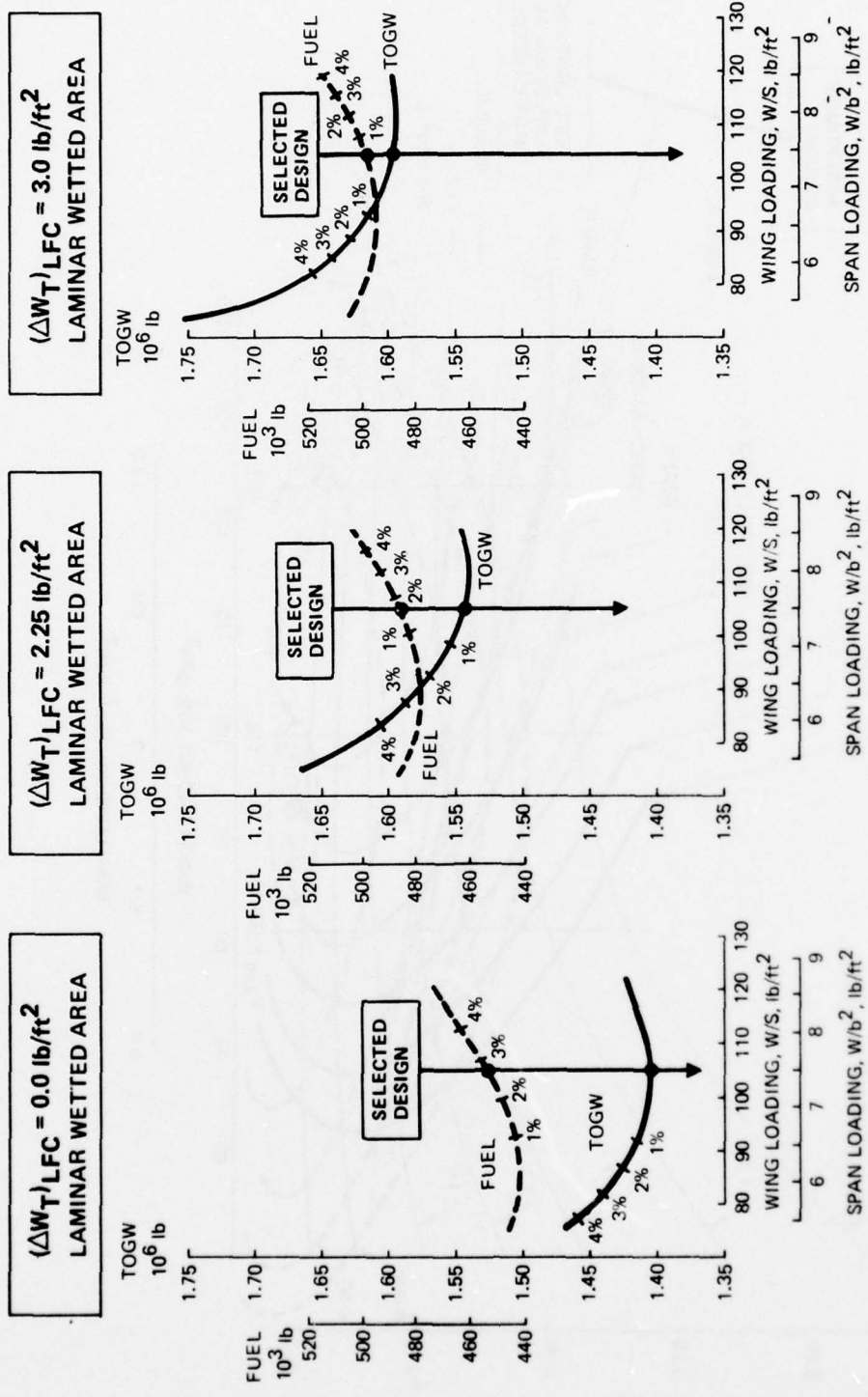


Figure 15 Engine/Airframe Matching for the Final Laminar Flow Control Airplane



RANGE = 10,000 nmi
 PAYLOAD = 350,000 lb
 MACH = 0.79
 MIL TOFL = 9,000 ft
 TURB CLIMB ALT = 35,000 ft

WING GEOMETRY
 AR = 14
 $\Lambda_c/4 = 10^\circ$
 t/c = 0.14/0.08

Figure 16 Final Laminar Flow Control Airplane Design Selection

4.3 LFC FUEL AND WEIGHT SAVINGS

Weight and performance characteristics of the reference turbulent airplane and the LFC configuration sized for different LFC system weight increments are summarized in Table 3.

The uncycled operating empty weight (OEW) buildup for the LFC configuration is shown in Figure 17. The wing and tails comprise a significant portion of the OEW. Therefore, the LFC structure and the systems weight increment per unit laminarized area, $(\Delta W_T)_{LFC}$, can significantly affect the OEW.

The final LFC configuration model 767-733 was sized with an LFC weight penalty of 2.25 lb/ft². The LFC systems, which include the suction pumps, suction engines, main collector ducts, and manifolds, and installation penalties to surrounding structure contribute about half of this weight increment. The other portion of the LFC weight increment is the impact on wing and empennage structural material weight.

Ongoing LFC systems development studies may result in integrated structural concepts, and systems load sharing/management techniques that may well reduce both the LFC structural and LFC system weight penalties.

An important objective of this study was to identify the sensitivity of the LFC benefits to the total LFC structural and system weight. Most of the performance and trade studies described in this section assumed an LFC total weight penalty of 2.25 lb/ft². LFC structural and system weight considerations are discussed further in Section 7.5.

The fuel saving, TOGW reduction, and OEW change of the LFC airplane sized with different $(\Delta W_T)_{LFC}$ relative to the reference airplane also are shown in Figure 17.

For a LFC weight increment of 2.25 lb/ft² of laminarized area, the impact of laminar flow on fuel and weight is:

- Fuel savings of 27 percent
- Reduction in TOGW of 7 percent
- Increase in OEW of 12.2 percent

Nearly all of the increase in OEW is due to the higher wing aspect ratio for the LFC configuration. This is shown in Section 4.7. Figure 17 also shows that a further reduction of the total LFC systems and structural weight penalty of 0.5 lb/ft² produces the following additional effects:

- Fuel savings of 1 percent
- Gross weight reduction of 2 percent
- OEW reduction of 4 percent

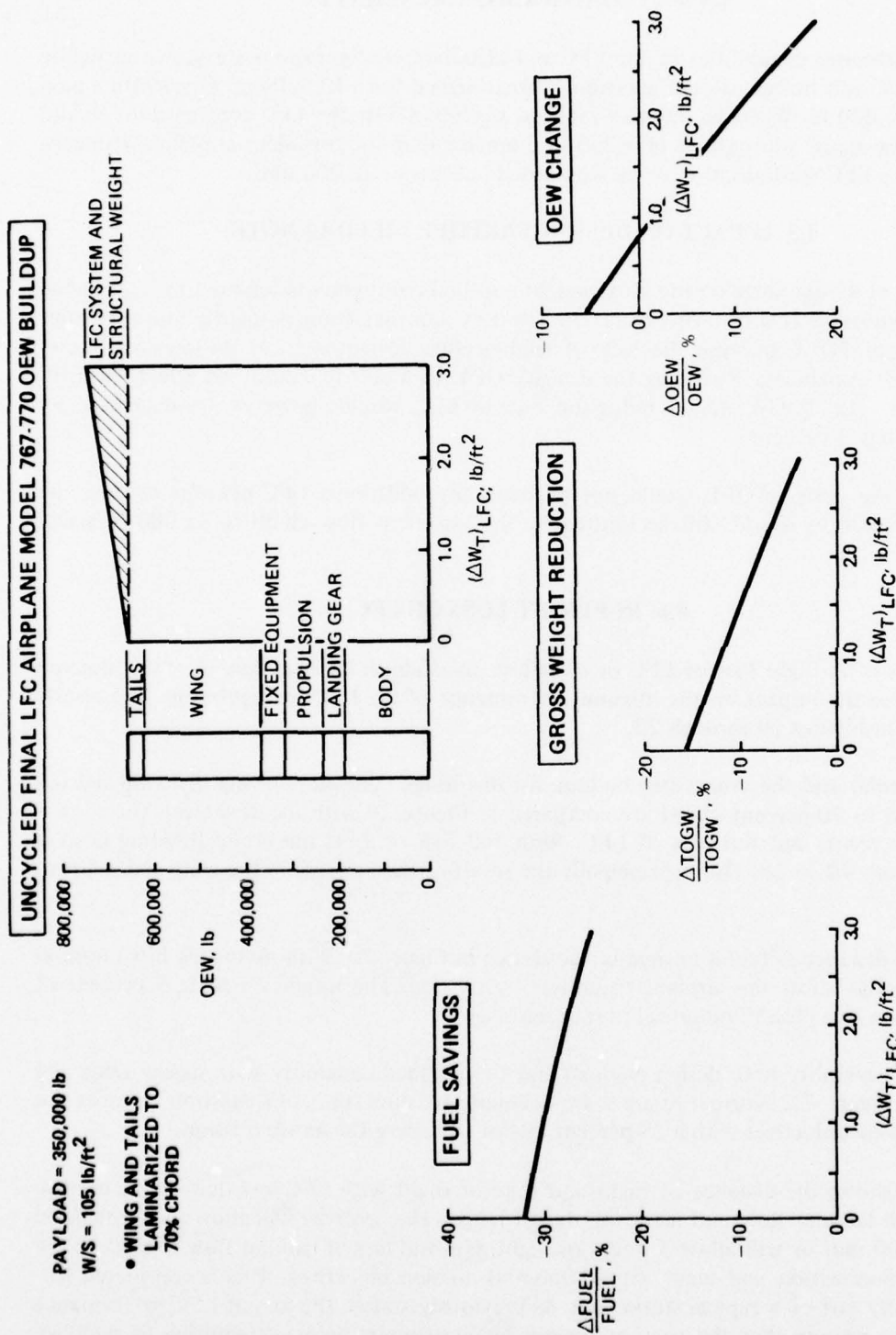
Table 3 Airplane Performance Characteristics Summary

ITEM		REFERENCE TURBULENT AIRPLANE MODEL 767-768	FINAL LFC CONFIGURATION		
			$(\Delta W_T)_{LFC}$ lb/ft ²		
			0.0	2.25	3.0
Design mission	Payload, lb Range, nmi	350,000 10,000			
Weights, lb	TOGW	1,665,800	1,408,980	1,551,560	1,607,650
	OEW	608,600	576,080	682,870	725,160
	Block fuel	668,600	455,960	489,640	502,650
	Reserves	43,300	30,870	33,250	34,160
Wing	Area, ft ²	14,785	13,420	14,780	15,310
	AR	12	14	14	14
	t/c Inboard/Outboard	0.14/0.08	0.14/0.08	0.14/0.08	0.14/0.08
	$\Lambda_{c/4}$, deg	20	10	10	10
	W/S, lb/ft ²	112.7	105	105	105
Engine	Engine type/no./BPR	STF 482/4/7.5			
	TSLS, lb	77,200	63,400	67,850	69,600
	T/W, lb/lb	0.185	0.180	0.175	0.173
Performance	Mach	0.78	0.79	0.79	0.79
	ICAC, ft	35,900	41,000	41,000	41,000
	h_{AVE} , CRU, ft	40,500	41,000	40,100	39,820
	L/D _{CRU}	27.9	(b) 38.9	(b) 40.1	(b) 40.5
	SFC _{CRU} , lb/hr/lb	(a) 0.603	(c) 0.643	(c) 0.642	(c) 0.641
	V_{APP} , keas	106.7	111.6	112.2	112.5
	TOFL (Mil), ft	9,000	8,650	8,950	9,050

(a) Includes 5% military mission fuel allowance

(b) Does not include suction drag

(c) Includes suction engine fuel flow plus 5 % military fuel allowance



NOTE: • REFERENCE TURBULENT AIRPLANE IS MODEL 767-768, (W/S = 112.7 lb/ft²)
• (ΔW_T) LFC = LFC STRUCTURAL AND SYSTEMS WEIGHT IN lb/ft² OF LAMINARIZED WETTED AREA

Figure 17 Laminar Flow Control Fuel and Weight Savings

4.4 PAYLOAD-RANGE CAPABILITY

The payload-range capabilities of the LFC and turbulent configurations are shown in Figure 18. The LFC and turbulent configurations were designed for a 10,000-nmi range with a payload of 350,000 lb. With the payload reduced to 200,000 lb, the LFC configuration would have a cruise range approximately 1,200 nmi greater than the turbulent airplane. With zero payload, the LFC configuration range would be in excess of 20,000 nmi.

4.5 IMPACT OF DESIGN TAKEOFF FIELD LENGTH

The effect of design range on the gross weight and fuel requirements for the LFC and turbulent configurations is shown in Figure 19. The LFC configuration is slightly more sensitive to the design TOFL because the lack of leading-edge devices reduces its low-speed aerodynamic lift capability. Reducing the design TOFL to 8,000 ft would not affect the LFC fuel saving. The TOGW weight reduction due to LFC would, however, be decreased by approximately 1 percent.

Increasing the design TOFL would not produce any additional LFC benefits because the LFC configuration would still be limited by the turbulent flow climb to 35,000-ft design constraint.

4.6 IN-FLIGHT LOSS OF LFC

The effects of in-flight loss of LFC or of failure to establish laminar flow were investigated to determine the impact on the mission performance of the LFC configuration. The results are shown in Figures 20 through 22.

The drag polar and the cruise drag buildup for the design condition having the wing and tail laminarized to 70-percent chord are compared in Figure 20 with the drag levels for 25 percent, 50 percent, and full loss of LFC. With full loss of LFC the cruise lift/drag ratio is reduced from 40 to 28. This is principally the result of the increase in the wing and tail profile drag.

The cruise distance as fuel is burned is also shown in Figure 20. With no loss of LFC, normal reserves would allow the airplane to cruise 11,000 nmi. The reserves include 5 percent of total mission fuel plus 30 minutes loiter at sea level.

The range capability with design payload and the payload capability with design range are shown in Figure 21. Normal reserves are adequate to allow the configuration to meet the design mission objectives with a 25-percent loss of LFC over the entire mission.

Figure 22 shows the distance of flight and time of flight with LFC loss that can be used to achieve full laminar flow and meet the design range. The reserves will allow the airplane to cruise 2,000 nmi or will allow 5 hours of flight with full loss of laminar flow to achieve the design laminarization and meet the 10,000-nmi mission objectives. This is considered sufficient to fly out of a typical storm area. As previously stated, the loss of LFC performance calculations assume that the suction engines remain running while attempting to establish laminar flow. Turning the suction engines off during complete loss of LFC would save fuel that could be used to further increase the allowable distance of flight or time of flight with loss of LFC.

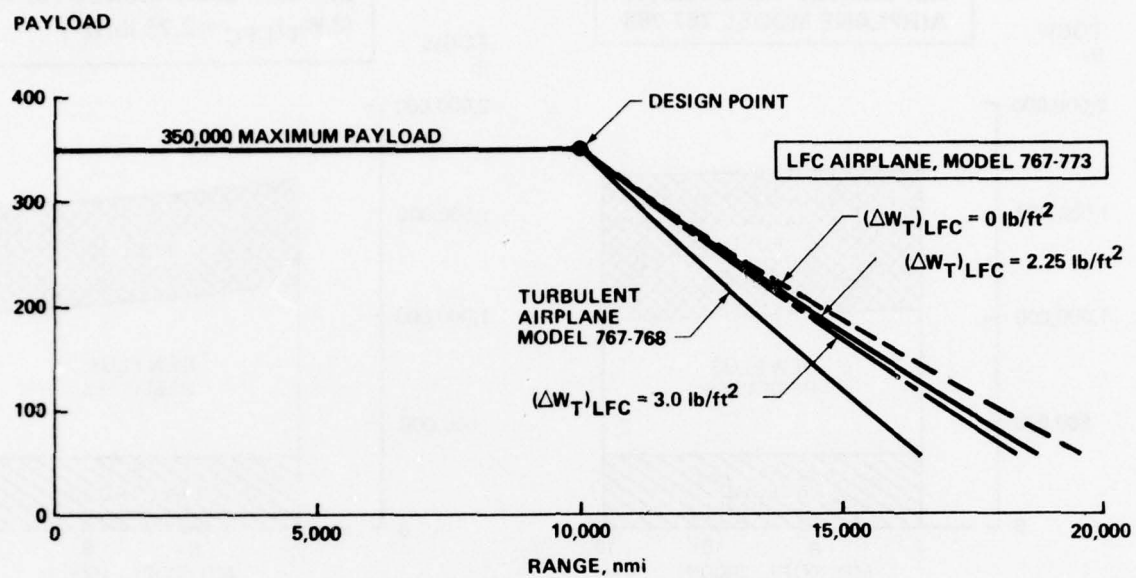


Figure 18 Payload-Range Capability

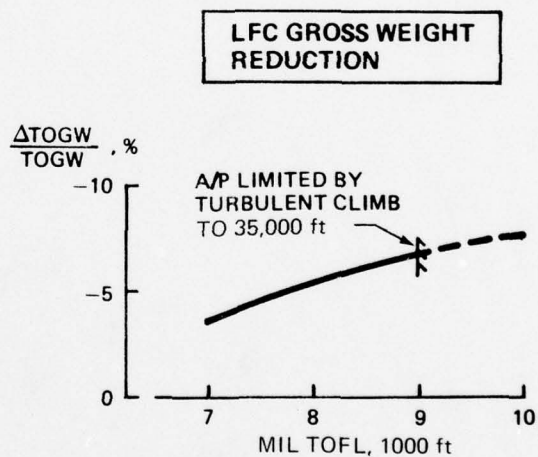
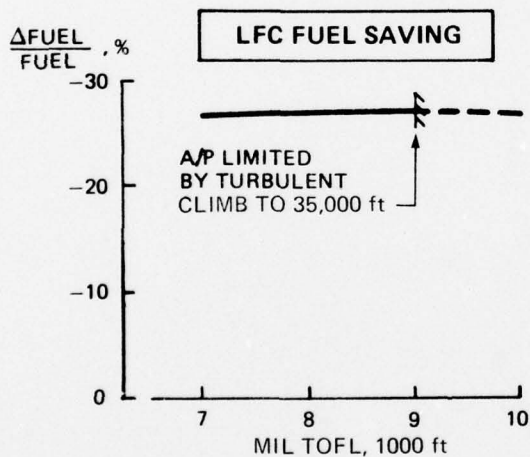
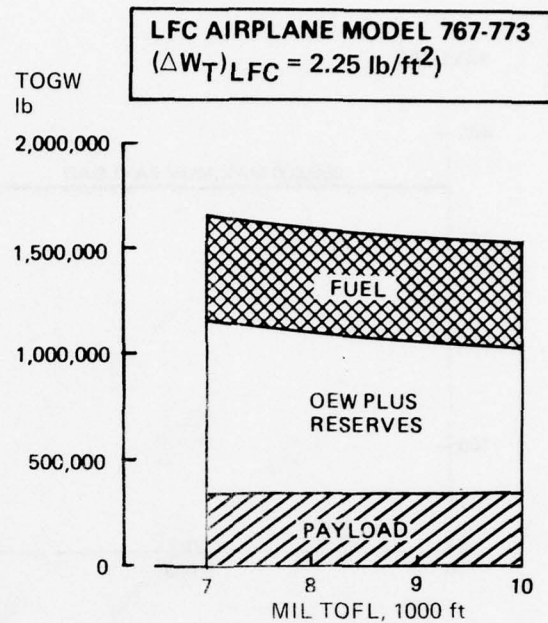
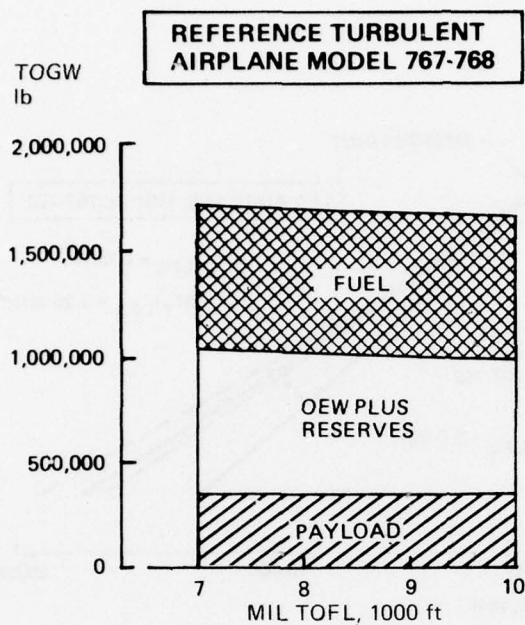


Figure 19 Effect of Design Takeoff Field Length on Fuel and Weight

- DESIGN RANGE = 10,000 nmi
- DESIGN PAYLOAD = 350,000 lb

MODEL 767-773 CRUISE DRAG
WITH LOSS OF LFC AT $C_L = 0.5$

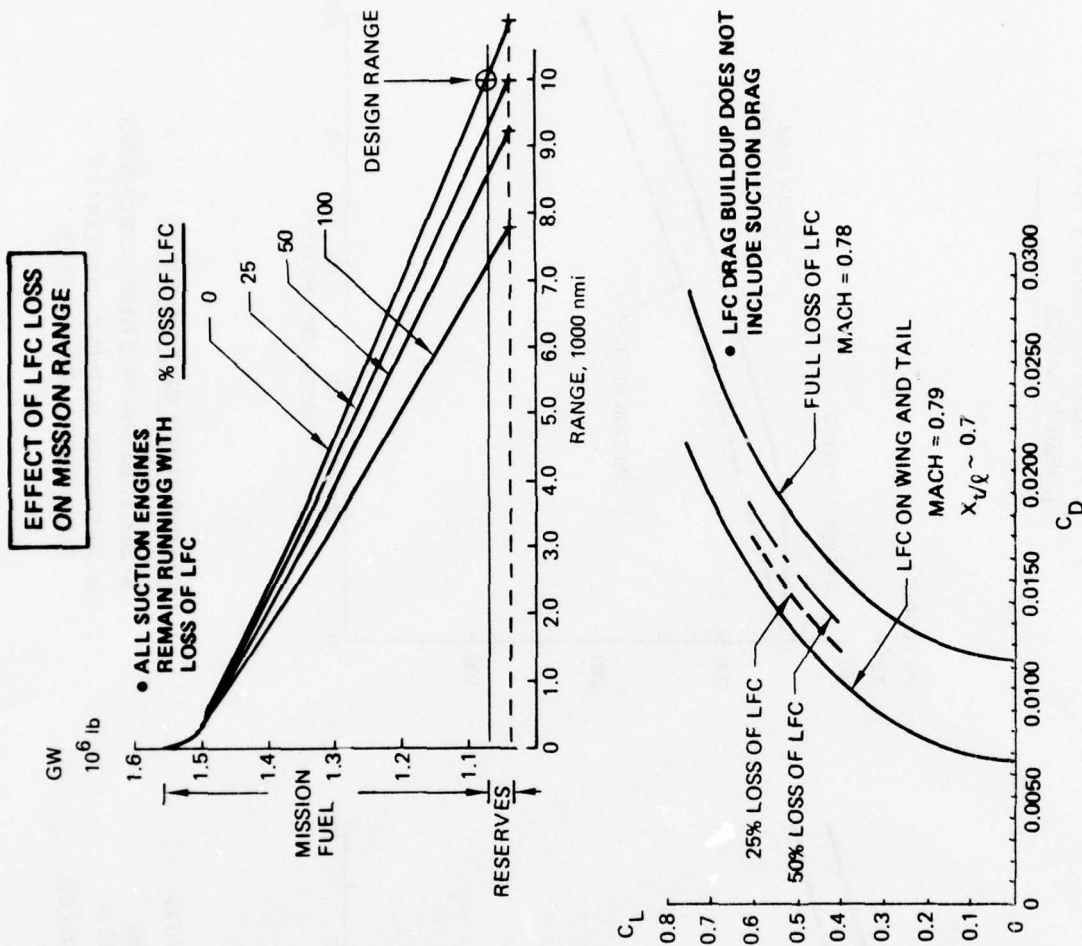
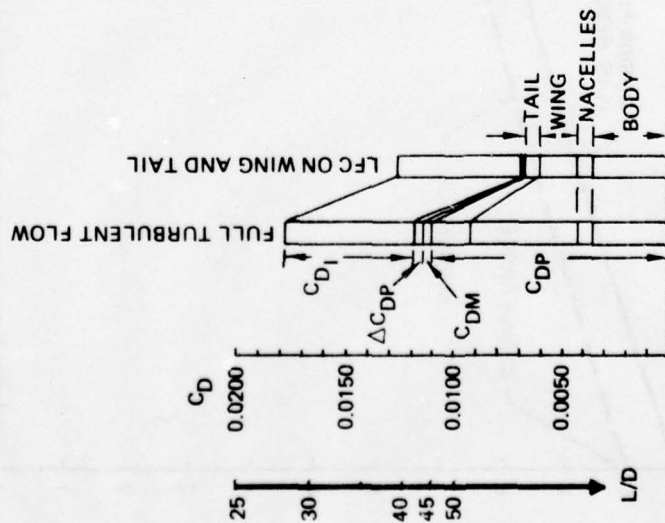
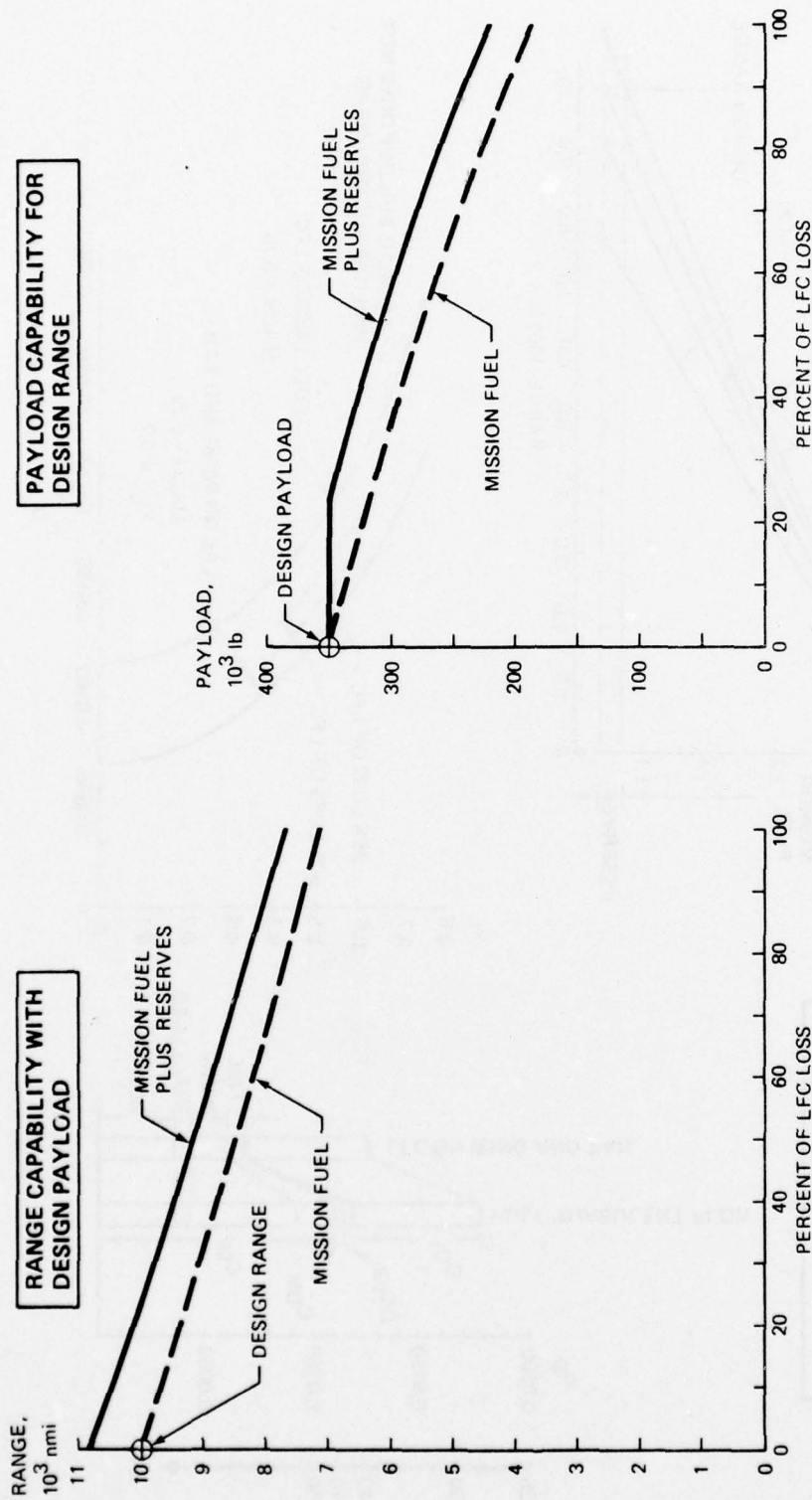


Figure 20 Effect of Loss of LFC on Mission Range

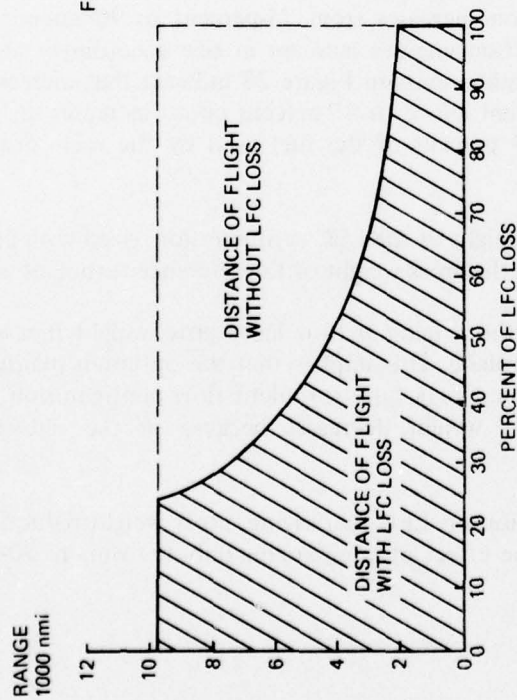


- LFC AIRPLANE MODEL 767-773
- DESIGN RANGE = 10,000 nmi
- DESIGN PAYLOAD = 350,000 lb
- WING AND TAILS LAMINARIZED TO 70% CHORD

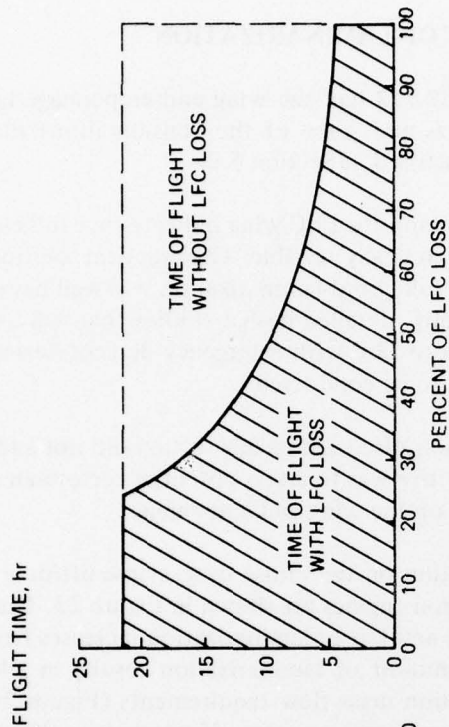
- LFC LOSS STUDY GROUND RULES**
- SUCTION ENGINES REMAIN RUNNING
 - RESERVES USED INCLUDE LOITER FUEL AND 5% MISSION FUEL

Figure 21 Performance Capability with Loss of Laminar Flow Control

**ALLOWABLE CRUISE DISTANCES
WITH LFC LOSS TO MEET DESIGN RANGE**



**ALLOWABLE CRUISE TIMES WITH
LFC LOSS TO MEET DESIGN RANGE**



- LFC AIRPLANE MODEL 767-733
- DESIGN RANGE = 10,000 nmi
- DESIGN PAYLOAD = 350,000 lb
- WING AND TAILS LAMINARIZED TO 70% CHORD

- LFC LOSS STUDY GROUND RULES**
- SUCTION ENGINES REMAIN RUNNING
 - RESERVES USED INCLUDE LOITER FUEL AND 5% MISSION FUEL

Figure 22 Allowable Cruise Time and Distance with Loss of Laminar Flow Control

These results indicate that normal reserves are adequate to meet the mission objectives with reasonable losses in LFC.

4.7 EXTENT OF LAMINARIZATION

The basic LFC configuration model 767-773 had the wing and empennage laminarized to 70-percent chord. The laminarized areas and some of the considerations that led to the selection of the laminarized areas are discussed in Section 5.2.

The results of a recent study⁽⁵⁾ of a composite LFC wing indicate that full chord laminarization of a wing with TE controls is technically feasible. The practical solution of the challenging design problems associated with full chord laminarization was well beyond the scope of the study reported herein. Additionally, detailed design studies that will be necessary to understand the compatibility of full chord LFC with emergency descent devices (e.g., spoilers) and moving active controls have yet to be conducted.

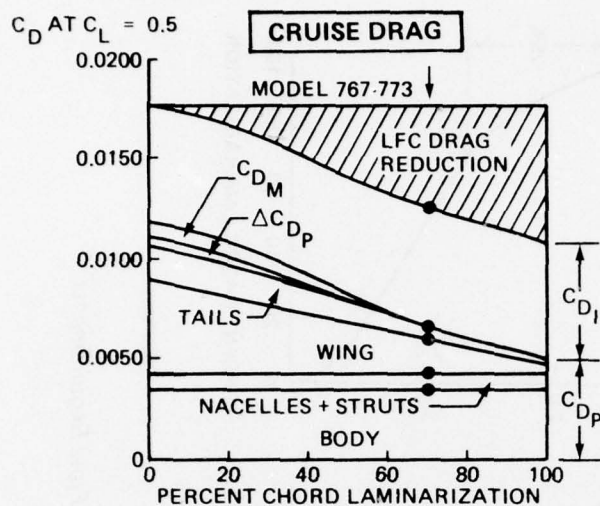
The extent of laminarization investigation discussed in this section did not address the solution of these design problems. The objective was to assess potential performance benefits by increasing the amount of laminarization on the wing and empennage.

The effects of the extent of laminarization on the cruise drag, cruise lift/drag ratio, and on the fuel flow requirements for the suction engines are shown in Figure 23. The cruise lift to drag ratio increases from 40 to 46 as the amount of laminarization increases from 70-percent to 95-percent chord. Increasing the amount of laminarization results in additional LFC structural and systems weight. The suction mass flow requirements (Figure 24) more than double as the amount of laminarization increases from 75-percent to 90-percent chord. Consequently, the compressor and suction engines increase in size accordingly and burn more fuel. The suction engine fuel requirements in Figure 23 indicate that increasing the amount of laminarization from 70-percent chord to 95-percent chord increases the suction engine fuel from 5 percent to over 13 percent of the fuel used by the main propulsion engines.

Figure 25 is a comparison of the gross weight of the LFC configuration, sized with different chordwise extents of laminar flow, and the gross weight of the reference turbulent airplane.

The LFC configuration arrangement without laminar flow has a gross weight that is higher than that of the reference turbulent airplane. This implies that the optimum planform for the LFC configuration is not an optimum for a fully turbulent flow configuration. As the configuration is laminarized, the gross weight decreases because of the reduced fuel requirements.

The effect of the extent of laminarization on LFC fuel saving, gross weight reduction, and OEW change is shown in Figure 25. The effect of laminarizing only the wing to 70-percent chord also is shown.



- MACH = 0.79
- ALTITUDE = 40,000 ft
- AR = 14
- $\Lambda_{c/4} = 10^\circ$
- $t/c = 0.14/0.08$
- DRAGS DO NOT INCLUDE SUCTION DRAG
- WING AND TAILS ARE LAMINARIZED

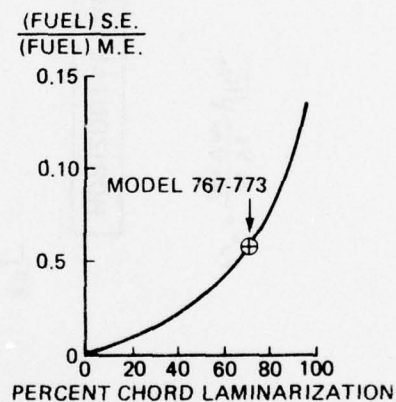
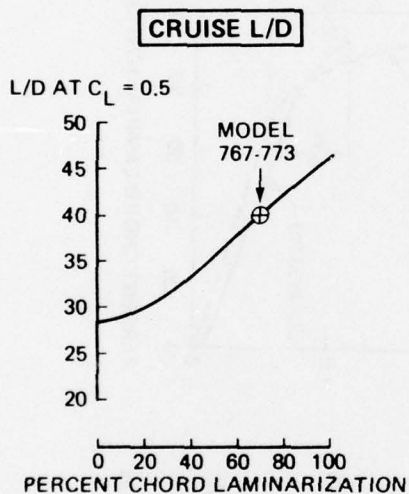


Figure 23 Effect of Extent of Laminarization on Cruise Drag and Suction Engine Fuel

$$Fo^* = \frac{\rho_s V_s}{\rho_\infty V_\infty} \sqrt{Re_c}$$

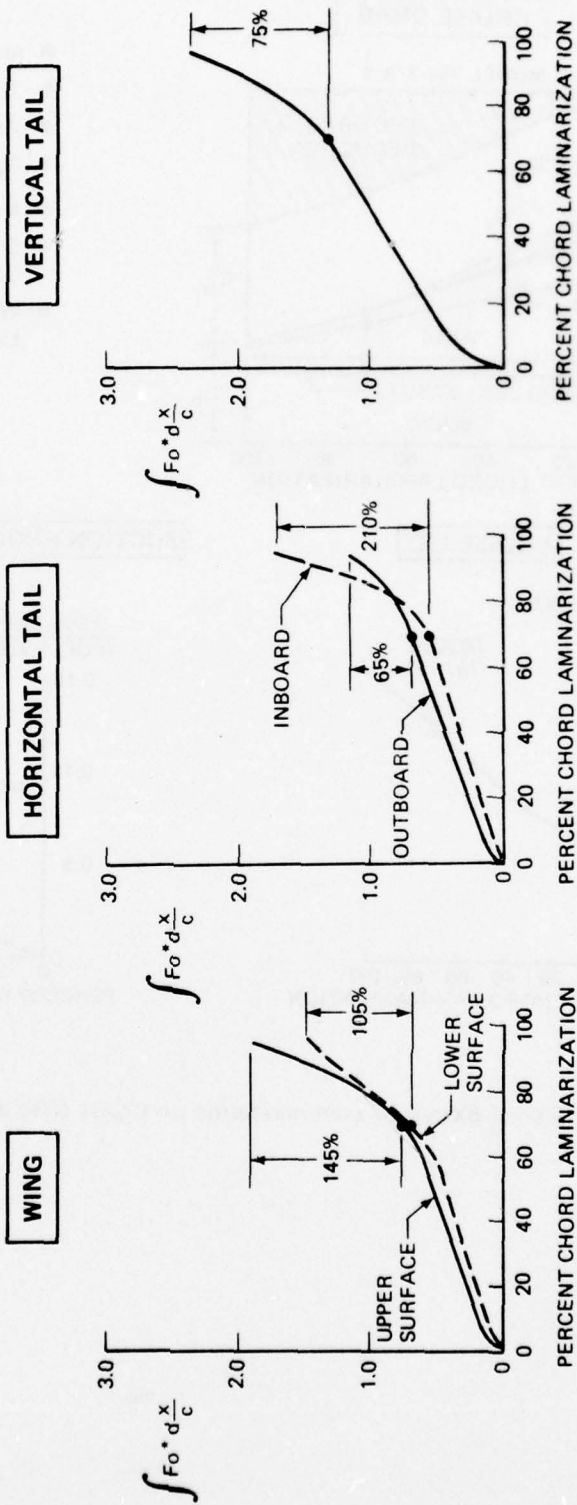


Figure 24 Effect of Extent of Laminarization on Suction Mass Flow Requirements

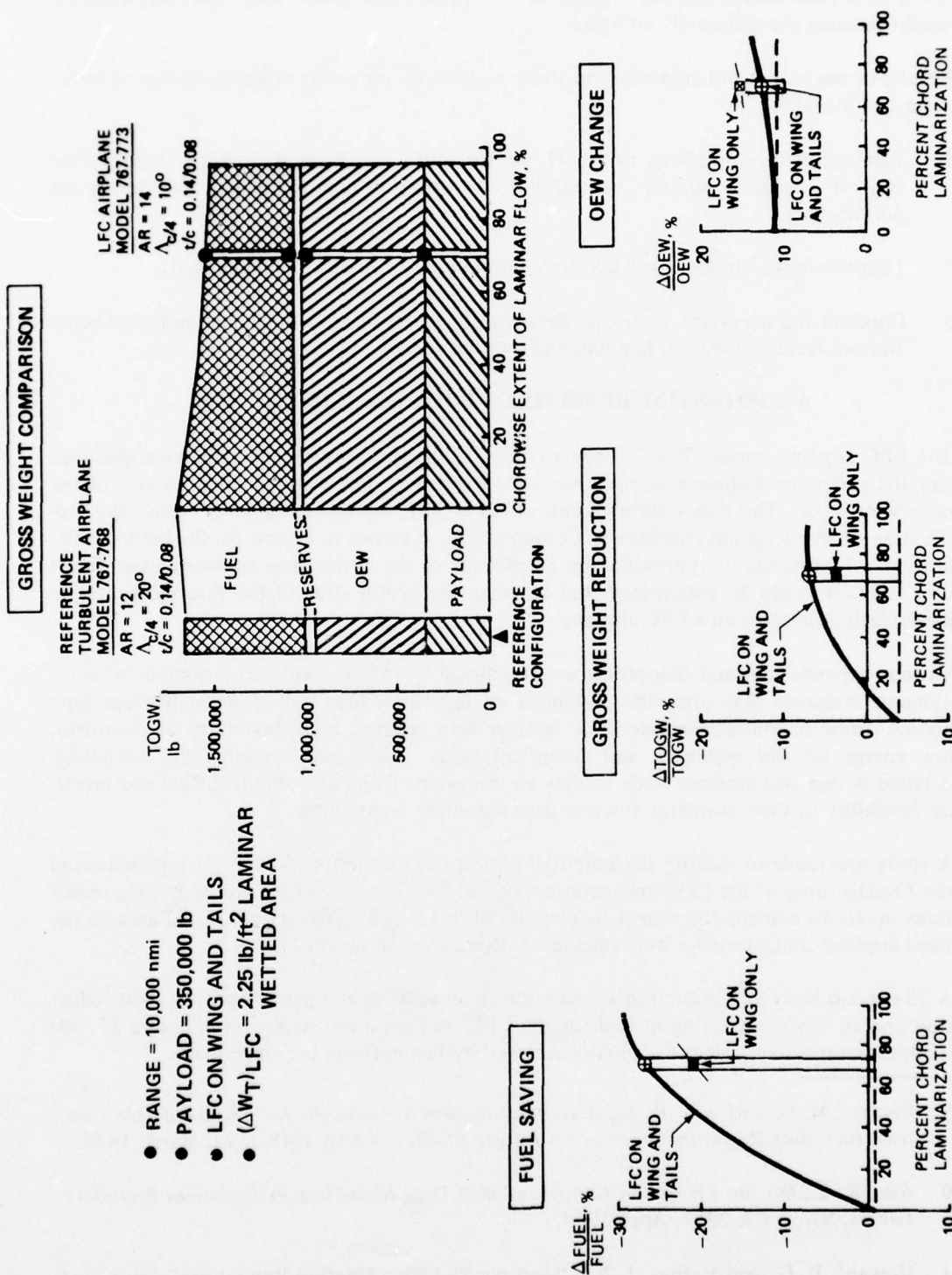


Figure 25 Effect of Extent of Laminarization on Fuel and Weight

The increase in OEW is primarily due to the wing planform change. Increasing the percent chord of laminarization beyond 70-percent chord continues to save fuel. However, the gross weight remains approximately constant.

Results of the extent of laminarization study suggest the following order for achieving maximum LFC benefits:

1. Laminarize the wing back to the TE control surfaces. The nested chord length of the control surfaces should be minimized without compromising the low-speed performance.
2. Laminarize the empennage back to minimum chord TE controls on the tails.
3. Conduct the necessary trade and detailed design studies to identify the practical benefits and technical risks of laminarizing over TE surface.

4.8 POTENTIAL BENEFITS OF BODY DRAG REDUCTION

The LFC airplane, model 767-773 has a cruise lift/drag ratio of 40. The LFC configuration and the reference turbulent configuration have relatively low induced drag because of the large wing spans. The major aerodynamic effect of LFC was to dramatically reduce the profile drag of the wing and empennage. Consequently, as shown in Figure 26, the body profile drag, which amounts to approximately 30 percent of the cruise drag, becomes a significant drag item. It might be anticipated that reducing the profile drag of the fuselage would be particularly attractive on a LFC airplane.

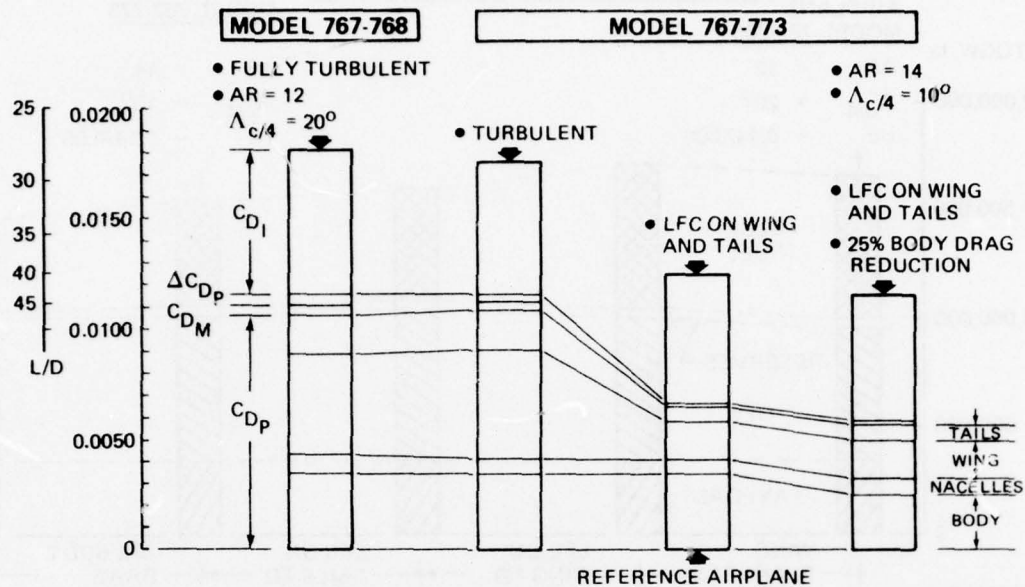
Various experimental and theoretical investigations⁽⁹⁻¹²⁾ have explored a number of aerodynamic concepts that offer the possibility of significant drag reduction on fuselage type bodies. These techniques include body laminar flow control, body boundary layer control, low energy air slot injection, and compliant skins. Additional experimental, analytical, detailed design and systems trade studies are necessary to identify the technical and practical feasibility of these potential fuselage drag reduction techniques.

A study was made to identify the potential performance benefits of achieving a reduction in the fuselage drag of the LFC configuration, model 767-773. The effects of body drag reductions up to 40 percent for weight increments of 0, 1.5 and 3.0 lb/ft² of treated area on the sized airplane characteristics were calculated. Results are shown in Figure 26.

A 25-percent body drag reduction would result in an additional 4-percent gross weight reduction and an 8-percent saving in fuel for the LFC configuration. As shown in Figure 27, this is approximately equivalent to benefits achieved by laminarizing the empennage.

9. Fischer, M. G. and Ash, R. L., *A General Review of Concepts for Reducing Skin Friction, Including Recommendations for Future Studies*, NASA TMS-2894, March 1974.
10. Ash, R. L., *On the Theory of Compliant Wall Drag Reduction in Turbulent Boundary Layers*, NASA CR-2387, April 1974.
11. Howard, F. G. and Hefner, J. N., "Multiple Slot Skin Friction Reduction," *Journal of Aircraft*, Vol. 12, No. 9, Sept. 1975, pp753-754.
12. Pfenninger, W., *Studies of Laminarized Underwater Suction Bodies*, Boeing Document D6-40283, March 1972.

CRUISE DRAG COMPARISON AT $C_L = 0.5$



BODY DRAG REDUCTION POTENTIAL FUEL AND WEIGHT SAVING

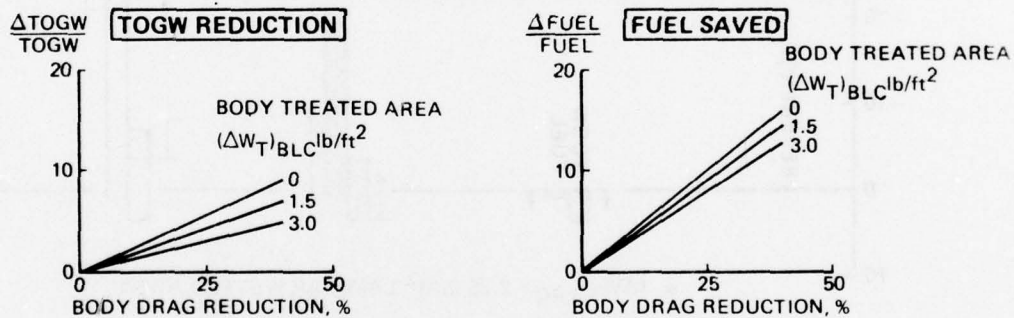


Figure 26 Body Drag Reduction Study

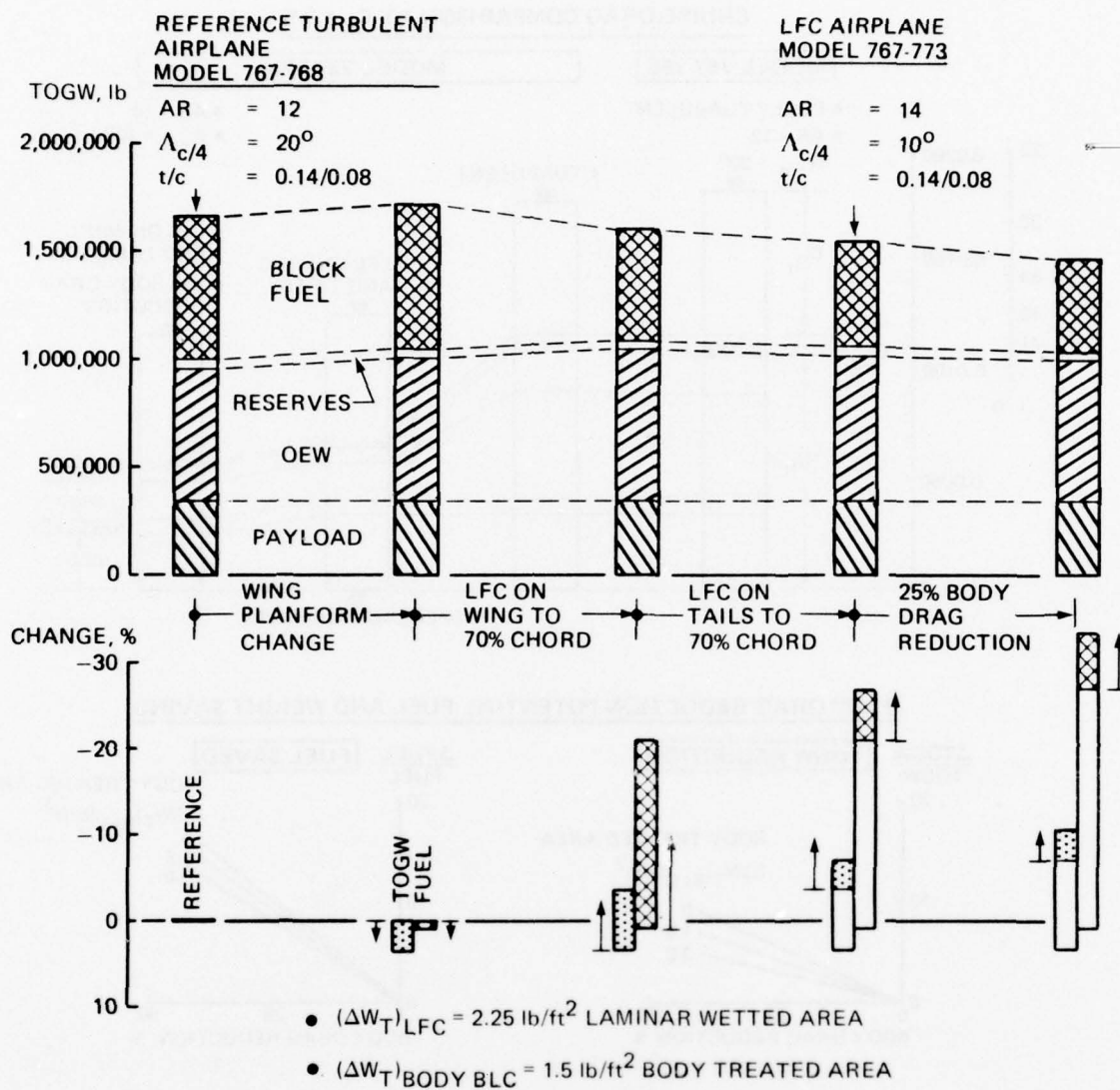


Figure 27 Potential Benefits of Body Drag Reduction

4.9 LIFE-CYCLE AND OPERATING COST COMPARISONS

Economic analyses were made to compare the 20-year life-cycle costs and surge condition operating costs of the LFC and turbulent configurations. Additional analyses were made to identify the sensitivity of the relative costs of the LFC configuration to the following:

- Fuel price
- Total LFC structural and systems weight penalty
- LFC technology complexity costs
- LFC maintenance costs

Ground rules for life-cycle cost calculations are summarized in Figure 20. The low utilization rate of 1080 flying hours per airplane used for the life-cycle cost calculations is about one-third to one-quarter that of the annual usage of commercial transports.

Results of the life-cycle calculations are shown in Figure 28. Fuel costs of the turbulent configuration make up a relatively small portion of the total life-cycle costs because of the low utilization rate. Production costs are the major cost items. Although LFC reduced the fuel costs significantly, the estimated production costs increased such that the relative life-cycle costs of the LFC configuration exceed those of the reference turbulent airplane.

Operating costs were determined for a surge condition with a higher utilization rate of 10 flying hours per day per airplane for a 60-day period. Ground rules and results are shown in Figure 29. Fuel costs comprise a major portion of the operating costs. Consequently, operating costs of the LFC are less than those of the turbulent airplane.

The life-cycle and operating costs of the LFC configuration are shown in Figure 30 as percent changes relative to the corresponding costs of the turbulent airplane at the same fuel price. The fuel price and the LFC systems and structural weight penalty have a significant effect on the relative life-cycle and operating costs of the LFC airplane.

For an LFC weight penalty of 2.25 lb/ft^2 , and with a fuel price of 40¢/gal , the life-cycle costs of the LFC configuration are 16.5 percent greater than the life-cycle costs of the turbulent airplane. The LFC airplane surge condition operating costs are, however, 9 percent less than those of the turbulent airplane.

At 80¢/gal the relative life-cycle costs and operating costs of the LFC airplane are, respectively, 13 percent more and 14 percent less than for the turbulent airplane.

These results also show that a reduction in the LFC systems and structural weight penalty of 0.5 lb/ft^2 will result in:

- Reduction in the LFC life-cycle costs of 2.5 percent
- Reduction in the LFC surge condition operating costs of 1 percent

GROUND RULES

- 1976 DOLLARS
- 20-YEAR OPERATIONS AND SUPPORT
- 112 UNIT-EQUIPPED AIRPLANES
- 12 COMMAND SUPPORT AIRPLANES
- 5 TEST VEHICLES, 4 REFURBISHED
- 1080 FLYING HOURS PER UNIT-EQUIPPED AIRPLANE PER YEAR—PEACE TIME
- 7 SQUADRONS
- +3.5% MAINTENANCE INCREASE FOR LFC
- 1500 FLIGHT TEST HOURS
- 24 MONTHS PRODUCT DEVELOPMENT PRECEDING GO-AHEAD
- 53 MONTHS FROM GO-AHEAD TO CERTIFICATION
- C-141 USED AS BASE FOR OPERATIONS AND SUPPORT COSTS
- BOEING COST MODELS FOR AIRPLANE, ENGINES, AVIONICS
- CACE COST MODEL AFR 173-10 FOR OPERATIONS AND SUPPORT COSTS

LIFE CYCLE COST ELEMENTS

- FUEL PRICE = 40¢/gal

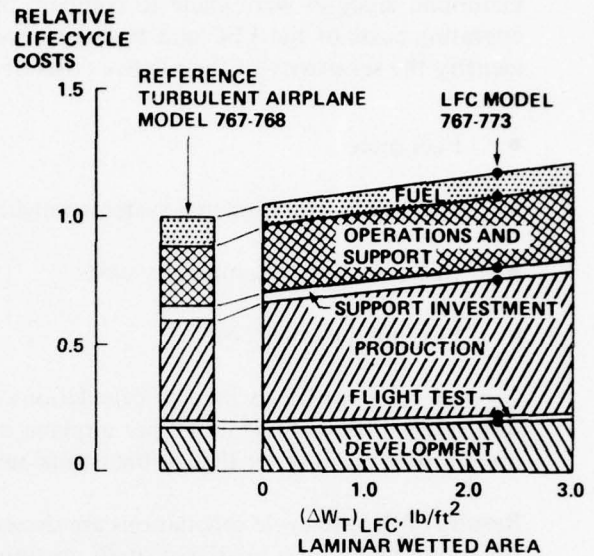


Figure 28 Twenty-Year Life-Cycle Cost Elements

OPERATING COST ELEMENTS

- FUEL PRICE = 40¢/gal.

GROUND RULES

- 1976 DOLLARS
- 60-DAY SURGE
- 112 UNIT-EQUIPPED AIRPLANES
- 10 FLYING HOURS PER UNIT-EQUIPPED AIRPLANES PER DAY
- 7 SQUADRONS
- 3.5% MAINTENANCE INCREASE FOR LFC
- C-141 USED AS BASE FOR OPERATIONS AND SUPPORT COSTS
- CACE COST MODEL AFR 173-10 FOR OPERATIONS AND SUPPORT COSTS

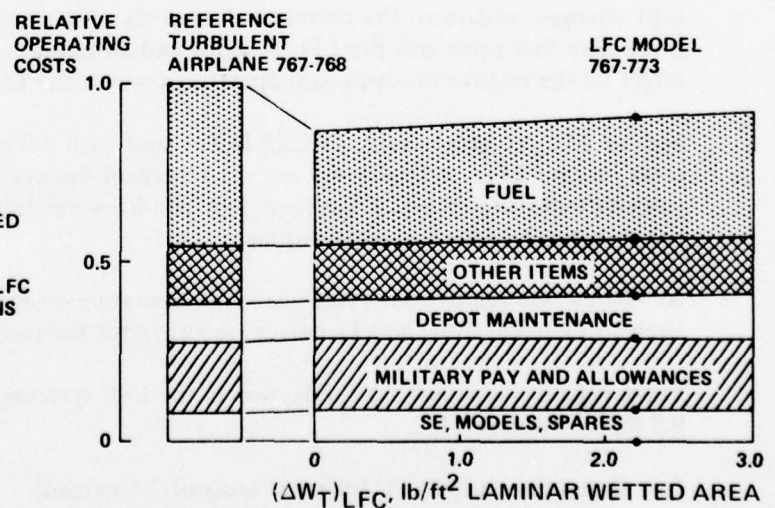
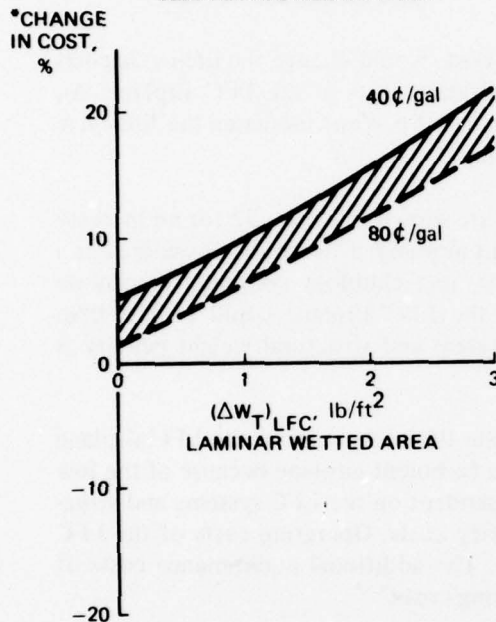


Figure 29 Sixty-Day Surge Condition Cost Elements

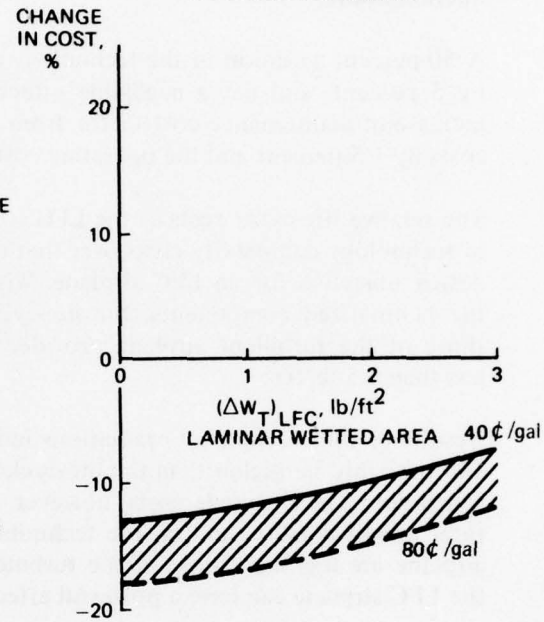
- 16 AIRPLANES PER SQUADRON
- 7 SQUADRONS

LIFE-CYCLE COSTS
20-YEAR PEACETIME OPERATION
 1080 FLYING HOURS/YEAR



- DESIGN RANGE = 10,000 nmi
- DESIGN PAYLOAD = 350,000 lb

OPERATING COSTS
ONE 60-DAY SURGE OPERATION
 10 FLYING HOURS/DAY



COST INCREASE
 ↑
 —
 ↓
 COST SAVING

*COST RELATIVE TO FULLY TURBULENT AIRPLANE
 AT SAME FUEL PRICE

Figure 30 Laminar Flow Control Cost Comparisons

The aforementioned economic assessments of the LFC configuration assumed a 3.5-percent increase in maintenance costs over a conventional turbulent airplane. The effect of variations in the maintenance costs on the economics of the LFC configuration is shown in Figure 31. This figure also shows the impact of LFC technology complexity cost variations relative to the current study estimates. The LFC technology complexity costs reflect the estimated impact of LFC on engineering hours, development hours, tooling hours, and production hours.

A 50-percent variation in the technology complexity costs would change the life-cycle costs by 5 percent, and has a negligible effect on the operating costs of the LFC airplane. An increase in maintenance cost factor from 3.5 percent to 10 percent increases the life-cycle costs by 1.5 percent and the operating costs by 4 percent.

The relative life-cycle costs of the LFC configuration are shown in Figure 32 for no increase in technology complexity costs over that of a turbulent airplane. This can be considered as a design objective for an LFC airplane. With no increase in technology complexity costs on the laminarized components, the life-cycle costs of the LFC airplane could be less than those of the turbulent airplane provided the LFC system and structural weight penalty is less than 1.5 lb/ft².

Results of these economic evaluations indicate that the life-cycle costs of the LFC airplane will probably be higher than the life-cycle costs of the turbulent airplane because of the low utilization. The life-cycle costs, however, are very dependent on the LFC systems and structural weight penalty, and on the technology complexity costs. Operating costs of the LFC airplane are less than those of the turbulent airplane. The additional maintenance costs of the LFC airplane can have a powerful effect on operating costs.

4.10 TOTAL LFC FUEL SAVINGS

Fuel savings that would be achieved through the use of laminar flow control are shown in Figure 33. The 20-year peacetime low-utilization rate would result in a fuel saving of over 2 billion gallons of fuel. Additionally, for every 60-day surge condition, the LFC configuration would save nearly 60 million gallons of fuel, which is equivalent to the total fuel burned by 104,000 cars operating for 1 year.

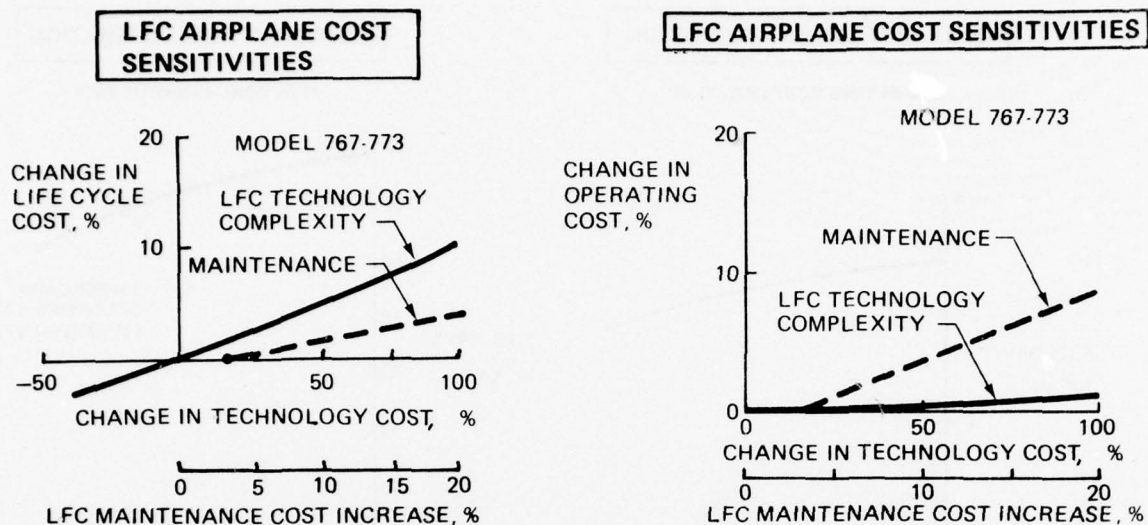


Figure 31 Life-Cycle and Operating Cost Sensitivities for LFC Configuration, Model 767-773

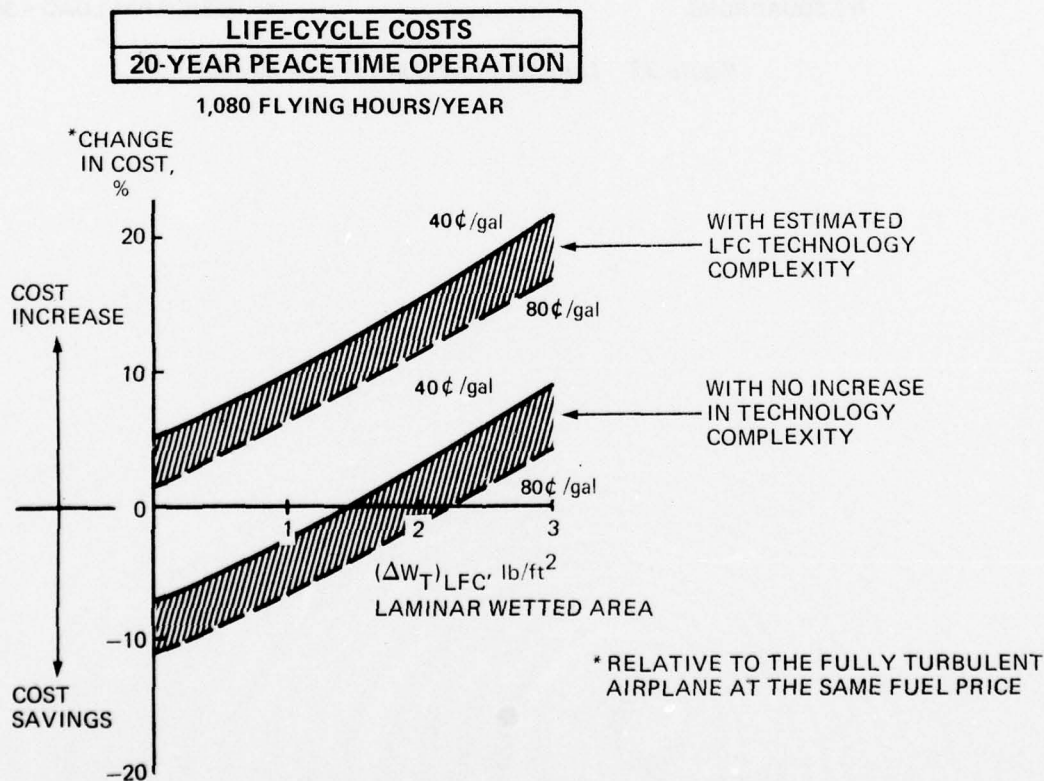


Figure 32 Effect of Technology Complexity on Relative Laminar Flow Control Life-Cycle Costs

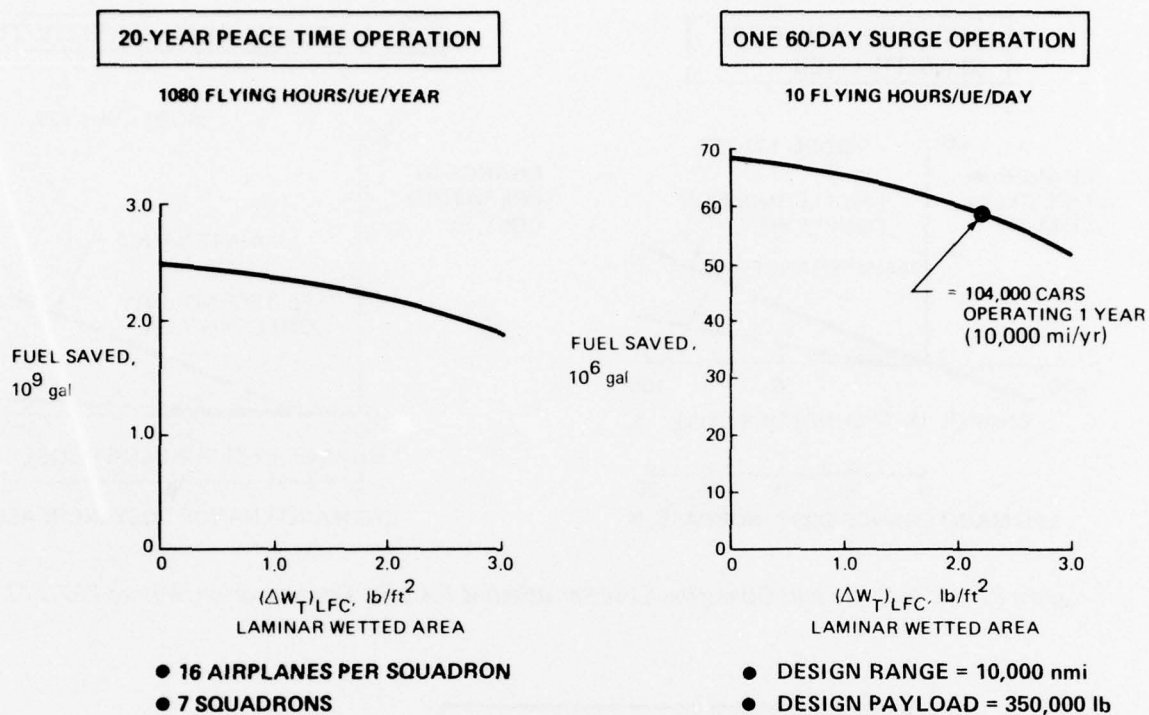


Figure 33 Laminar Flow Control Fuel Savings

5.0 LFC DESIGN CONSIDERATIONS

Some considerations that led to the design and assessment of the study LFC configurations are discussed in this section.

5.1 FACTORS AFFECTING LAMINARIZATION

Figure 34 illustrates some design and operational factors that can affect the achievement or maintenance of laminar flow. The Northrop X-21 flight test program demonstrated the technical feasibility of laminar flow control and established the suitability of existing LFC design criteria to address these factors.

To identify the practical and economic feasibility of LFC in either a military or commercial aircraft operational environment, additional LFC wind tunnel, flight test, analytical and system studies are required. An important objective of these investigations would be to develop such areas as design guidelines, system and structural concepts, and manufacturing techniques that will permit development of an LFC airplane with minimum weight penalties, development and production costs, and maintenance requirements.

Current NASA-sponsored LFC development studies are directed at providing this necessary information for smaller commercial transport aircraft.

5.2 LAMINARIZED FLOW AREAS

The study final LFC configuration Model 767-773 has wing and tail surfaces laminarized to 70-percent chord, which corresponds to the start of the trailing-edge control surfaces. Laminarized areas are shown in Figure 35. Some design considerations for selecting this extent of laminarization instead of full chord laminarization also are summarized in this figure.

Laminarization to 70-percent chord on the study configurations was selected primarily because of reduced design complexity and lower technical risk. The potential performance benefits from increasing the extent of laminarization were explored. (Results were discussed in Section 4.7.)

5.3 SUCTION SURFACES

To achieve laminar flow control, a surface and an internal ducting system must be designed and developed with internal aerodynamics and controls that permit a desired inflow through the suction surface over a specified range of operating conditions. A continuously porous surface might be ideal. However, both theory and experiment have shown that a laminar boundary layer can be kept stable by applying suction at suitable discrete intervals.

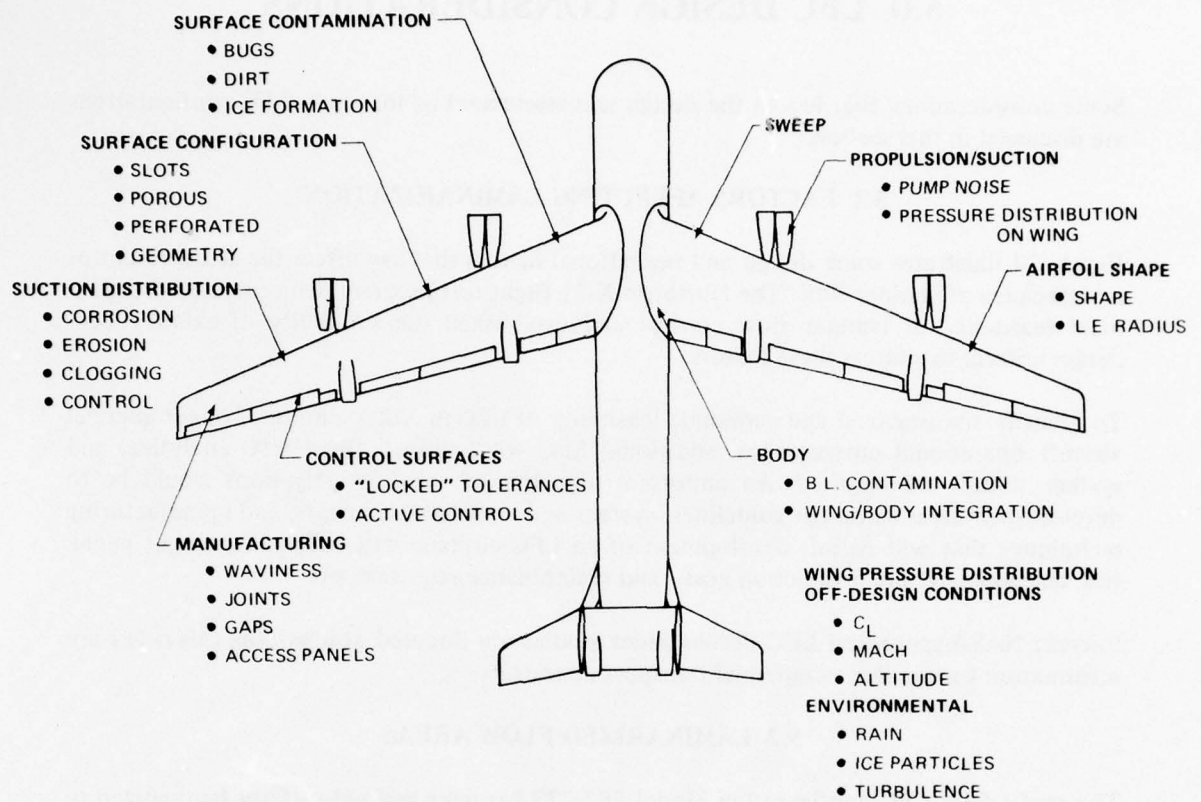


Figure 34 Factors Affecting Laminar Flow

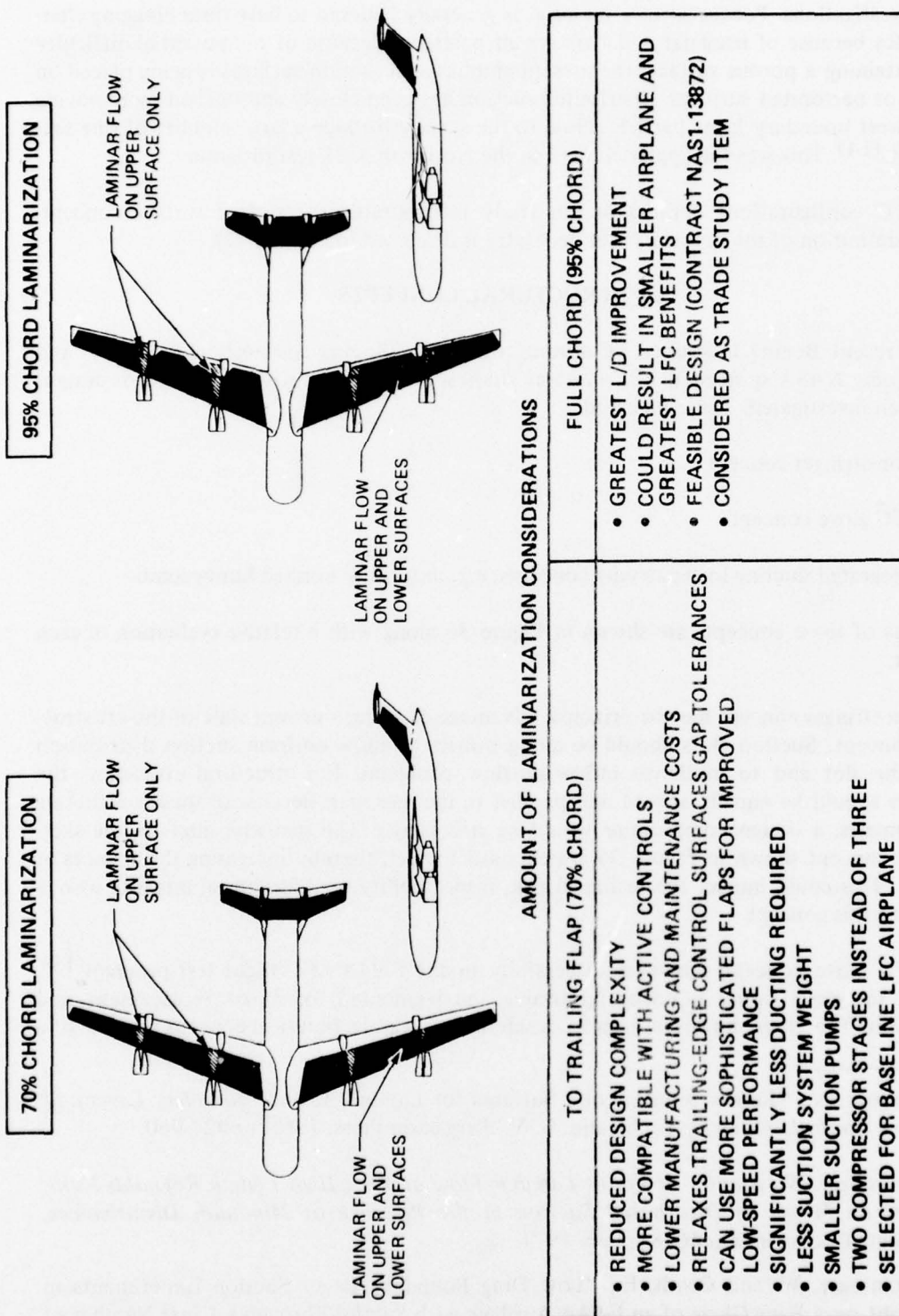


Figure 35 Laminarized Flow Areas

Porous, perforated, and slotted surfaces have been considered in past⁽¹³⁾ and recent^(3,4,5) LFC investigations. Porous-surface material is generally believed to have poor clogging characteristics because of irregular and twisting air passages. Because of the potential difficulty of maintaining a porous surface, the present emphasis on suction surfaces is being placed on slotted or perforated surfaces. Distributed suction has been closely approached by removing the slowest boundary layer particles close to the surface through a large number of fine suction slots⁽¹⁴⁾. This was the approach used in the Northrop X-21 test program.

The LFC configurations defined in this study incorporated the slotted surface concept. Design definition of the necessary slot geometry is discussed in Section 7.4.

5.4 STRUCTURAL CONCEPTS

During recent Boeing in-house LFC studies, the NASA/Boeing composite LFC study, and the ongoing NASA sponsored LFC systems studies, a number of structural concept designs have been investigated. These included:

- Skin-stringer concept
- LFC glove concept
- Integrated ducting load-carrying concepts; e.g., integrally bonded honeycomb

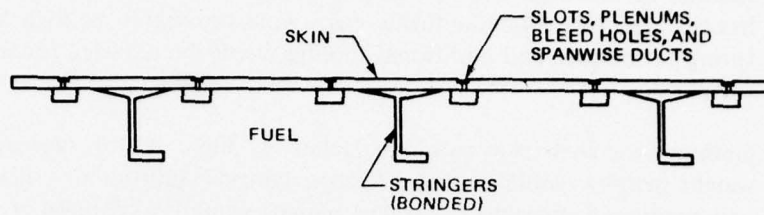
Sketches of these concepts are shown in Figure 36 along with a relative evaluation of each concept.

The skin-stringer concept has the principal advantage of being a proven state-of-the-art structural concept. Suction slots should be along isobars to allow uniform suction distribution along the slot and to minimize inflow/outflow problems. For structural efficiency, the stringers should be equally spaced and parallel to the rear spar. Because of these conflicting requirements, a design compromise would be necessary. The spanwise ducts in the skin-stringer concept shown in Figure 36 are exposed to fuel, thereby increasing the chances of leakage. This could impact the technical risk, inspectability, and structural integrity associated with this concept.

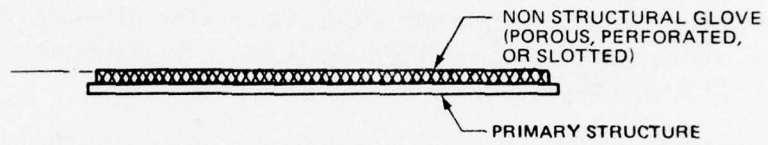
The LFC glove concept was used successfully in the F-94A LFC flight test program⁽¹⁵⁾. Ideally, the glove would be made removable and segmented for repair, replacement, and inspection. The glove, however, is not considered as a viable, practical concept because of a

-
13. Gregory, N., "Research on Suction Surfaces for Laminar Flow," *Boundary Layer and Flow Control*, edited by Lachmann, G. V., Pergamon Press, 1961, pp924-960.
 14. Pfenninger, W., *Studies to Verify Laminar Flow at Very High Length Reynolds Numbers by Means of Distributed Suction in the Presence of Minimum Disturbances*, Boeing Document D6-40281, Feb. 1971.
 15. Pfenninger, W. and Groth, E., "Low Drag Boundary Layer Suction Experiments in Flight on a Wing Glove of an F-94A Airplane with Suction through a Layer Number of Fine Slots," *Boundary Layer and Flow Control*, edited by Lachmann, G. V., Pergamon Press, 1961, pp961-999.

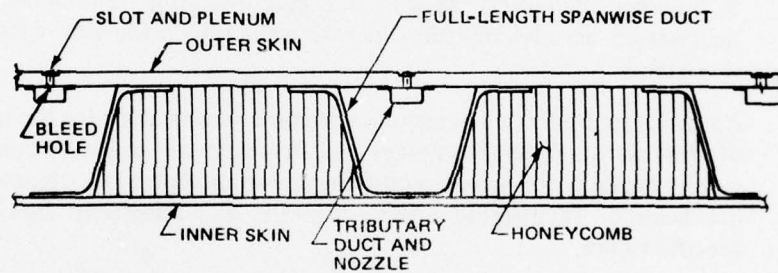
1. SKIN STRINGER



2. GLOVE CONCEPT



3. INTEGRAL BONDED HONEYCOMB CONCEPT



TECHNICAL AND OPERATIONAL CONSIDERATIONS	SKIN STRINGER	GLOVE CONCEPT	INTEGRAL BONDED HONEYCOMB CONCEPT
• WEIGHT	●	○	●
• PRODUCTION COST	●	○	●
• MAINTENANCE	●	○	●
• STRUCTURAL INTEGRITY	●	○	●
• INSPECTION	●	○	●
• CERTIFICATION	●	○	●
• TECHNICAL RISK	●	○	●
• EASE OF LAMINARIZATION	●	○	●

RELATIVE RATING	
●	BEST
●	GOOD
○	POOR

Figure 36 Laminar Flow Control Structural Concept Considerations

number of technical and operational concerns. The glove weight is parasitic and results in a heavier structure. Manufacturing costs would probably be high because different manufacturing techniques and additional tooling would be required for the basic wing structure and the glove.

Maintenance costs also would be relatively high. A glove designed to reduce the inherent weight penalty would be susceptible to damage. Additionally, a large inventory of expensive and noninterchangeable replaceable panels would be required at each maintenance station. A nonload-carrying glove must allow for wing flexing. This offers structural concerns such as fatigue effects and scrubbing of the panels against each other, and the problem of water ingestion later turning to ice. Routine inspection of a glove would be difficult because the basic load-carrying structure is hidden from view. This fact, together with the possible loss of one or more panels in flight, could also make certification difficult and greatly increase the technical risk.

The X-21 LFC wing was an early version of an integrated duct load-carrying structure. Current NASA-sponsored LFC studies include an effort to develop integrated duct load-carrying structural concepts that will effectively utilize existing and projected advanced technology, materials, design, and manufacturing techniques. This concept promises a lightweight aerodynamically smooth structure with low technical risk through design innovation.

An integrated duct load-carrying structure was assumed for the large military configurations of this study. Extensive design and development studies would be necessary to identify weight characteristics and production/development costs. Hence, the emphasis in this study has been on identifying relative benefits and sensitivity data rather than on calculating specific values.

5.5 SUCTION SYSTEM

The suction system design was based on location of two suction pump compressors on each wing, two suction engines in the empennage, and 0 to 70-percent chord laminarization of the wing, and vertical and horizontal stabilizer. This is shown schematically for the wing in Figure 37.

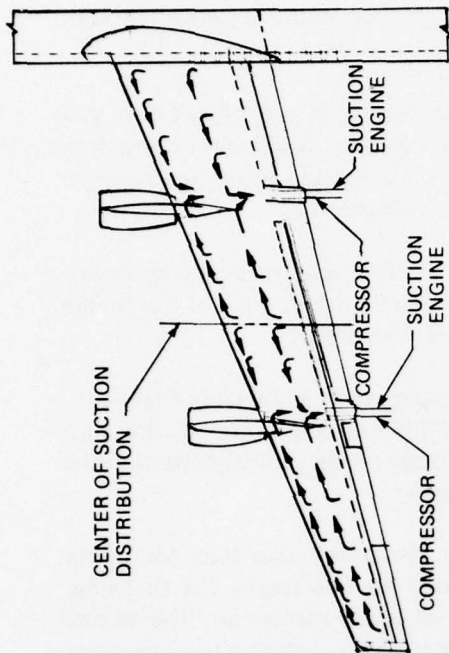
Specific design criteria applied to the wing duct system included: two separate levels of suction (upper surface and lower surface); duct airflow velocity of $Mach=0.2$ maximum; slot Reynolds number of from 50 to 80; slot velocity of 75 to 100 ft/sec; and suction duct pressure level equal to minimum surface pressure minus 15-percent free-stream dynamic pressure. Spanwise collection ducts provide for collection of air from 0 to 70 percent of wing chord for both upper and lower surfaces. Mixing of local chord suction air is accomplished at the suction engine location for each surface.

The same duct and slot design velocities and pressure level considerations were used for the horizontal and vertical stabilizers. The horizontal stabilizer pressure level and suction distributions are similar to the wing. The vertical stabilizer system operates at a different pressure level.

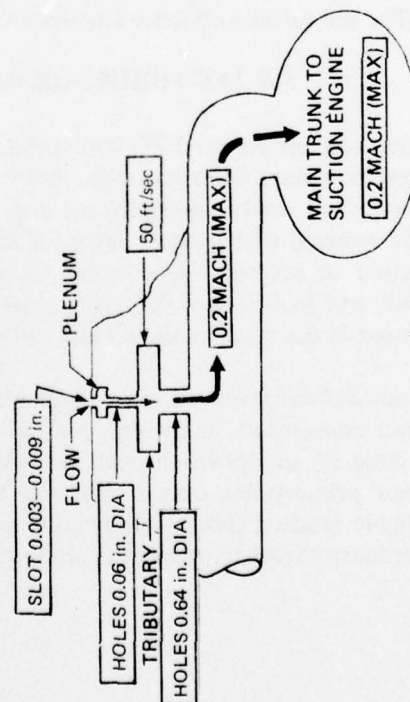
Therefore, each aft unit has three levels of suction and three compressor sections.

SUCTION SYSTEM CHARACTERISTICS

- SUCTION APPLIED OVER 0 TO 70% CHORD ON WING, HORIZONTAL, AND VERTICAL SURFACES, AND ACCESS DOORS
- TWO SUCTION ENGINES PER WING AND TWO SUCTION ENGINES ON EMPENNAGE
- TWO LEVELS OF SUCTION PROVIDED BY AXIAL FLOW COMPRESSORS
- DUCT VELOCITY: MACH = 0.2
- SLOT REYNOLDS NUMBER = 50 TO 80
- SLOT VELOCITY = 75 TO 100 fps



SUCTION SYSTEM CONCEPT



SLOT, PLENUM AND HOLE GEOMETRY BASED ON NORAIR RPT NOR 67-36

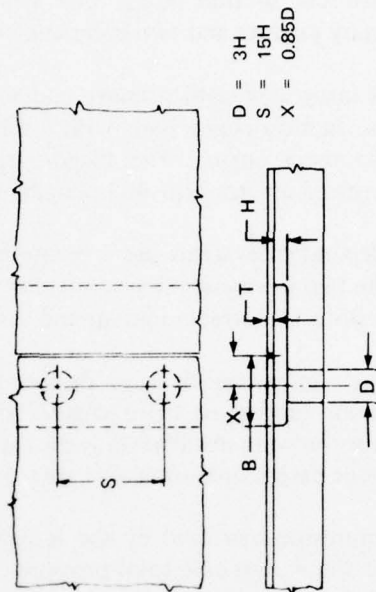


Figure 37 Wing Suction Duct Characteristics

The suction system geometry used for slots, plenums, and ducts is also shown in Figure 37. Typical duct system diameters are shown in Figure 38.

Four different suction pump drive systems were considered: Two systems integrated with the primary engines and two independent systems.

Systems integrated with primary engines include a direct drive system and a bleed-burn system. The suction compressor with a direct drive system is driven by shaft power extraction from the main engine. The bleed-burn system consists of a turbine using heated high-pressure bleed air from the main engine to drive the suction compressor.

The independent systems use a separate turboshaft engine to drive each suction compressor unit. The two independent systems that were considered differed in the source of the engine airflow. Both free-stream ram-air and suction-air sources were examined.

A relative comparison of these different suction pump drive systems is shown in Figure 39. The ram-air turboshaft drive engine concept was selected for this study. The suction unit design for the wing installation is shown in Figure 40. The basic design requirements and the compressor design operation also are summarized in this figure.

The compressor was sized by the required suction airflow, the compressor inlet total pressure and the design exit total pressure. The wing compressor has two stages. The first stage compresses upper surface air to match the pressure level of lower surface air. The second stage compressor increases the pressure of the discharged air to the free-stream total pressure. The tail suction compressors have an additional stage to handle air sucked from the vertical tail. The tail turboshaft drive engines are, however, identical to the wing units.

5.6 LFC THRUST-DRAG-WEIGHT BOOKKEEPING SYSTEM

Suction engines on the LFC configuration drive pumps that provide suction to remove the slowest boundary layer particles close to the surface. This process retains a laminar boundary layer and results in significant drag reduction relative to the turbulent airplane. Because of the removal of boundary layer air and the additional suction engines, some care must be exercised in properly accounting for the impact of the suction engines on thrust, drag, weight, and fuel flow of the entire airplane system. The thrust-drag-weight bookkeeping system used in the study is shown in Figure 41.

Suction airflow removed from laminarized areas is pumped to free-stream conditions. The suction compressor, therefore, produces a gross thrust that exactly cancels the suction or sink drag of air drawn through the surface plus the internal flow losses. The turboshaft engines' primary function is to supply the shaft power necessary to drive the compressor. A negligible residual thrust is, however, produced by these engines. The main engines provide the primary thrust to propel the aircraft.

● SYSTEMS INTEGRATED WITH PRIMARY ENGINES

- DIRECT DRIVE: SHAFT POWER EXTRACTION FROM THE MAIN ENGINE DRIVING A SUCTION COMPRESSOR
- BLEED AND BURN: TURBINE USING HEATED HIGH-PRESSURE BLEED AIR FROM THE MAIN ENGINE TO DRIVE A SUCTION COMPRESSOR

● INDEPENDENT SYSTEMS

- RAM-AIR TURBOSHAFT ENGINE DRIVING A SUCTION COMPRESSOR
- SUCTION-AIR TURBOSHAFT ENGINE DRIVING A SUCTION COMPRESSOR

RELATIVE RATING	
●	GOOD
◐	FAIR
○	POOR

DESIGN ITEM	INTEGRATED SYSTEMS		SEPARATE SYSTEMS	
	BLEED AND BURN	DIRECT DRIVE	RAM AIR *	SUCTION AIR
● DESIGN/LOCATION FLEXIBILITY	◐	○	●	●
● CONTROL FOR OFF-DESIGN OPERATION	◐	○	●	●
● AFFECTS/DEPENDS ON ENGINE OPERATION	○	◐	●	●
● NET SYSTEM FUEL CONSUMPTION	○	●	◐	◐
● SYSTEM WEIGHT	●	◐	○	○
● DESIGN COMPLEXITY	◐	○	●	◐
● DESIGN HAZARD POTENTIAL	◐	◐	●	○
● DISTURBANCE TO BOUNDARY LAYER	●	●	◐	◐

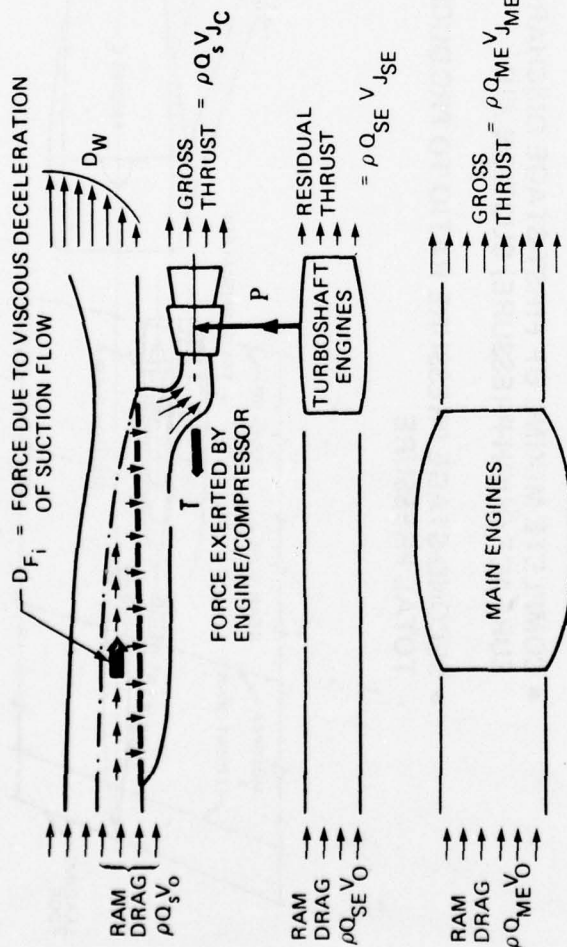
*SELECTED FOR THIS STUDY

Figure 39 Suction Pump Drive System Selection

- BASIC REQUIREMENTS
 - FLOW QUANTITY
 - COMPRESSOR INLET P_t
 - DESIGN EXIT P_t
- COMPRESSOR DESIGN OPERATION
 - TWO STAGES
 - FIRST-STAGE COMPRESSOR RATIO TO MATCH TWO LEVELS OF SUCTION AIR PRESSURE
 - COMPLETE MIXING OF FIRST-STAGE DISCHARGE WITH LOWER WING SURFACE (HIGH-PRESSURE) SUCTION AIR
 - SECOND-STAGE PRESSURE RATIO TO PRODUCE FREE STREAM TOTAL PRESSURE

Figure 40 Compressor/Suction Engine Design

LFC SYSTEM MOMENTUM BALANCE



$$\text{TOTAL NET THRUST} = \rho Q_{ME} (V_{JME} - V_0) + \rho Q_{SE} (V_{JSE} - V_0)$$

STUDY PERFORMANCE EVALUATION

- LFC WEIGHT ITEMS VARY WITH LAMINARIZED AREA
- MAIN ENGINE SIZE AND FUEL FLOW DEPEND ON AIRPLANE DRAG
- SUCTION ENGINE SIZING INCLUDES INTERNAL DUCT LOSSES
- SUCTION ENGINE FUEL FLOW VARIES WITH LAMINAR AREA
- TOTAL FUEL FLOW = SUCTION ENGINE PLUS MAIN ENGINE FUEL FLOW

DRAG BOOKKEEPING

- AIRPLANE DRAG = WING AND TAILS WAKE DRAG + PROFILE DRAG + INDUCED DRAG + COMPRESSIBILITY DRAG
- EQUIVALENT SUCTION DRAG = $\frac{P_i}{V_0}$
- LFC DRAG CONVENTION = AIRPLANE DRAG + EQUIVALENT SUCTION DRAG

Figure 41 LFC System Bookkeeping Method

In cruise, thrust produced by the main engines balances airplane drag. Airplane drag includes the wake drag of the laminarized surfaces; the profile drag of the nacelles, struts, and fuselage; and the airplane compressibility drag, trim drag, and induced drag.

In airplane sizing calculations, the LFC-related weight items including the weight of the turboshaft engines and compressors, internal ducting, and structural weight increment all varied with the laminarized areas. Fuel flow of the main engines depends on the previously defined airplane drag. Size of the main engines was determined by the TOFL and turbulent climb requirements. The suction engine fuel flow varies with the laminarized area. The total fuel flow includes the suction engine plus main engine fuel flow.

The standard convention in discussing the aerodynamic efficiency of an LFC airplane is to define total drag as the sum of the airplane drag plus an equivalent suction drag. Equivalent suction drag is defined in terms of the power, P_i , required to drive the pumps in the absence of internal duct losses. This is a convenient way to identify the net aerodynamic benefits of an LFC configuration. However, to be consistent with the previously defined bookkeeping system, the aerodynamic drag buildup of the LFC configurations does not include the equivalent suction drag. The suction engines and compressors are, however, sized to balance momentum loss of the suction airflow including the internal duct losses.

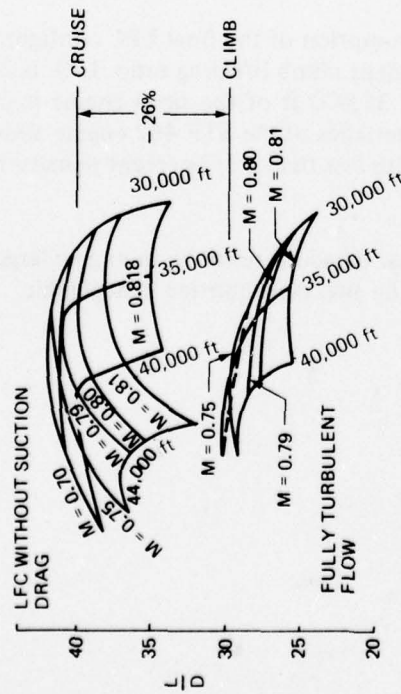
5.7 TAKEOFF-CLIMB-CRUISE THRUST MATCHING

An LFC airplane has varied thrust demands because of low cruise thrust requirements. Engines for the study LFC configurations were required to have a TOFL not to exceed 9000 ft. Additionally, the engines also were required to allow the configurations to climb to 35,000 ft with fully turbulent flow drag levels. The turbulent climb to altitude condition generally determined the size of the engines.

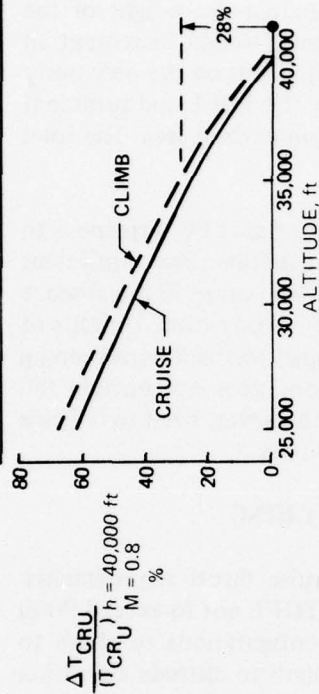
The lift/drag ratios, thrust characteristics, and fuel consumption of the final LFC configuration Model 767-773 are shown in Figure 42. The turbulent climb lift/drag ratio, L/D , is 26 percent less than the LFC cruise L/D . Climb thrust at 35,000 ft of the sized engine is 28 percent greater than cruise thrust at 40,000 ft. Characteristics of the STF 482 engine allow the engine in cruise to be throttled up to 17 percent with less than a 1/2-percent penalty in SFC.

These data show that takeoff and turbulent climb thrust demands result in an engine larger than would be required for cruise. However, the impact on fuel consumption is negligible.

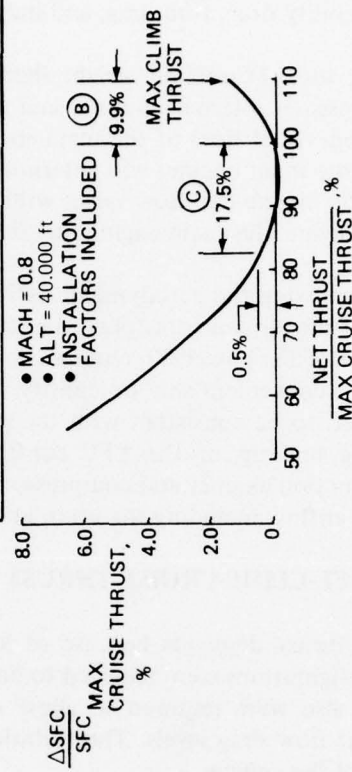
MODEL 767-773 L/D COMPARISONS



STF-482 CRUISE/CLIMB THRUST VARIATIONS



STF-482 SFC vs THRUST CHARACTERISTICS



THRUST DEMANDS

- TAKEOFF-HIGH TAKEOFF THRUST AT SEA LEVEL
- TURBULENT CLIMB-HIGH CLIMB THRUST TO 35,000 ft
- LFC CRUISE-LOW CRUISE THRUST AT 40,000 ft

THRUST MATCH CONSIDERATIONS

- TURBULENT CLIMB L/D = 26% LESS THAN LFC CRUISE L/D
- CLIMB THRUST AT 35,000 ft = 28% GREATER THAN CRUISE THRUST AT 40,000 ft
- CAN THROTTLE 17% FOR 0.5% SFC PENALTY

Figure 42 Takeoff, Climb, and Cruise Thrust Match Considerations

6.0 LFC CONFIGURATION EVOLUTION

This section summarizes studies and results that led to the evolution of the final LFC configuration. The initial baseline LFC configuration was derived from the reference turbulent airplane by incorporating only the minimum design changes necessary to laminarize the wing and tails. A braced-wing LFC configuration was then developed from the initial baseline LFC configuration. Additionally, LFC wing geometry/cruise speed optimization study was conducted to select the wing planform for the final LFC configuration.

6.1 INITIAL BASELINE LFC CONFIGURATION

The initial baseline uncycled LFC configuration, Model 767-769, that was derived from the reference turbulent airplane is shown in Figure 43. This configuration was derived from the reference turbulent airplane Model 767-768 by removing leading-edge devices and adding six separate turboshaft-driven suction pump units. Four of these suction units are located on the wing, and two units are located on the empennage. The wing and tails are slotted to provide laminar flow over 70 percent of the surfaces. The LFC suction ducts are integral with the primary structure. Internal suction duct design permits low duct Mach numbers.

The initial baseline LFC configuration was sized to achieve design mission objectives. The design selection, which was constrained by both the TOFL and turbulent climb altitude, is shown in Figure 44. A wing loading of 90 lb/ft^2 , which corresponds to a span loading of 7.5 lb/ft^2 , was selected. The selected design is within approximately 1 percent of the minimum fuel burned and 2 percent of the constrained minimum gross weight configuration arrangements.

The initial baseline configuration was sized for a wide range of LFC structural and system weight penalties. Results are shown in Figure 45. The unit LFC structural and systems weight impact on laminar flow control fuel savings and gross weight reduction is significant. For this initial LFC configuration, a 1 lb/ft^2 LFC weight penalty change results in a 2.5-percent change in fuel savings and a 5-percent change in the TOGW reduction.

6.2 LFC BRACED WING STUDY

Previous LFC configuration studies and recent work by Dr. W. Pfenninger have indicated that a strut-braced wing might be a desirable arrangement for an LFC configuration. The strut-braced wing could allow use of a large wing span. Additionally, maximum wing chords that normally occur near the side of the fuselage are reduced by using an untapered planform inboard of the strut-attachment station. The shorter chords reduce the maximum chord Reynolds number and, thereby, ease the task of laminarization.

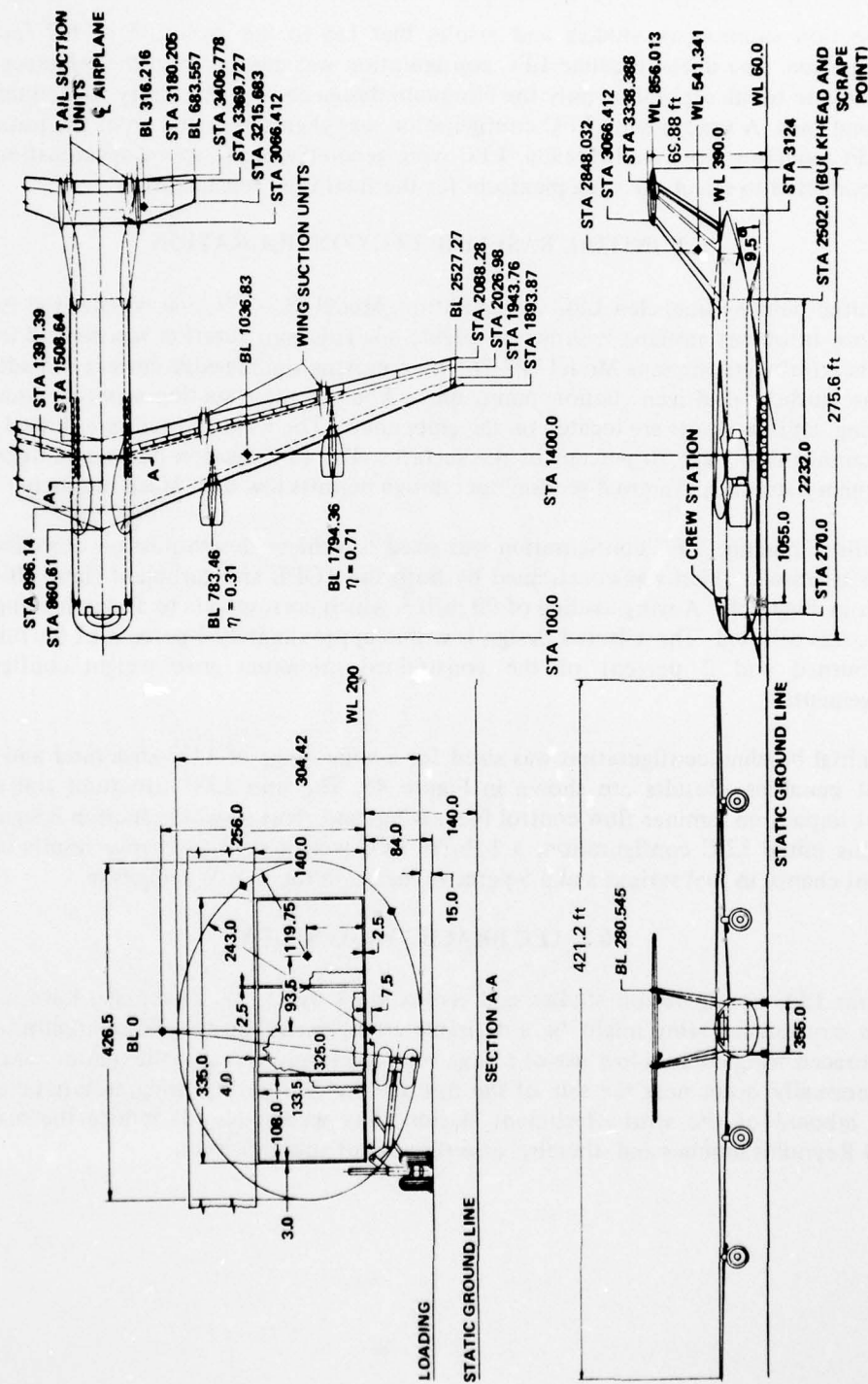


Figure 43 Uncycled Initial Baseline Laminar Flow Control Airplane, Model 767-769

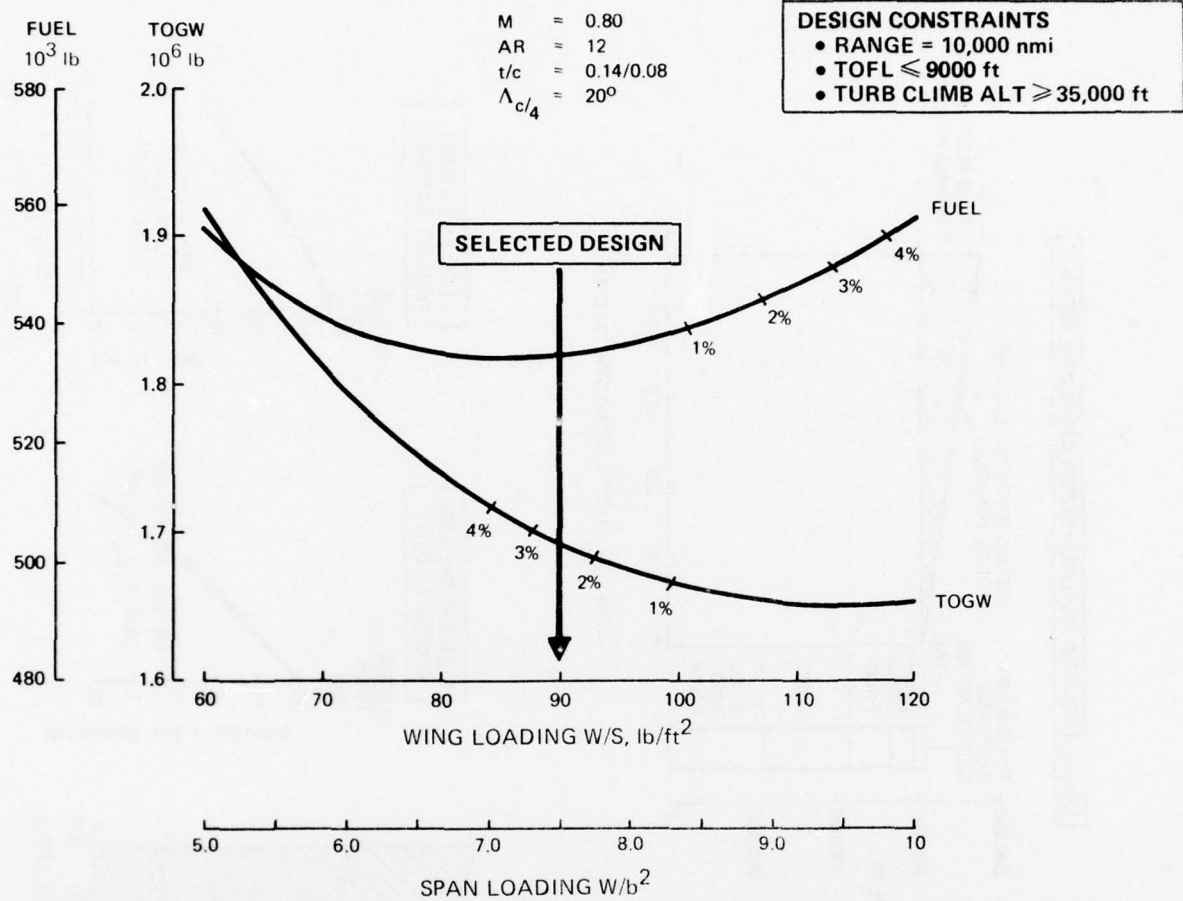
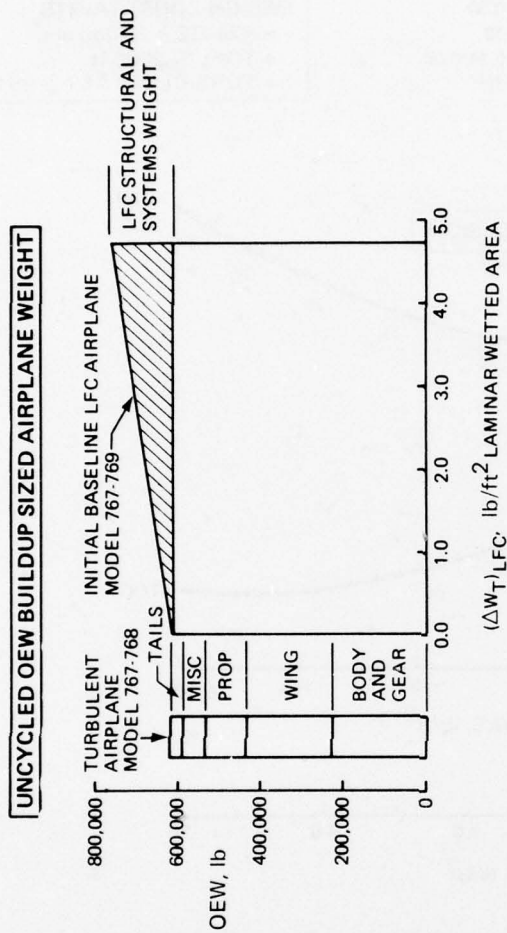


Figure 44 Baseline Laminar Flow Control Airplane Design Selection



PAYLOAD = 350,000 lb
 RANGE = 10,000 nmi
 AR = 12
 $\Lambda_{c/4} = 20^\circ$
 $t/c = 0.14/0.08$

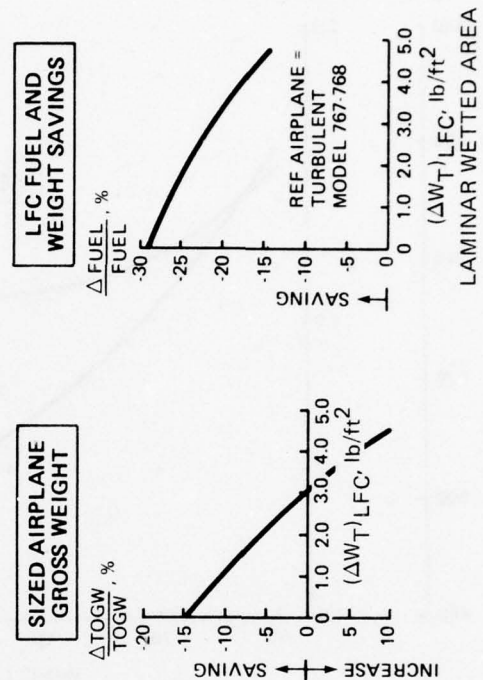
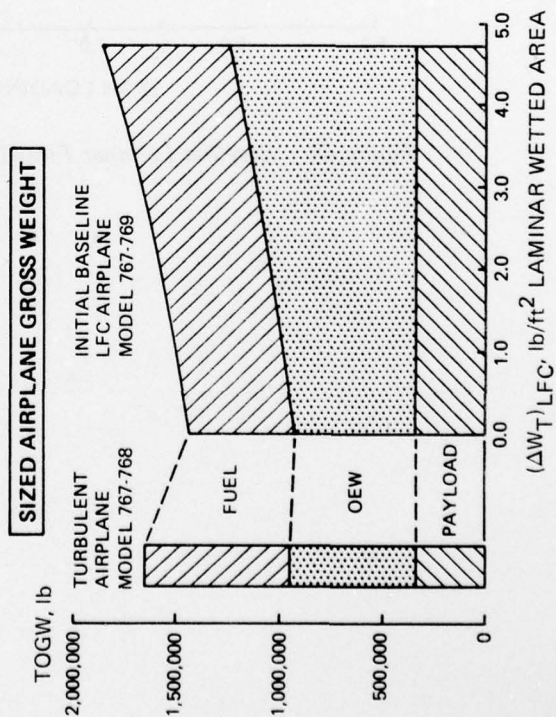


Figure 45 Initial Baseline Laminar Flow Control Airplane Structural and System Weight Sensitivity Study

Previous Northrop studies shown in Figure 46, and recent unpublished Boeing wind tunnel test results, indicate that aerodynamic interference between wing and strut can be made negligible by proper tailoring of the wing and/or strut, particularly near the strut-wing intersection. Results of recent Boeing large freighter braced-wing studies, were used to provide design guidance for defining an LFC braced-wing arrangement. Strut-attachment studies shown in Figure 46 indicate that the spanwise extent of a simple single-strut brace is limited by a minimum attachment angle of 13 to 15 deg. The optimum strut spanwise extent could perhaps be increased with use of a more sophisticated jury strut arrangement, or a modified body with increased depth between wing-body intersection and the strut-body intersection.

The strut-braced wing LFC configuration developed for this study is shown in Figure 47. The strut is unswept to allow achievement of natural laminar flow on the relatively short chords. The wing planform has an aspect ratio of 15. The wing inboard of the strut attachment is untapered. The minimum strut attachment angle for this simple strut arrangement resulted in an attachment station at approximately 33 percent of the wing semispan.

Results of the braced-wing study are shown in Figure 48. The selected design has a wing loading of 113 lb/ft^2 and a span loading of 7.5 lb/ft^2 . Gross weights of the sized LFC braced-wing configuration and the initial LFC cantilever wing configurations are compared in Figure 48. Both configurations were sized with an early assessment of the total LFC structural and systems weight penalty. As previously mentioned in Section 4.3, the ongoing NASA-sponsored LFC systems studies may result in integrated LFC structural and systems concepts with a significantly lower LFC weight penalty.

Gross weight for the strut-braced wing LFC configuration Model 767-767 is slightly less than the cantilever configuration. This reduction is the result of a lower OEW associated with a higher wing loading and consequently lower wing area.

The strut-braced wing concept offers a number of design variables, such as strut chord, spanwise attachment, strut thickness, sweep, and strut concept (jury or simple struts), in addition to the usual wing planform parameters, that must be considered to fully optimize the configuration arrangement. Consequently, the study effort was directed at optimizing the cantilever wing arrangement.

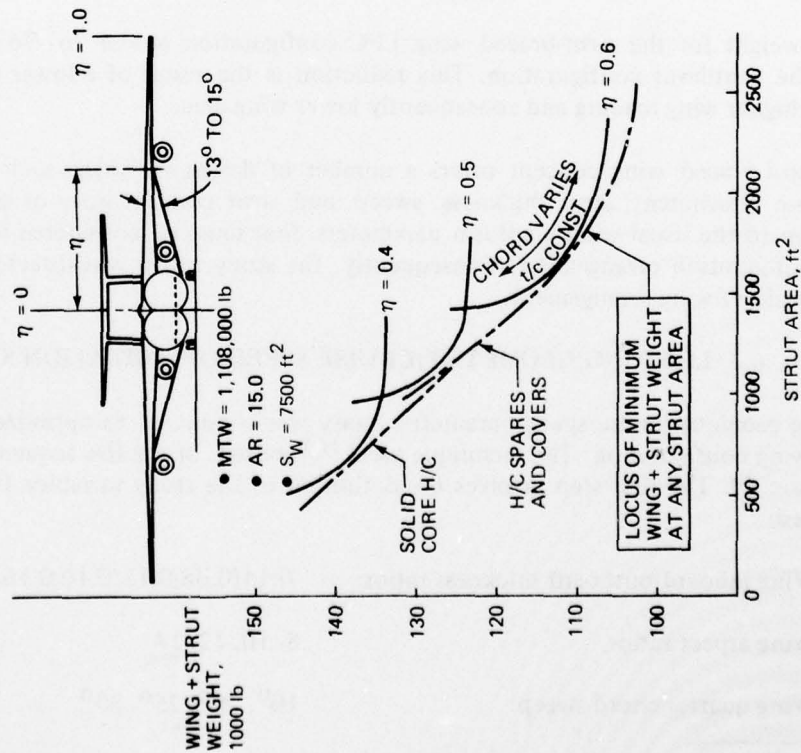
6.3 LFC WING GEOMETRY/CRUISE SPEED OPTIMIZATION STUDY

A wing geometry/cruise speed parametric study was conducted to optimize the LFC cantilever wing configuration. The technique used⁽¹⁶⁾ consists of the five sequential steps shown in Figure 49. The first step involves the definition of the study variables. Primary variables included:

- Wing inboard/outboard thickness ratios: 0.14/0.08;0.15/0.10;0.16/0.12;0.17/0.14
- Wing aspect ratio: 8, 10, 12, 14
- Wing quarter chord sweep: 10° , 20° , 25° , 30°

16. Healy, M. J.; Kawalik, J. S.; and Ramsay, J. W., "Airplane Engine Selection by Optimization on Surface Fit Approximations," *Journal of Aircraft*, Vol. 12, No. 7, July 1975, pp593-599.

● STRUT ATTACHMENT



● AERODYNAMIC DESIGN

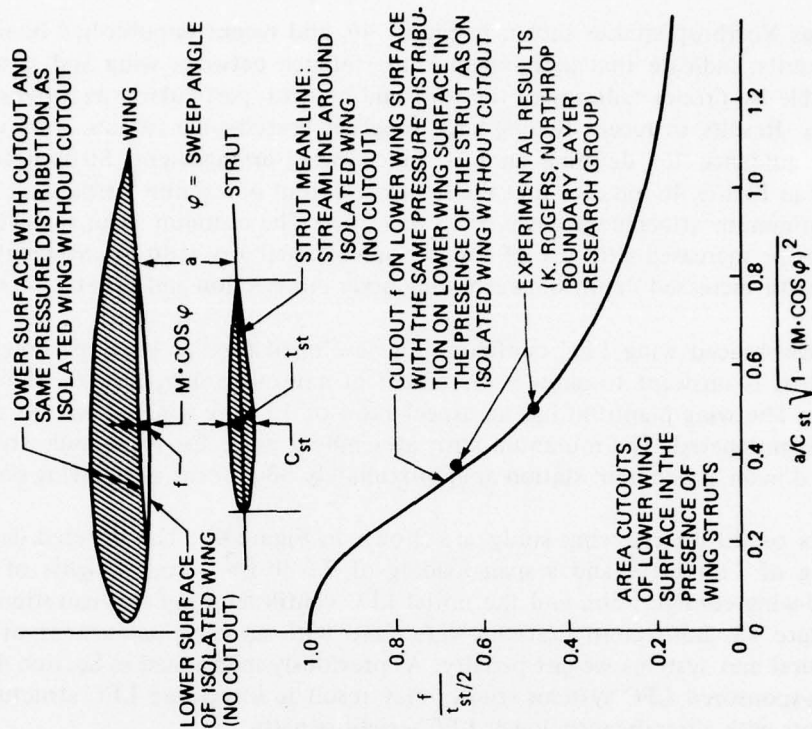


Figure 46 Laminar Flow Control Braced-Wing Design Considerations

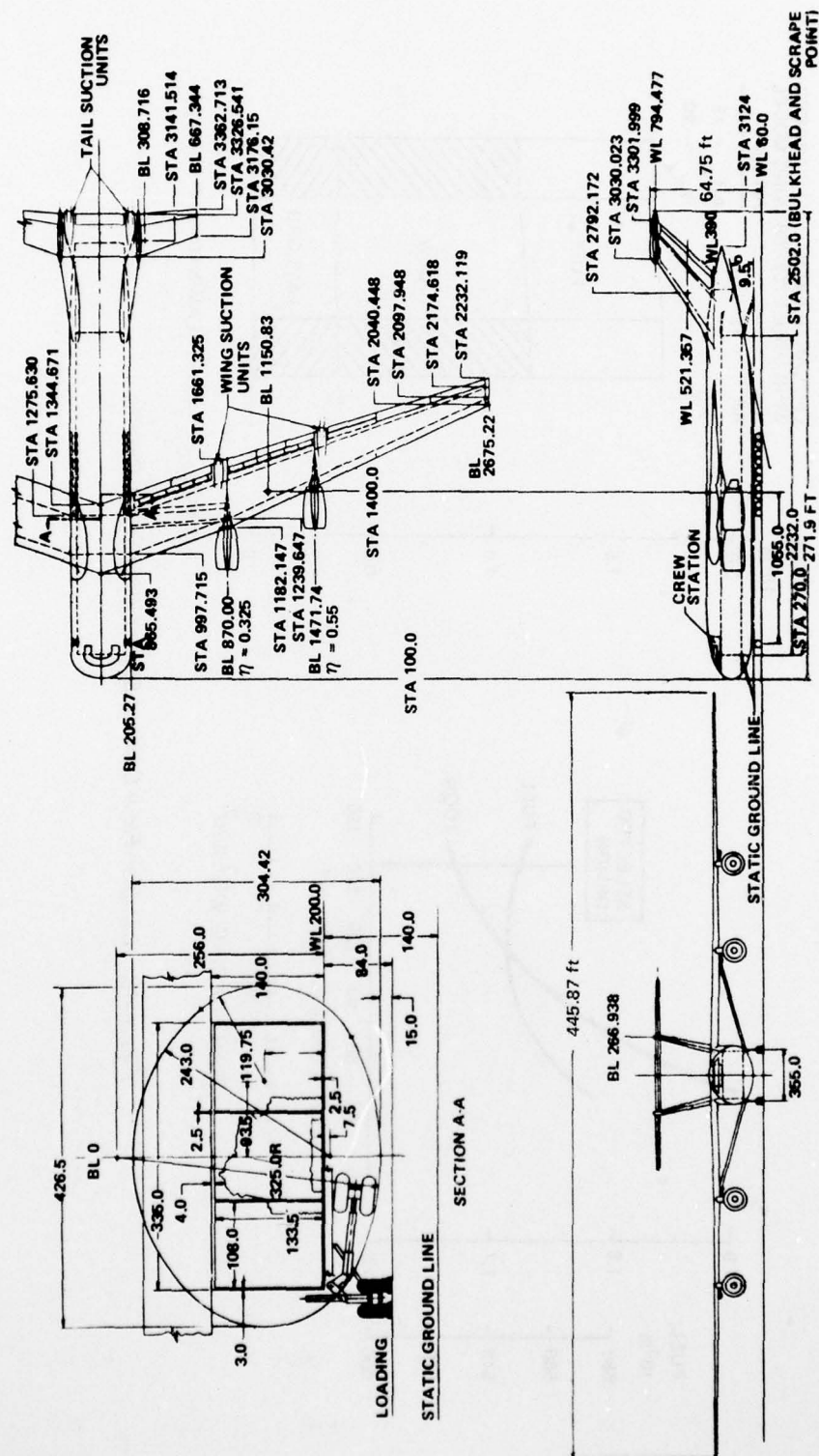
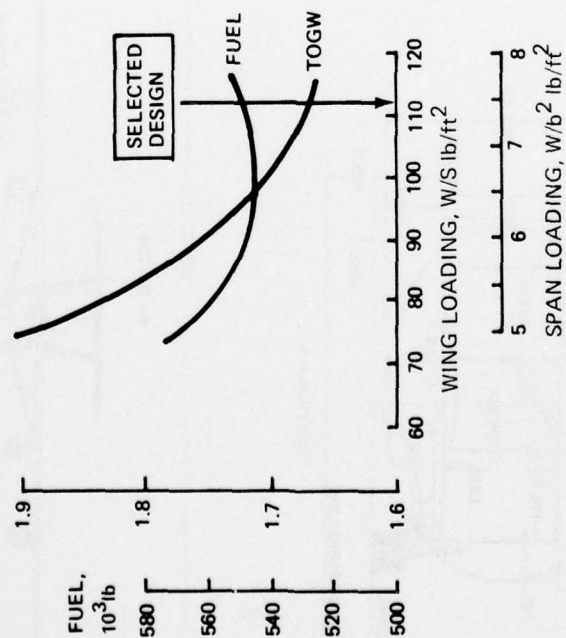
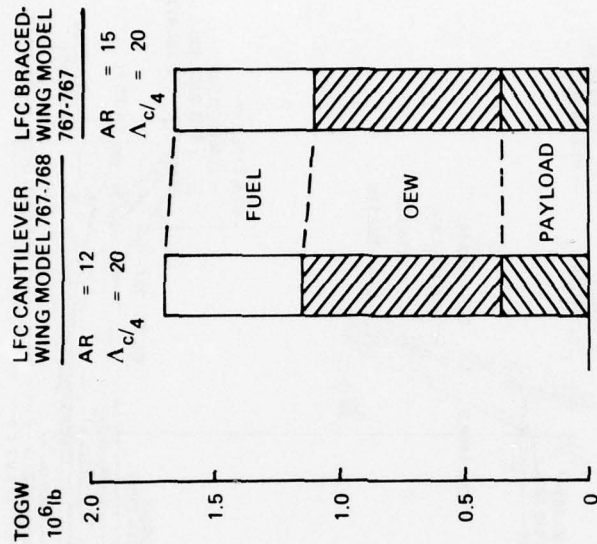


Figure 47 Uncycled Braced-Wing Laminar Flow Control Airplane, Model 767-767

LFC BRACED-WING MODEL 767-767 ENGINE/AIRFRAME MATCHING



GROSS WEIGHT COMPARISON



$(\Delta W_T)_{LFC} = 3.3 \text{ lb/ft}^2 \text{ LAMINAR WETTED AREA}$

Figure 48 Laminar Flow Control Braced-Wing Study Results

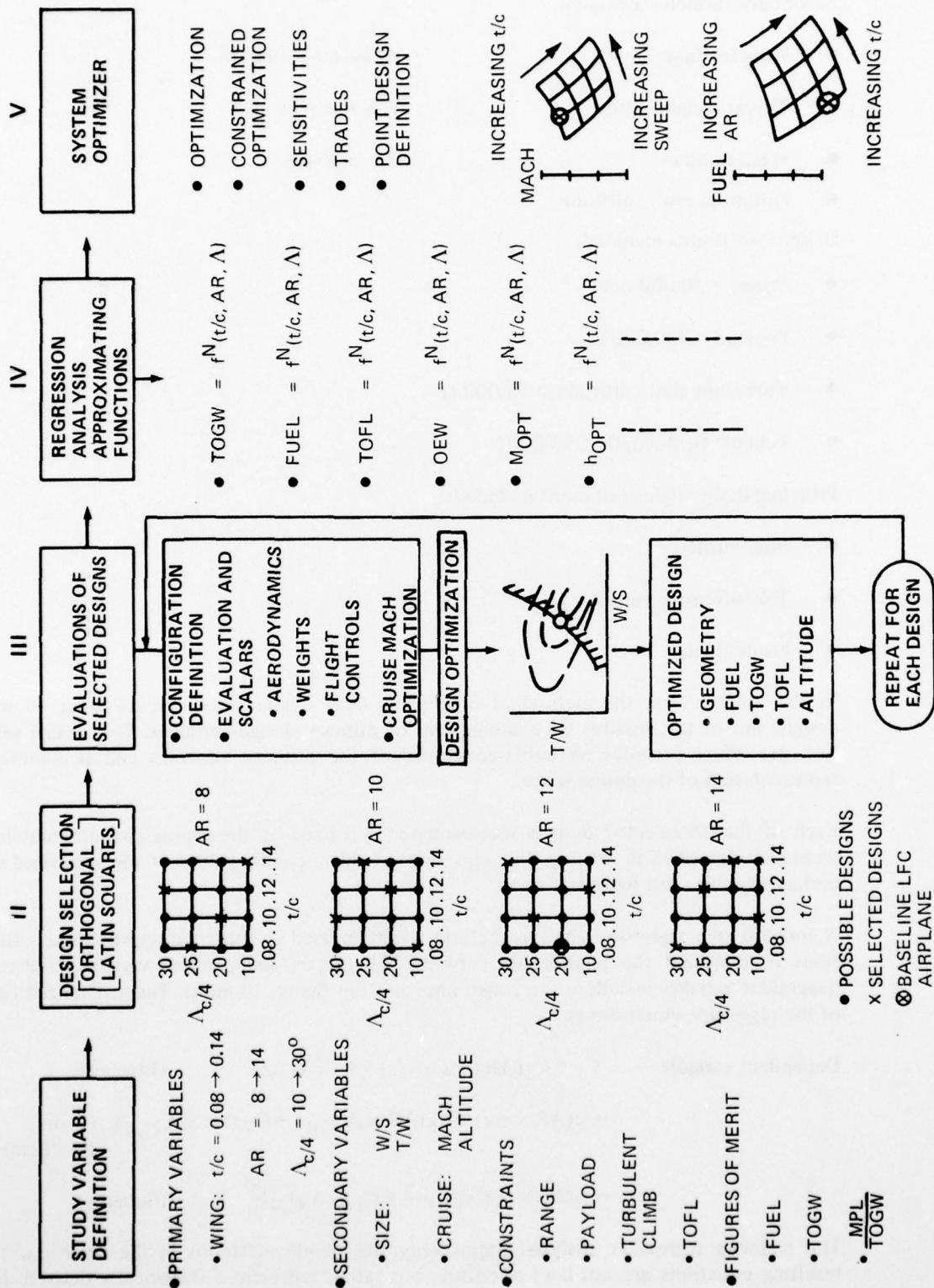


Figure 49 Laminar Flow Control Wing Parametric Optimization Study

Secondary variables included:

- Wing loading: $W/S = 60-120 \text{ lb/ft}^2$
- Thrust/weight ratio: $T/W = 0.10-0.30$
- Mach number: $M = 0.70-0.85$
- Optimum cruise altitude

Design constraints included:

- Range = 10,000 nmi
- Payload = 350,000 lb
- Turbulent climb altitude > 35,000 ft
- Takeoff field length < 9,000 ft

Principal design figures of merit included:

- Fuel burned
- Takeoff gross weight
- Productivity

In the second step, the method of orthogonal latin squares was used to select 16 wing designs out of the possible 64 combinations of primary design variables. This design selection procedure provides an unbiased choice of the primary variables and is a uniform representation of the design space.

Each of the 16 selected designs was evaluated and sized by the engine/airframe matching technique described in Section 4.2. This step provides specific values of the optimized secondary variables and figures of merit.

A forward step regression analysis method was then used to construct approximating functions to represent the relationship between the primary independent variables and each dependent variable including the constraints and the figures of merit. The generalized form of the regression equations is:

$$\begin{aligned}
 \text{Dependent variable} = & C_1 + C_2(AR) + C_3(t/c) + C_4 (\Lambda_{C/4}) && \text{(Linear)} \\
 & + C_5(AR \times t/c) + C_6(AR \times \Lambda_{C/4}) + C_7 (t/c \times \Lambda_{C/4}) && \text{(Cross Products)} \\
 & + C_8(AR)^2 + C_9 (t/c)^2 + C_{10} (\Lambda_{C/4})^2 && \text{(Squares)}
 \end{aligned}$$

The stepwise regression analysis retains only the significant terms in the equation. The resulting equations are not laws of nature, but rather represent a statistically derived data enrichment procedure.

The approximating functions can then be used in a powerful nonlinear optimizer to conduct constrained or unconstrained optimization, sensitivity, and trade studies. This parametric optimization process is described in Reference 16.

The design selections for each of the sixteen configurations that were analyzed are shown in Figures 50 through 53. The selected designs all have a span loading of $W/b^2 = 7.5 \text{ lb/ft}^2$. These designs were close to the constrained minimum fuel configuration and generally within 2 percent of the constrained minimum gross weight configurations. The corresponding wing loadings vary from $W/S = 60$ to 105 lb/ft^2 . These results imply that the LFC configurations tend to optimize with approximately the same span length irrespective of aspect ratio, sweep, or thickness.

6.3.1 PERFORMANCE OPTIMIZATION

Results of the wing planform/cruise speed optimization study are shown in Figures 54 through 57. These results illustrate the impact of the wing planform geometry on the cruise Mach number, fuel requirements, TOGW, and productivity of the LFC cantilever wing configurations. The surface fit equations are shown to be a good representation of the initial baseline LFC configuration and the additional 15 LFC study configurations.

The spanwise variation of thickness/chord ratio is shown in Figure 54. The thickness/chord ratio referred to in the subsequent figures corresponds to the thickness/chord ratio on the outboard portion of the wing. In all cases the inboard thickness/chord is greater than that outboard on the wing.

Characteristics of the optimum LFC wing planform geometry are summarized in Figure 58.

The optimum planform for minimum fuel as the figure of merit has the highest aspect ratio, lowest thickness/chord ratio, and a quarter chord sweep of approximately 12 degrees. This results in a cruise Mach number $M = 0.78$. The sensitivity data show that achieving a high aspect ratio is most important for minimum fuel consumption. Reducing the aspect ratio from 14 to 8 would increase the fuel consumption by nearly 13 percent. Increasing the wing thickness from 8 percent to 14 percent would increase fuel consumption by 4 percent. Wing sweep is seen to be a rather unimportant parameter.

The minimum gross weight configuration has the same high aspect ratio and a slightly lower sweep angle than the minimum fuel-burned configuration. The minimum gross weight configuration favors a higher thickness ratio (11 percent). The corresponding optimum cruise Mach number $M = 0.75$. The sensitivity data show that a low sweep angle and high aspect ratio are most important for gross weight as a figure of merit. Wing thickness ratio is an insignificant design variable in this case.

The maximum productivity configuration favors a high aspect ratio. Because cruise speed is important for productivity, the optimum configuration desires a high sweep, and low wing thickness. This results in a cruise Mach number $M = 0.85$. The sensitivity data indicate that having a low t/c wing with a high aspect ratio is most important. Wing sweep is seen to have only a small effect on productivity.

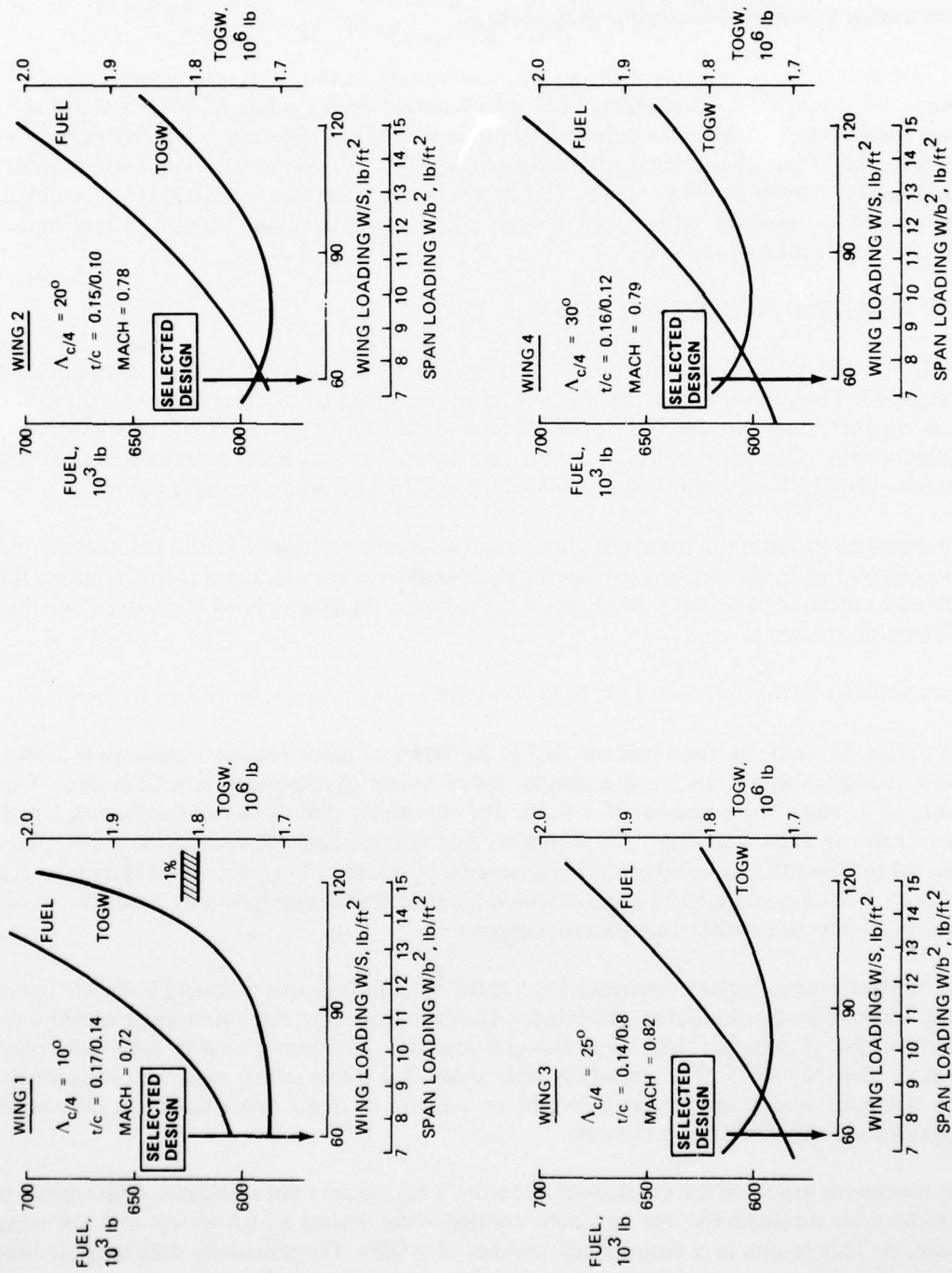


Figure 50 Design Selection for AR=8 Laminar Flow Control Configurations

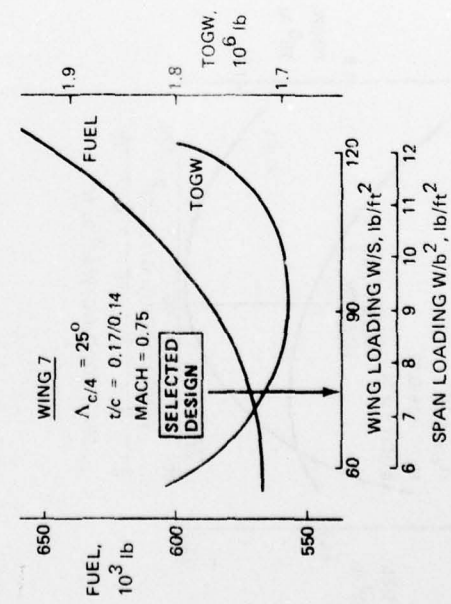
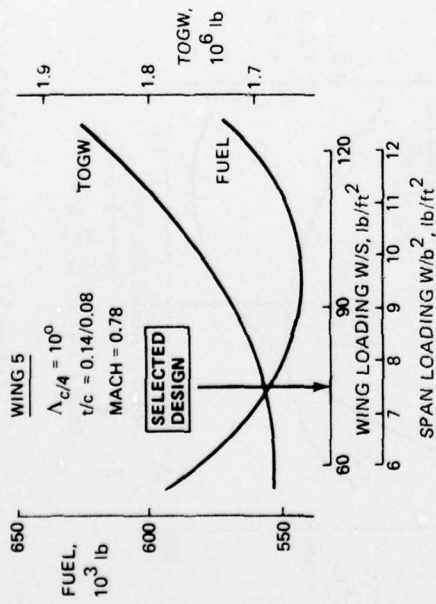
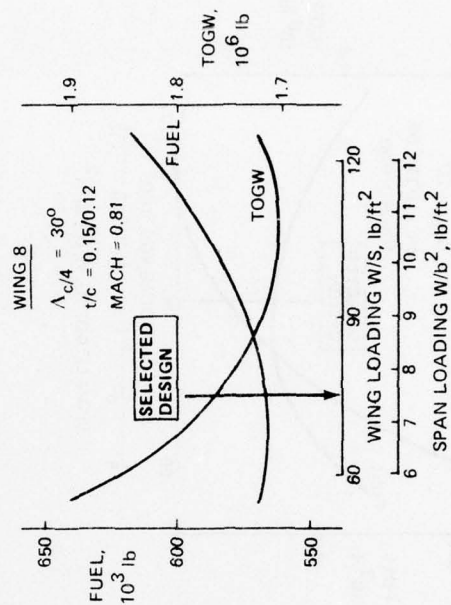
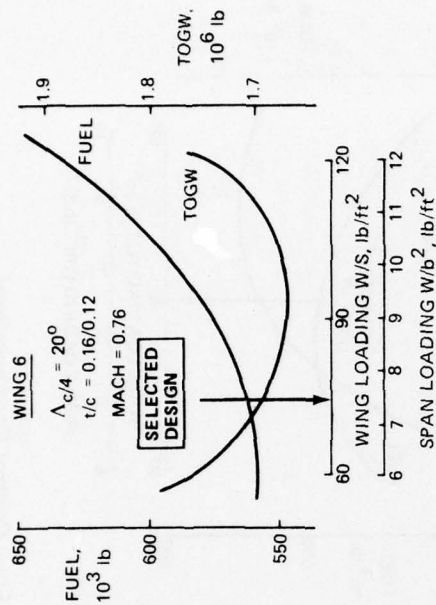


Figure 51 Design Selection for AR=10 Laminar Flow Control Configurations

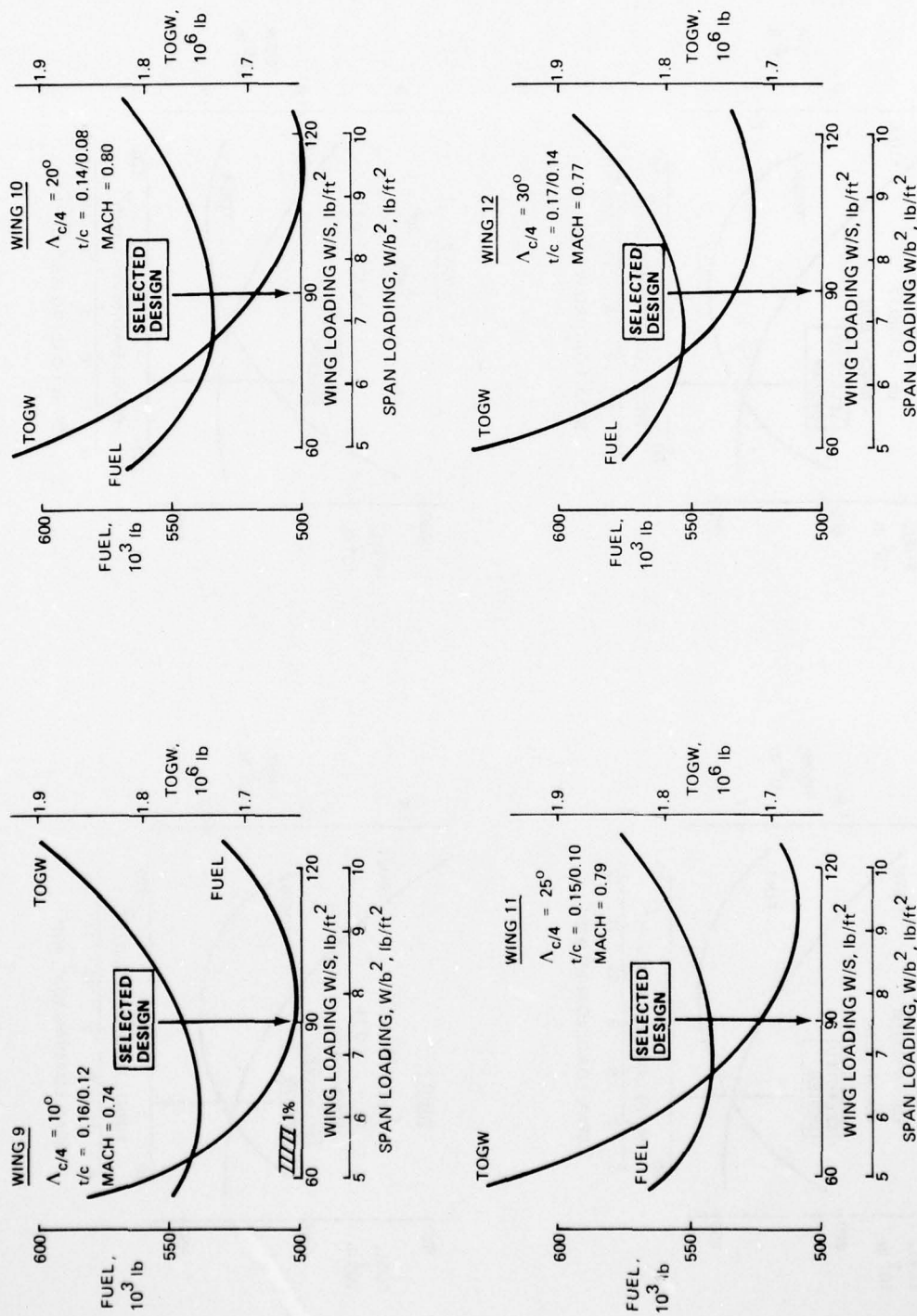


Figure 52 Design Selection for AR=12 Laminar Flow Control Configurations

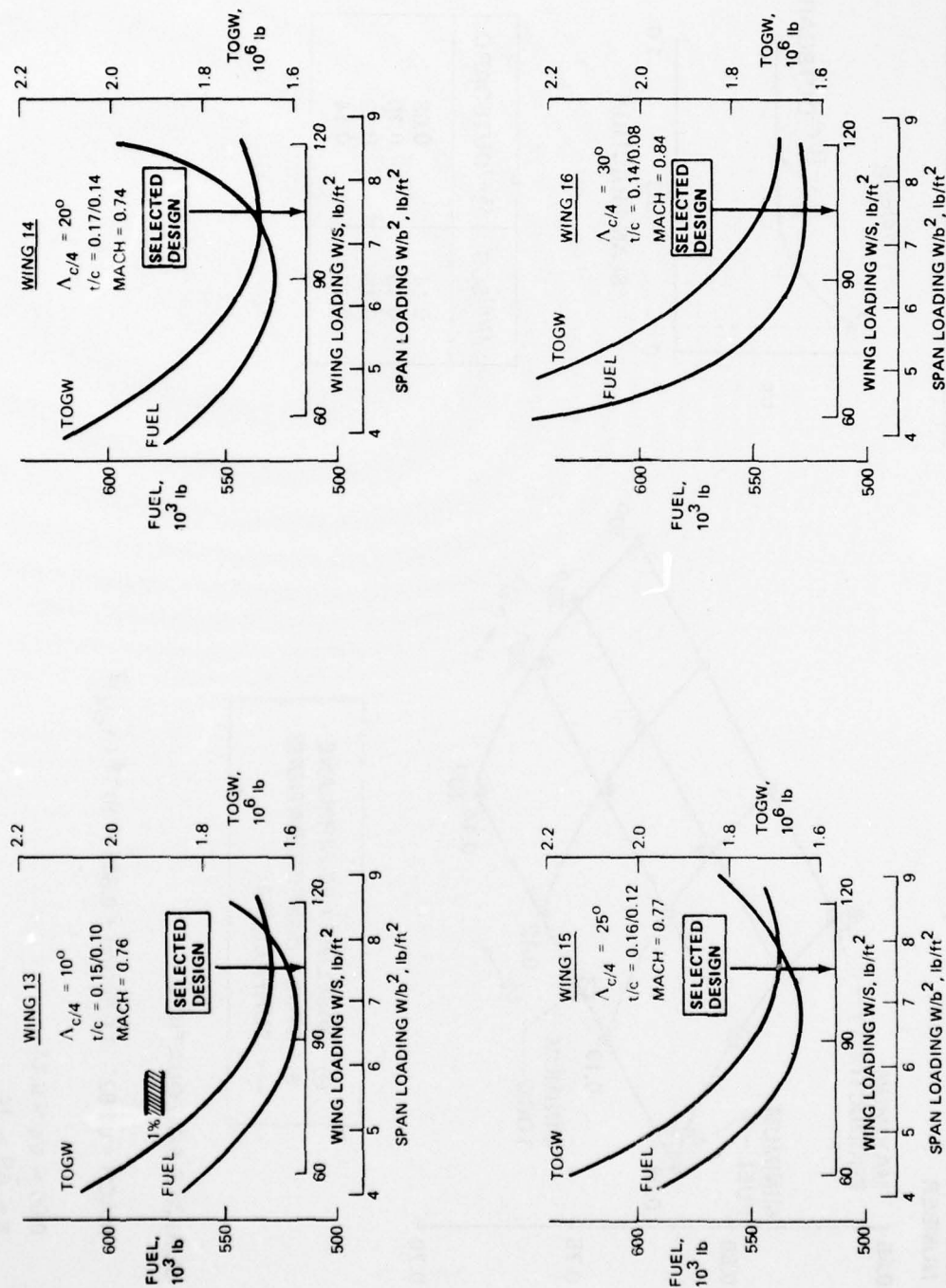


Figure 53 Design Selection for AR = 14 Laminar Flow Control Configurations

AD-A052 422

BOEING COMMERCIAL AIRPLANE CO SEATTLE WASH

F/G 1/3

APPLICATION OF LAMINAR FLOW CONTROL TO LARGE SUBSONIC MILITARY --ETC(U)

JUL 77 R M KULFAN, J D VACHAL

F33615-76-C-3035

UNCLASSIFIED

D6-45148

AFFDL-TR-77-65

NL

2 OF 2

AD
A052422

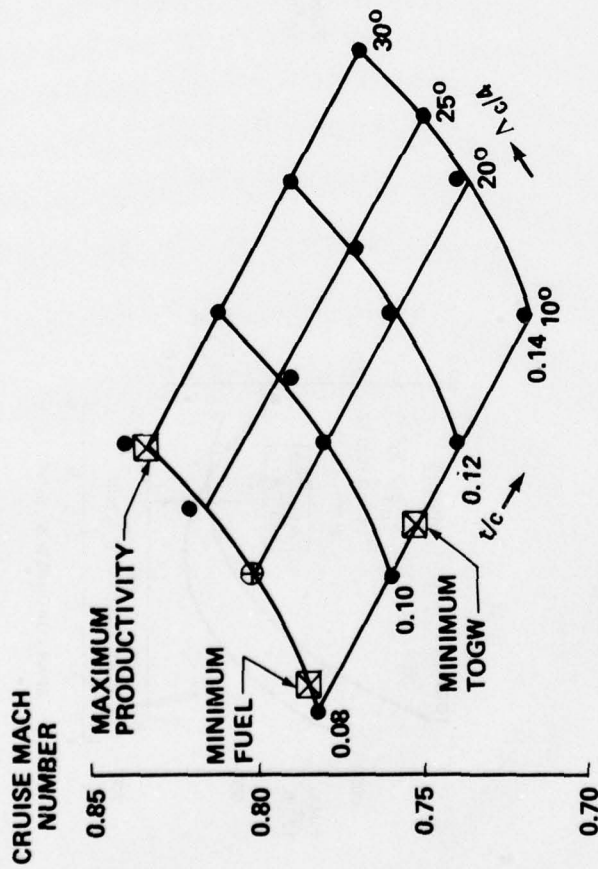


END

DATE
FILMED

5 -78

DDC



⊕ BASELINE LFC AIRPLANE
● STUDY CONFIGURATIONS
— SURFACE FIT

SURFACE FIT EQUATION:

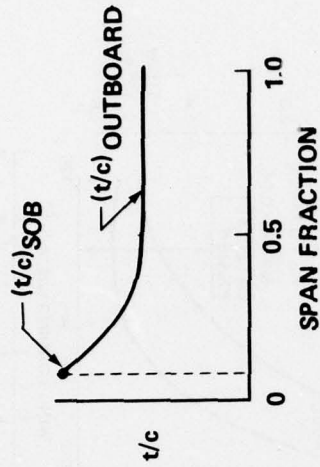
$$\text{MACH} = 0.862 - 1.075 (t/c) + 0.649 \times 10^{-4} (\Lambda_{c/4})^2$$

$$0.08 \leq t/c \leq 0.14$$

$$8 \leq \text{AR} \leq 14$$

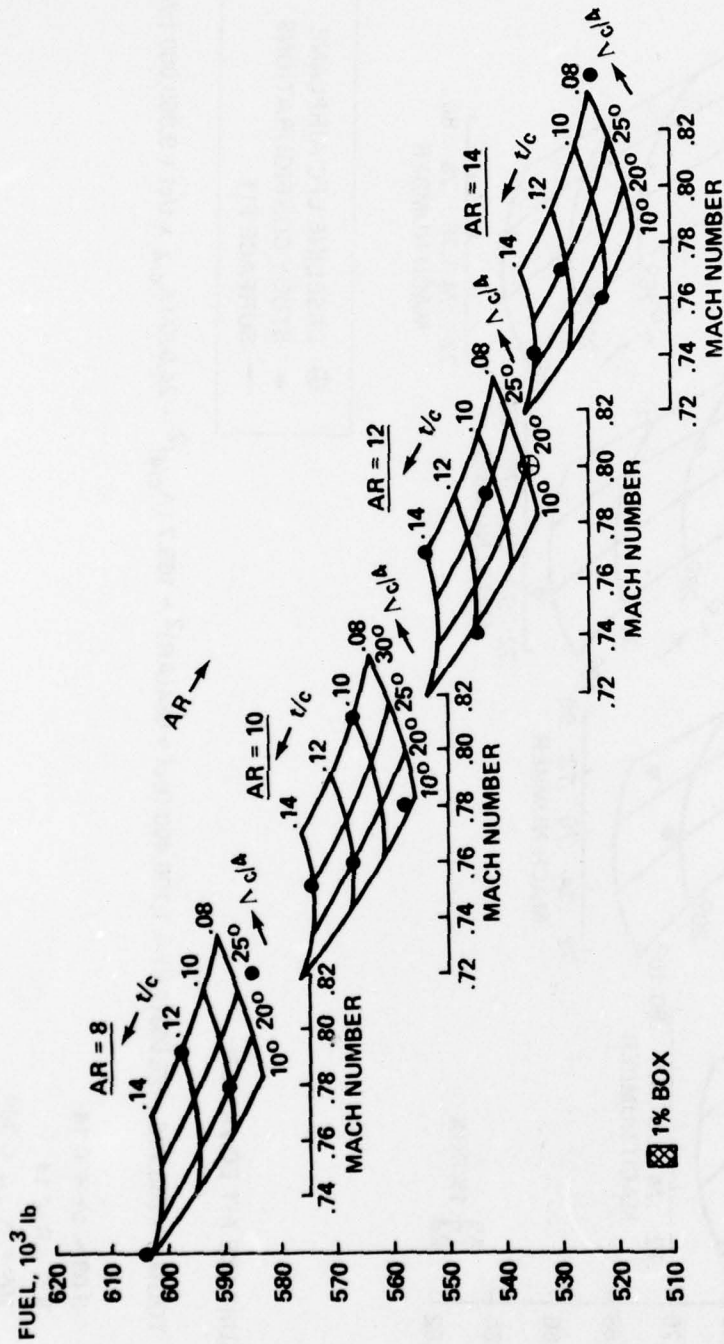
$$10^\circ \leq \Lambda_{c/4} \leq 30^\circ$$

STUDY THICKNESS DISTRIBUTION



(t/c)SOB	(t/c)OUTBOARD
0.14	0.08
0.15	0.10
0.16	0.12
0.17	0.14

Figure 54 Effect of Wing Planform Geometry on Cruise Mach



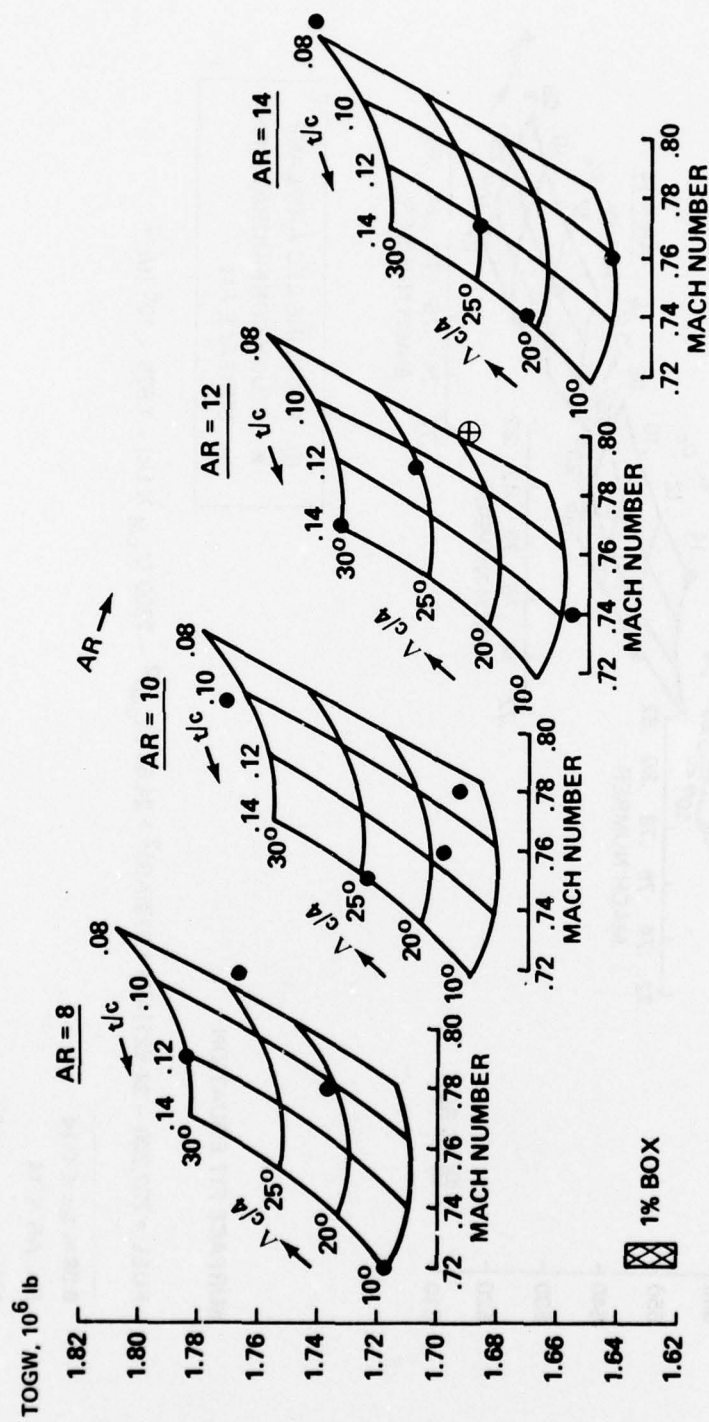
- ⊕ BASELINE LFC AIRPLANE
- STUDY CONFIGURATIONS
- SURFACE FIT

SURFACE FIT EQUATION:

$$\text{FUEL} = 732,200 - 24,621(\text{AR}) + 613(\text{AR})^2 + 24.59 (\Lambda_{c/4} \times t/c) - 7209 (\Lambda_{c/4})^2 - 1.875 \times 10^6 (t/c)^2$$

- $0.08 \leq t/c \leq 0.14$
- $8 \leq \text{AR} \leq 14$
- $10^\circ \leq \Lambda_{c/4} \leq 30^\circ$

Figure 55 Effect of Wing Planform Geometry on Fuel



SURFACE FIT EQUATION:

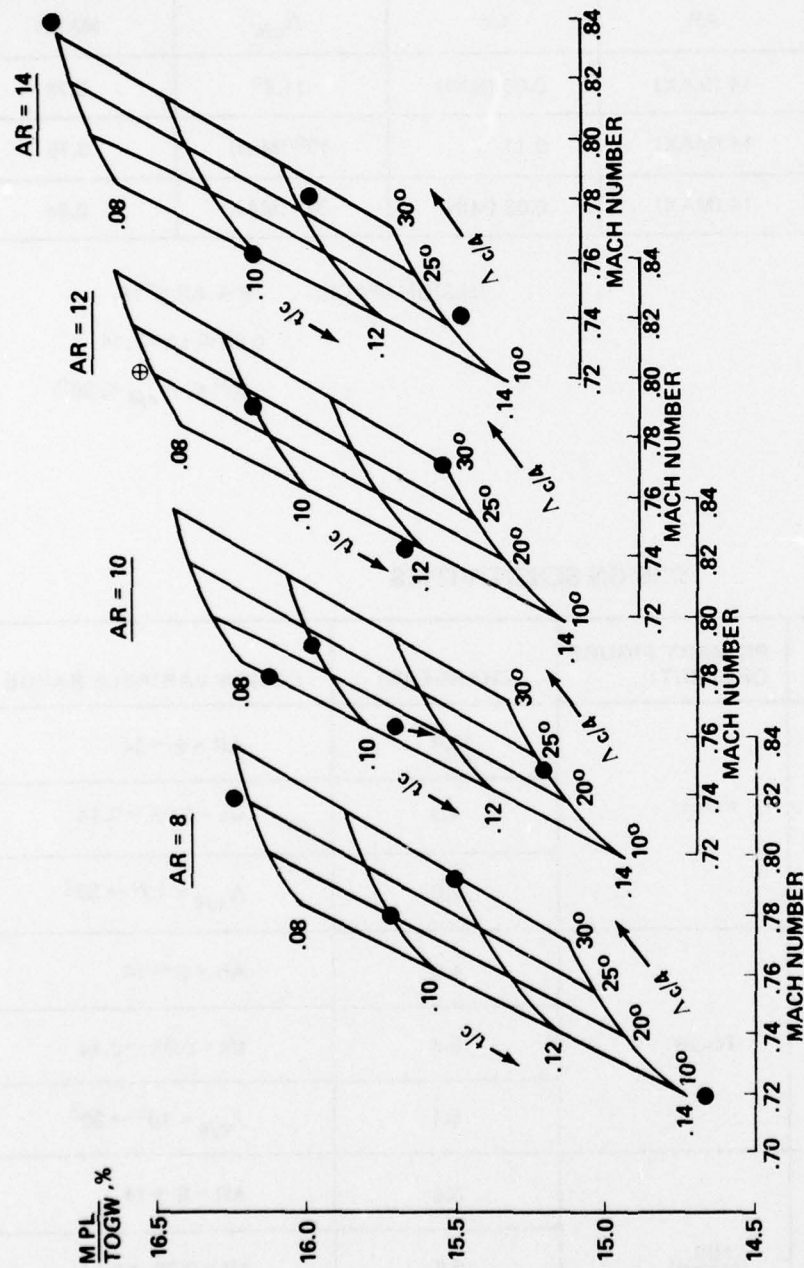
$$\text{TOGW} = 1,958,790 - 25,968(\text{AR}) - 1,700,400 (t/c) + 684(\text{AR})^2 + 165.7 (\Delta c/4)^2 - 24,070 (\Delta c/4 \times t/c) + 9,060,000 (t/c)^2$$

$$0.08 \leq t/c \leq 0.14$$

$$8 \leq \text{AR} \leq 14$$

$$10^\circ \leq \Delta c/4 \leq 30^\circ$$

Figure 56 Effect of Wing Planform Geometry on Weight



- ⊕ BASELINE LFC AIRPLANE
- STUDY CONFIGURATIONS
- SURFACE FIT

SURFACE FIT EQUATION:

$$\frac{M PL}{TOGW} = 16.93 + 0.1008(AR) - 22.92(t/c) + 0.1446(\Lambda_{c/4} \times t/c)$$

$$0.08 \leq t/c \leq 0.14$$

$$8 \leq AR \leq 14$$

$$10^\circ \leq \Lambda_{c/4} \leq 30^\circ$$

Figure 57 Effect of Wing Planform Geometry on Productivity

OPTIMUM CONFIGURATIONS

FIGURE OF MERIT	AR	t/c	$\Lambda_{c/4}$	MACH
MINIMUM FUEL	14 (MAX)	0.08 (MIN)	11.6°	0.78
MINIMUM TOGW	14 (MAX)	0.11	10° (MIN)	0.75
MAXIMUM $\frac{MPL}{TOGW}$	14 (MAX)	0.08 (MIN)	30° (MAX)	0.84

DESIGN SPACE: $8 < AR < 14$

$0.08 < t/c < .14$

$10^\circ < \Lambda_{c/4} < 30^\circ$

DESIGN SENSITIVITIES

CONFIGURATION	PRIMARY FIGURE OF MERIT:	CHANGE (%)	DESIGN VARIABLE RANGE
MINIMUM FUEL A/P	FUEL:	12.9	AR = 8 → 14
		4.0	t/c = 0.08 → 0.14
		1.6	$\Lambda_{c/4} = 10^\circ \rightarrow 30^\circ$
MINIMUM TOGW A/P	TOGW:	4.0	AR = 8 → 14
		0.6	t/c = 0.08 → 0.14
		5.1	$\Lambda_{c/4} = 10^\circ \rightarrow 30^\circ$
MAXIMUM $\frac{MPL}{TOGW}$ A/P	$\frac{MPL}{TOGW}$:	3.6	AR = 8 → 14
		6.6	t/c = 0.08 → 0.14
		1.4	$\Lambda_{c/4} = 10^\circ \rightarrow 30^\circ$

Figure 58 Laminar Flow Control Wing Optimization Study Results

6.3.2 EASE OF LAMINARIZATION

A low chord Reynolds number and a low unit Reynolds number are desirable to ease the task of laminarization. All of the LFC wing parametric study configurations represented by the regression analysis equations have average cruise maximum chord length Reynolds numbers and average unit Reynolds number contained in the shaded bands of data in Figure 59.

The maximum chord Reynolds number achieved by the X-21 flight test program was 47.3×10^6 (17 18). Reynolds numbers of approximately 60×10^6 have been achieved in wind tunnel tests (19 20). Results in Figure 59 show that a high aspect ratio is necessary to limit the maximum chord Reynolds number.

Study results also indicate that all configurations cruised at a Mach number and cruise altitude combination such that the unit Reynolds was 1.5×10^6 . To cruise at a higher altitude without incurring a significant performance penalty would probably require a different engine-cycle selection.

Another important parameter that affects the ease of laminarization is the attachment line momentum thickness Reynolds number, $R_{\theta_{AL}}$. If the attachment line momentum thickness Reynolds number exceeds approximately 100, disturbances may propagate spanwise along the wing LE, destroying laminar flow over a significant portion of the wing (20 21). Exceeding this limit would require special treatment, such as suction around the LE with chordwise slots, or locally reduced LE radii (20 21). The effect of typical values of LE suction on the allowable equivalent unsucked momentum thickness Reynolds number is shown in Figure 60. Low wing sweep is seen to be most important to achieve low values of $R_{\theta_{AL}}$. Low thickness ratios and high aspect ratio are also desirable. Low sweep also is desirable to eliminate boundary layer crossflow instability concerns.

17. Wheldon, W. G. and Whites, R. C., *Flight Testing of the X-21A Laminar Flow Control Airplane*, AIAA Paper No. 66-734, Sept. 1966.
18. Kosin, R. E., *Laminar Flow Control by Suction as Applied to the X-21 Airplane*, AIAA Paper No. 64-284, July 1964.
19. Gross, L. W., *Experimental and Theoretical Investigation of a Reichardt Body of Revolution with Low Drag Suction in the NASA Ames 12 ft Pressure Tunnel*, Northrop Report NOR-63-46, BLC-148, July 1963.
20. Gross, L. W., *Investigation of a Reichardt Body of Revolution with Low Drag Suction in the Norair 7 x 10 ft Wind Tunnel*, Northrop Report BLC-143, NOR 62-126, 1962.
21. Pfenninger, W. and Reed, V. D., "Laminar Flow Research and Experiments," *Astrodynamics and Aeronautics*, July 1966, pp44-50.

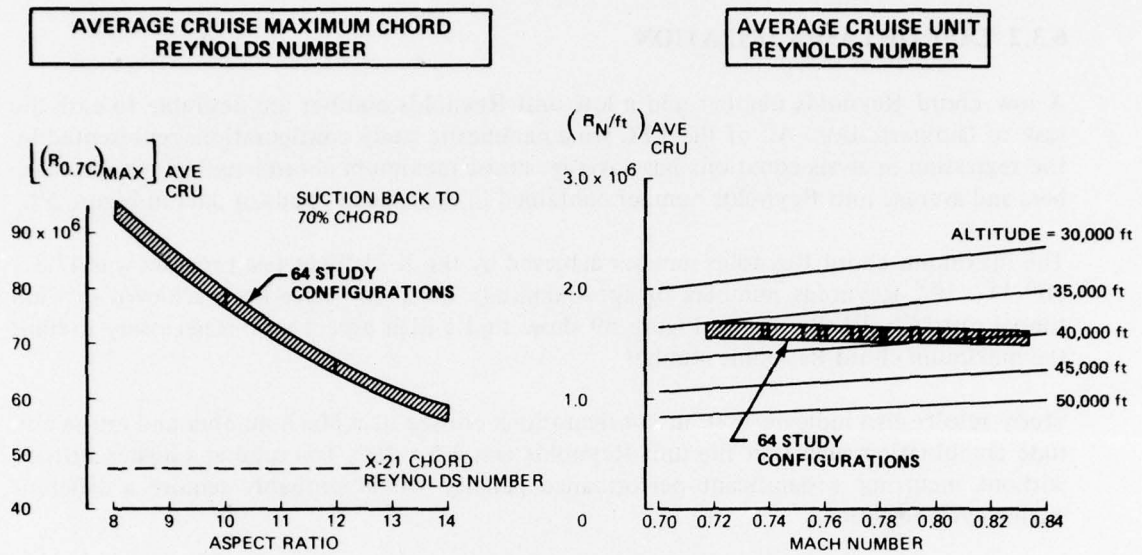


Figure 59 Effect of Wing Planform Geometry on Ease of Laminarization

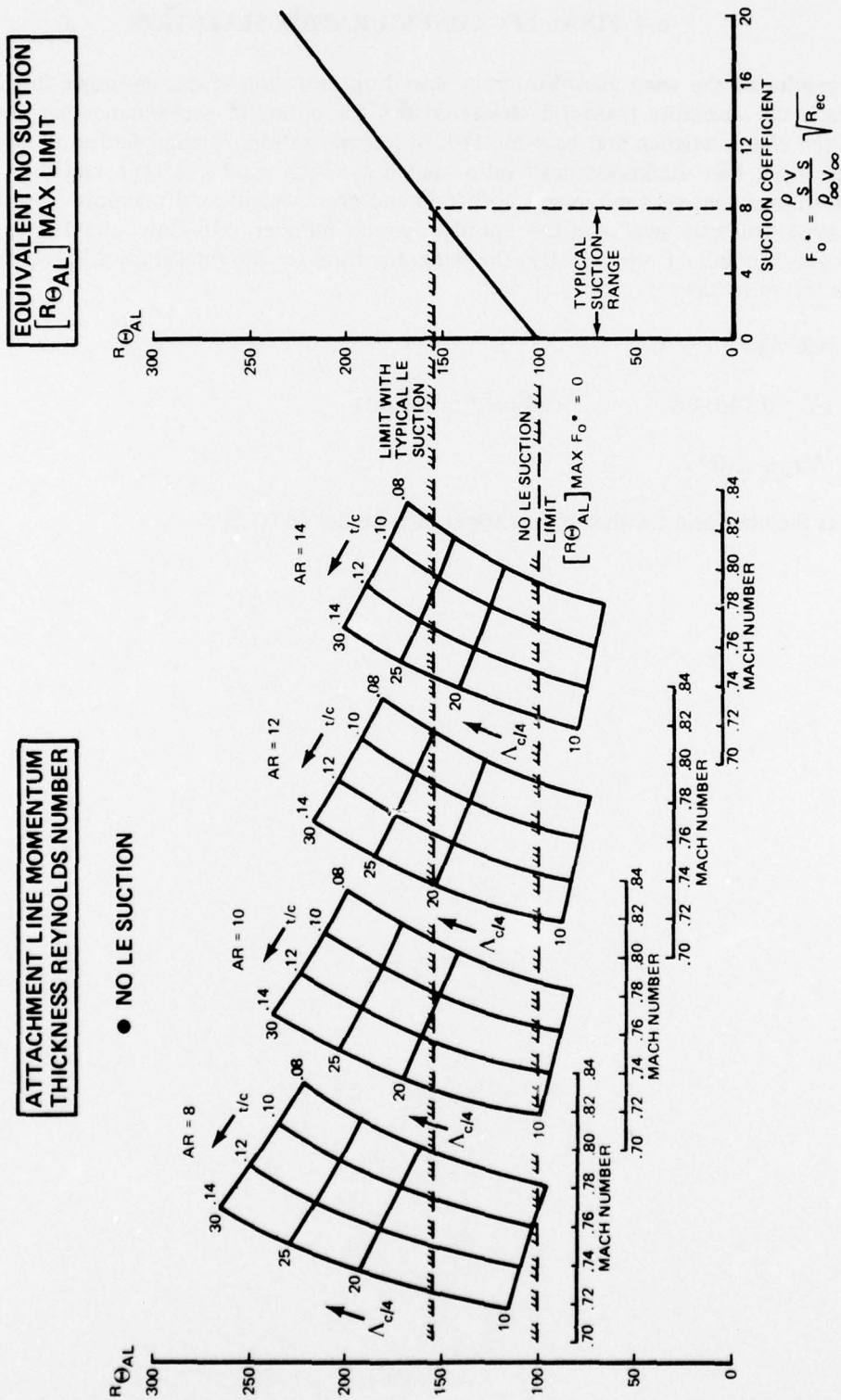


Figure 60 Effect of Wing Planform Geometry on Ease of Laminarization (Cont)

6.4 FINAL LFC CONFIGURATION SELECTION

The results of the wing planform/cruise speed optimization study, as shown in Figure 61, indicate the desirable planform characteristics for optimum performance are compatible with the characteristics that ease the task of laminarization. A wing planform having a high aspect ratio, low thickness/chord ratio, and low sweep results in approximately the optimum arrangement that minimizes both fuel and gross weight, and maximizes productivity. The same geometry results in low chord Reynolds number, crossflow, and attachment line Reynolds numbers. Consequently, the wing planform for the final study LFC configuration was selected to have:

- $AR = 14$
- $t/c = 0.14/0.08$ (inboard/outboard)
- $\Lambda_{C/4} = 10^\circ$

This is the planform for the LFC configuration Model 767-773.

FIGURE OF MERIT		WING DESIGN PARAMETER		
		ASPECT RATIO	THICKNESS RATIO	SWEEP
PERFORMANCE	MINIMUM FUEL	HIGH	LOW	NMC
	MINIMUM TOGW	HIGH	NMC	LOW
	MAXIMUM $\frac{MPL}{TOGW}$	HIGH	LOW	NMC
EASE OF LAMINARIZATION	LOW CHORD REYNOLDS NUMBER	HIGH	NMC	NMC
	LOW UNIT REYNOLDS NUMBER	NMC	NMC	NMC
	MINIMIZE CROSS FLOW	NMC	LOW	LOW
	MINIMIZE LE CONTAMINATION	HIGH	LOW	LOW

• NMC: NOT A MAJOR CONSIDERATION

Figure 61 Desirable Laminar Flow Control Wing Planform Characteristics

7.0 CONFIGURATION ANALYSIS AND METHODS

This section contains a description of design and analysis methods used in the study. Technology levels assumed in development of the configurations are identified. Some of the configuration analyses also are presented.

7.1 AERODYNAMICS

Aerodynamic tasks included the following:

- Definition of advanced aerodynamic technology levels for the study configurations
- Development of necessary aerodynamic design definitions of the study configurations
- Definition and evaluation of the high lift systems
- Calculation of suction flow requirements for laminarization of the wing and tail surfaces
- Calculation of the aerodynamic characteristics of study configurations to provide necessary data for performance and economic evaluations in addition to trade, sensitivity and optimization studies.

7.1.1 AERODYNAMICS TECHNOLOGY

Advanced aerodynamic technology assumptions included in the study configurations are summarized in Figure 62. This figure shows drag divergence boundaries for airfoils having different technology levels. The indicated progress in achieving higher Mach capability has been accomplished by the design of upper surface shapes with extensive supersonic regions at cruise condition with negligible wave drag, and by the distribution of lift towards the rear of the airfoil.

The maximum level of local Mach number on the upper surface is limited by the onset of significant wave drag. The chordwise extent of supersonic flow is limited by the ability of the airfoil to retain attached flow through the steep recovery pressure gradients near the trailing edge. Progress beyond the current level of airfoil technology will probably require the use of boundary layer control by suction or blowing to prevent separation in the closure regions of the airfoil. Hence, improvements in critical Mach number might be achievable with a properly designed LFC system. A critical Mach improvement of $Mach = 0.01$ was assumed for the LFC configurations. The LFC configurations also incur an indirect improvement in critical Mach number because the cruise lift coefficient, and, therefore, the design lift coefficient of an LFC wing, is less than that of an equal aspect ratio turbulent flow wing. A reduced design C_L allows either an increase in speed for the same thickness or an increase in thickness at the same speed.

The study configurations have high aspect ratio wings, and low trim drag through an aft cg location permitted by the augmented stability system. These are aerodynamic benefits derived from advances in structures, materials, and flight control technology.

- ADVANCED HIGH-SPEED AIRFOILS
- ADVANCED AERODYNAMIC DESIGN METHODOLOGY
- WING-BODY-NACELLE DESIGN INTEGRATION
- AFT-BODY AND FORE-BODY SHAPE
- LOW TRIM DRAG (AFT CG)
- HIGH ASPECT RATIO WING
- (BOUNDARY LAYER CONTROL)
- (LAMINAR FLOW CONTROL)

AIRFOIL TECHNOLOGY ENVELOPES

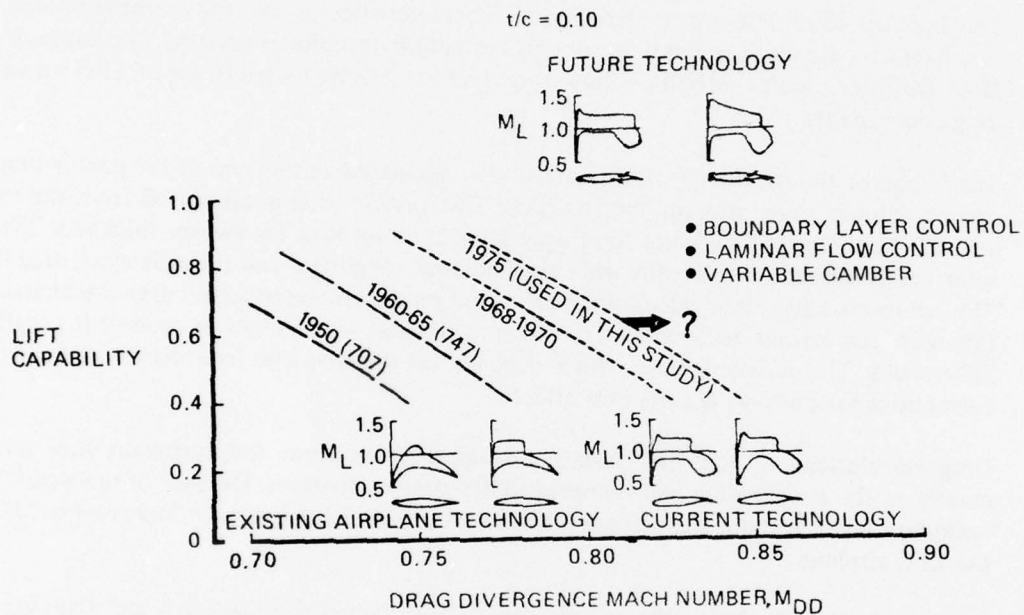


Figure 62 Advanced Aerodynamic Technology

The reference turbulent and the LFC configurations have engines located on the wing. This location of the engines, as previously mentioned in Section 3, was required to balance the airplane. It has been assumed that advanced aerodynamic design methodology would allow the development of an integrated wing-body-nacelle design with minimum interference drag. Furthermore it has been assumed that aerodynamic design methods together with the development of a suitable quiet engine would allow locating the engines on the wing without destroying laminar flow.

7.1.2 CRUISE AERODYNAMIC ANALYSES

The flaps-up climb and cruise aerodynamic characteristics of the study configurations were calculated by standard preliminary design evaluation techniques used by the contractor for large freighter studies. Modifications were made to account for effects of LFC on various drag components.

Total drag of the turbulent configuration was calculated as the sum of the profile drag and compressibility drag, plus the induced drag. The profile drag is calculated from the wetted area friction drag by applying form drag factors to account for sweep, thickness, lift, and interference effects. The profile drag also includes roughness and miscellaneous drag items. The compressibility drag calculations are based on experimental airfoil drag rise characteristics with corrections to account for sweep, thickness, and design or cruise lift coefficient differences. The induced drag, which depends on the spanwise load distribution, includes corrections for body-wing carryover effects.

Drag calculations of the LFC configurations differed from the turbulent flow analyses mainly in the profile drag and compressibility drag evaluations. Because of the reduction in boundary layer growth, the critical Mach number was assumed to be increased by 0.01 for the LFC airplane.

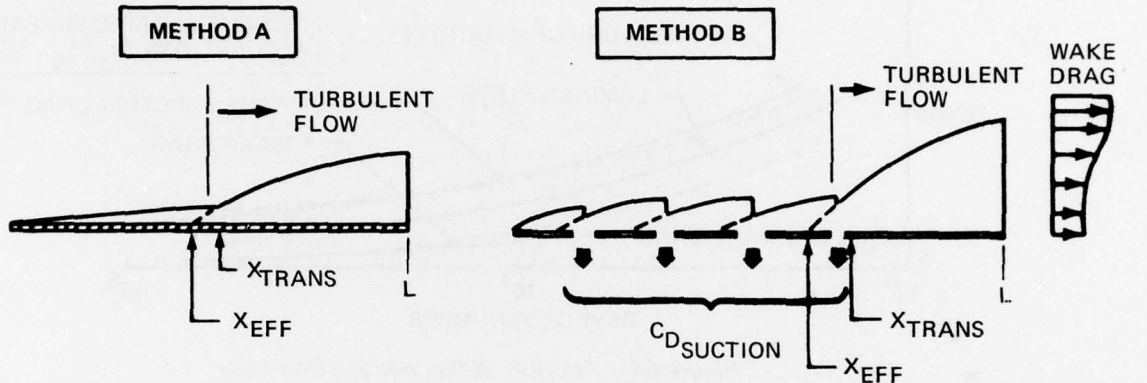
Procedures for calculating the profile drag of the laminarized surfaces are summarized in Figure 63. Two methods that differed only in the initial step were used initially. In both methods, transition was assumed to occur immediately downstream of the last suction slot. In method A, the effective origin of the downstream turbulent boundary layer was determined using the LFC wake drag coefficient data in Figure 64 obtained from Reference 23.

In Method B, a piecewise laminar boundary layer calculation procedure similar to the method of Reference 24 is used to calculate boundary layer growth along the slotted surface. The suction flow for each slot is determined from the boundary layer suction calculations in Section 7.1.4. Downstream laminar boundary layer growth matches the momentum remaining in the boundary layer passing over the slot after the lower portion is sucked off. At the last slot, the downstream turbulent boundary layer growth match is the remaining momentum of the flow over the last slot. This method also provides an evaluation of the suction drag that equals the sum of the momentum of the flow sucked through each slot. The calculated suction drag and wake drag coefficients agree well with corresponding drag curves in Figure 64. Because of its simplicity, method A was used for most of the drag evaluations.

23. Boyd, B. B., et al, *A Comparison of Medium Range Laminar Flow Control and Turbulent Airplane Designs*, Boeing Document D6-E10251-1, May 1974.
24. Smith, A. M. O., "Rapid Laminar Boundary-Layer Calculations by Piecewise Application of Similar Solutions," *Journal of Aeronautical Sciences*, Vol. 23, No. 10, Oct. 1956, pp901-912.

$$\text{LFC PROFILE DRAG} = C_{DF} [1 + K_F K_{XT} + K_L(C_L) K_{XT}] + C_{DP, \text{TURB WEDGE}}$$

STEP 1: CALCULATE " X_{EFF} "_{TURB}



- USE C_{DW} (FIGURE 64) TO DETERMINE X_{EFF}

$$\frac{\Delta C_{FT} X_{EFF}}{2} = \Theta_{TRANS} = \frac{X_{TRANS} C_{DW}}{2}$$

- PIECEWISE LAMINAR BOUNDARY LAYER CALCULATION
- SUCK OFF LOWER PORTION OF BOUNDARY LAYER
- START DOWNSTREAM GROWTH MATCHING REMAINING MOMENTUM THICKNESS TO DETERMINE EFFECTIVE ORIGIN FOR EACH SLOT
- AT LAST SLOT, MATCH REMAINING MOMENTUM THICKNESS TO DETERMINE TURBULENT EFFECTIVE ORIGIN

STEP 2: $C_{DF} = C_{FTURB} \left(\frac{L - X_{EFF}}{L} \right) \frac{A_{NET}}{A_{WET}} \dots$ CALCULATE C_{FTURB} FROM X_{EFF}

STEP 3: CALCULATE " K_F ", TURBULENT FLOW THICKNESS, SWEEP FORM FACTOR

STEP 4: CALCULATE " $K_L(C_L)$ " TURBULENT FLOW LIFT EFFECT FORM FACTOR, THIS VARIES WITH THE LIFT COEFFICIENT

STEP 5: CALCULATE " K_{XT} " PARTLY LAMINAR FLOW FACTOR (FIGURE 65)

STEP 6: CALCULATE $C_{DP, \text{TURB WEDGE}}$... PROFILE DRAG OF TURBULENT WEDGE AREAS

Figure 63 Laminar Flow Control Profile Drag Calculation Procedure

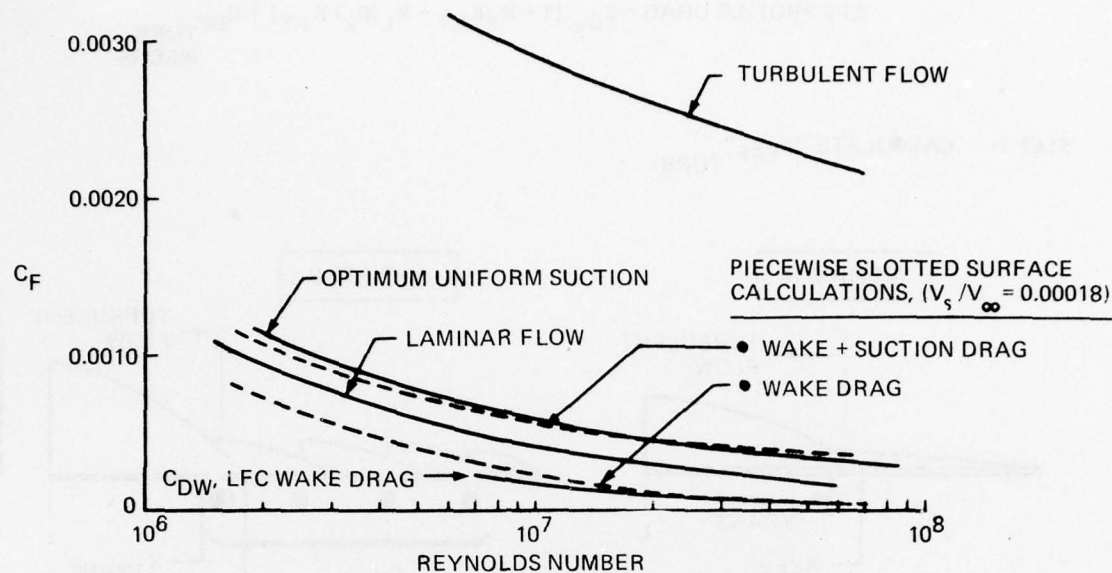


Figure 64 Friction, Wake, and Suction Drag

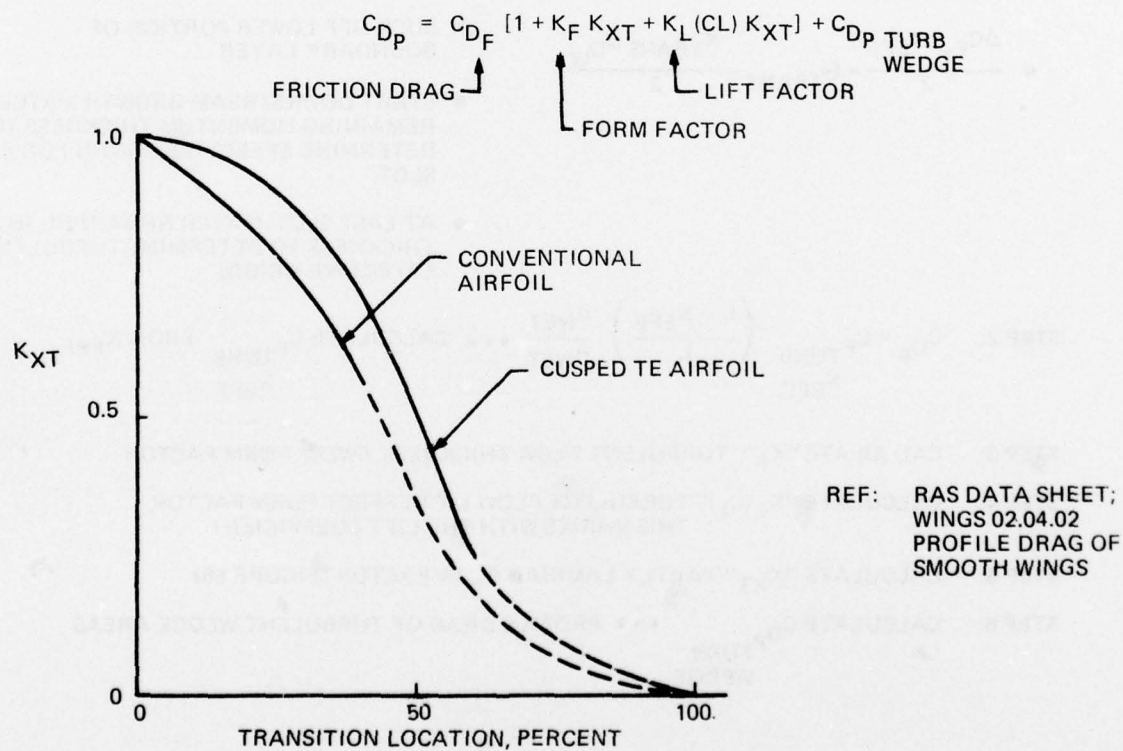


Figure 65 Profile Drag Factor for Transition Location

The second step of the calculation procedure is to compute the friction drag coefficient using the effective origin of the turbulent boundary layer.

Turbulent flow correction factors are then determined to account for airfoil shape, sweep, and thickness effects, and for lift coefficient variations.

In Step 5 (Figure 63), the partly laminar flow factor is determined using the data from Reference 25, (shown in Figure 65). The final step involves the calculation of the profile drag of the wedge areas of turbulent flow near the wing-body intersection, wing tip, and wing-nacelle strut intersections on the lower surface.

The calculated climb and cruise drag polars for the turbulent flow airplane Model 767-768 and the LFC Model 767-773 are shown in Figure 66.

7.1.3 LOW-SPEED AERODYNAMIC ANALYSES

The low-speed aerodynamic characteristics of the study configurations were estimated by methods used by the contractor for preliminary design configurations on which wind tunnel data do not exist. In general, the procedures are based on theoretical considerations, but are tempered by flight test and wind tunnel data wherever applicable. For rapid evaluation of low-speed characteristics, the procedures described briefly below have been programmed for processing by the CDC 6600 computer.

The basic flaps-up lift curve was constructed from a zero angle of attack intercept and a lift curve slope that is a function of aspect ratio, thickness ratio, and quarter-chord sweep angle. The slope was adjusted for the effect of the body and for the addition to wing planform area affected by the extension of leading- and trailing-edge flaps. The maximum lift coefficient of the basic, flaps-up wing was determined according to aspect ratio and quarter-chord sweep angle.

Leading-edge devices reduce the lift coefficient in the linear lift range, and this effect was computed using a theoretical value for flap effectiveness and part span effects. The lift increments due to trailing-edge flaps were determined from empirical section flap effectiveness data. Adjustments were made to account for three-dimensional effects and the geometry of the flap system.

The maximum lift increments due to leading-edge and trailing-edge flaps were determined from empirical data that have been correlated in terms of the ratio of leading-edge-device area to wing area, ratio of trailing-edge-device area to wing area, and ratio of wing area subtended by flaps to total wing area.

Drag polars were constructed by estimating the minimum parasite drag of the flaps-up configuration at typical takeoff and landing Reynolds numbers at sea level. Increments to minimum parasite drag for leading- and trailing-edge devices were added from test data correlated on the basis of flap-to-wing area ratios, flap-chord ratios, type of flaps, and flap deflection. Slotted, trailing-edge-flap parameters were evaluated in terms of the extended flap-chord ratios.

-
25. R. A. S. Aerodynamic Data Sheets, WINGS 02.04.02, *Profile Drag of Smooth Wings*, May 1969.

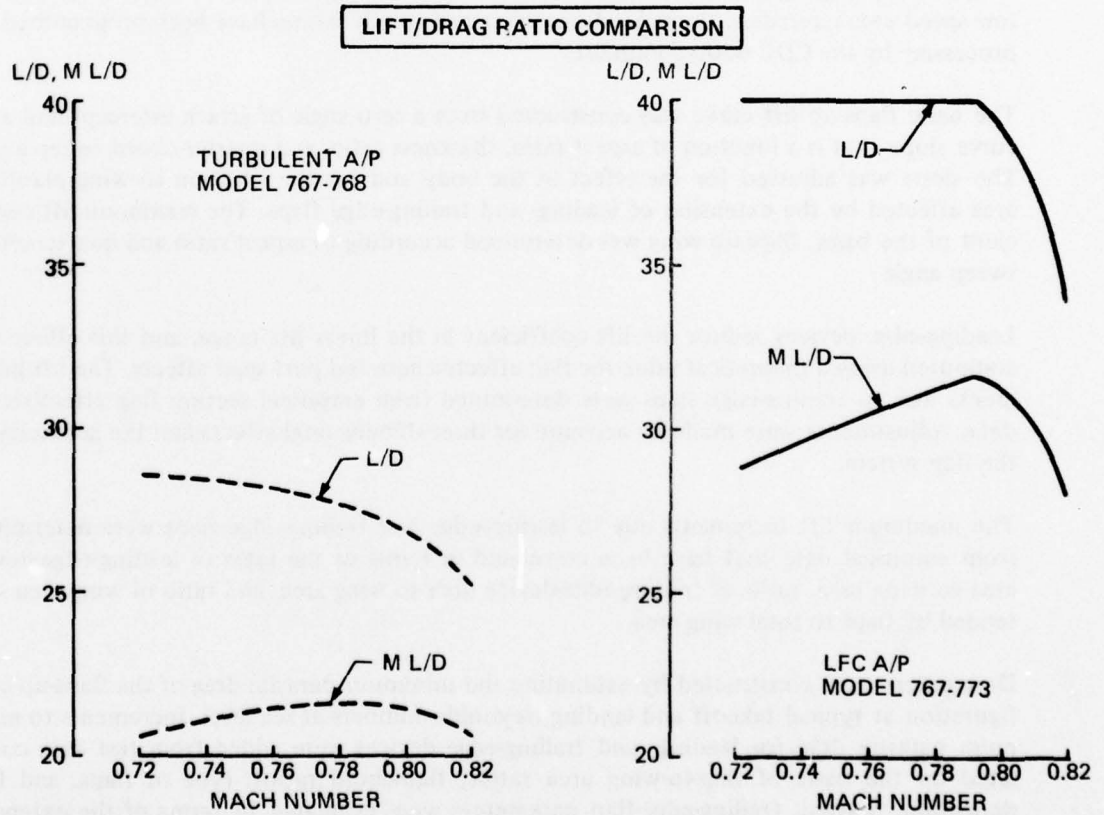
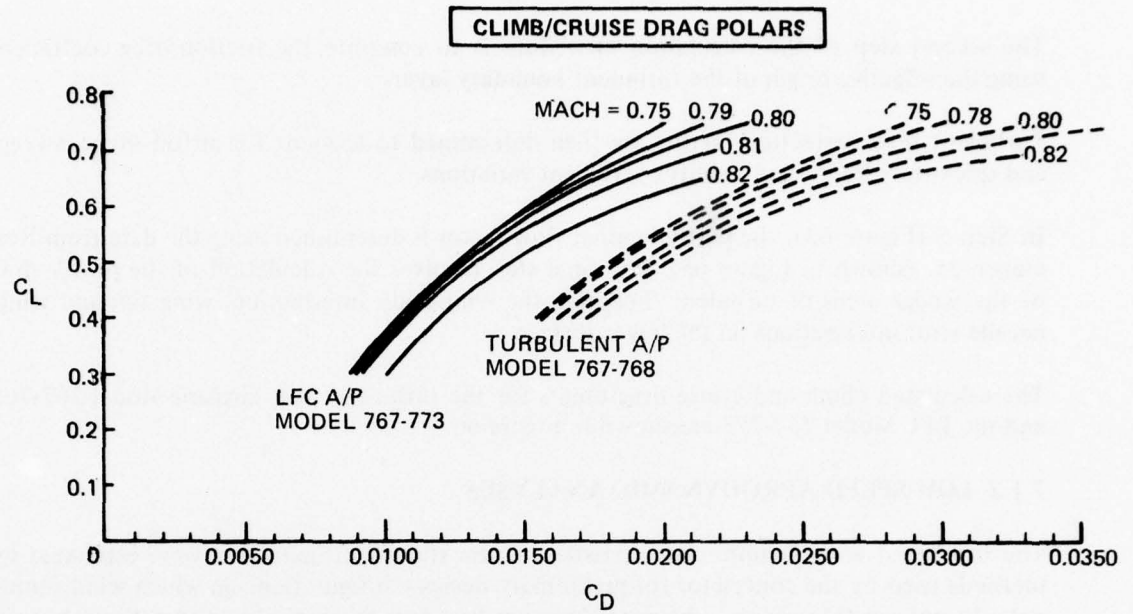


Figure 66 Laminar Flow Control and Turbulent Configurations Cruise Aerodynamic Data

Drag due to lift was added as $C_L^2/\pi AR$ then modified by additional drag terms. Additional parasite drag, ΔC_{DP} , was applied as a function of $C_L - C_{LP}$, necessitating the determination of an increment to C_{LP} for leading- and trailing-edge devices. Again, this was evaluated from empirical data as a function of planform area to wing area for the leading-edge flap and as a function of lift increment for the trailing-edge flap. An additional drag due to lift, ΔC_{DITE} , term was added to account for the discontinuous span loading due to the part-span flaps. This term was evaluated using constants obtained from Royal Aeronautical Society data sheets.

Pitching moments were evaluated by first estimating the zero lift pitching moment, C_{MO} and aerodynamic center of the basic flaps-up configuration, then adding the increment produced by the flap lift acting at its estimated center-of-lift position.

The high-lift system of the reference turbulent configuration, Model 767-768, includes Boeing 747 SP-type single-slotted trailing-edge flaps and variable camber leading-edge flaps. The trailing-edge flap has a chord ratio, (C_F/C) , of 0.225 and a flap Fowler motion, (C'/C) , of 1.08. Figure 67 summarizes the low speed aerodynamic data of this configuration. A 1-g stall was assumed in the generation of these data along with a 1.1 scale factor for correction from wind tunnel to full-scale C_{LMAX} values.

The high lift systems of the LFC configurations considered in this study had the same trailing- but no leading-edge devices. The inboard and outboard ailerons of the LFC configurations can be dropped to 10 deg.

The low-speed lift and drag characteristics of the final LFC configuration, Model 767-773, are shown in Figure 68. This figure also includes estimated takeoff and landing speeds. The LFC configurations were assumed to have fully turbulent flow drag levels for takeoff and landing.

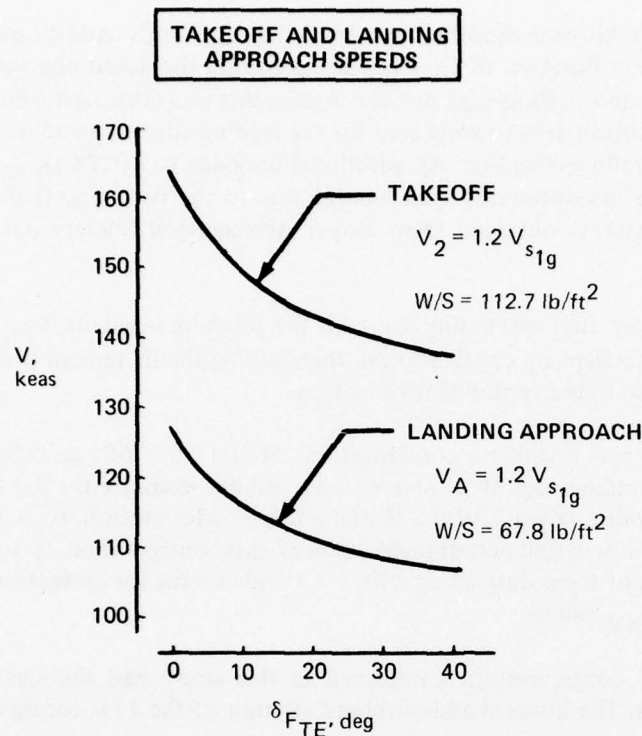
7.1.4 LAMINAR BOUNDARY LAYER ANALYSES

Boundary layer suction requirements for the laminarized surfaces of the study LFC configurations were calculated by the iteration procedure shown in Figure 69. Three types of boundary layer instabilities were considered:

- Tollmien-Schlichting tangential instability
- Crossflow instability
- Leading edge spanwise flow contamination

The method used is a mixture of empirical transition criteria and analytical boundary layer growth calculations.

The first step of the calculation procedure is to define airfoil and planform geometry and generate surface pressure distribution. An initial suction distribution is then selected.



MODEL 767-768

- $S_W = 14,785 \text{ ft}^2$
- $AR = 12$
- $\Lambda_{c/4} = 20^\circ$
- FULL-SPAN LE DEVICES
- SINGLE SLOTTED TE FLAPS
- $b_F/b = 0.684$
- $c_{F/c} = 0.225$
- $c'/c = 1.08$

MILITARY RULES (MIL-C-5011A)

- $V_2 \geq 1.2 V_{s1g}$
- $V_A \geq 1.2 V_{s1g}$

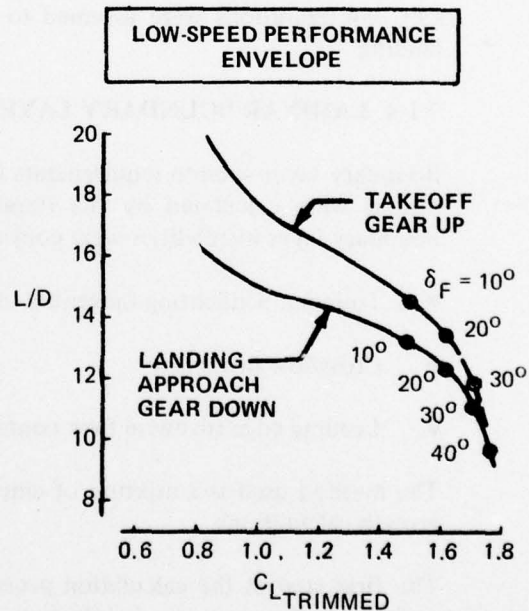
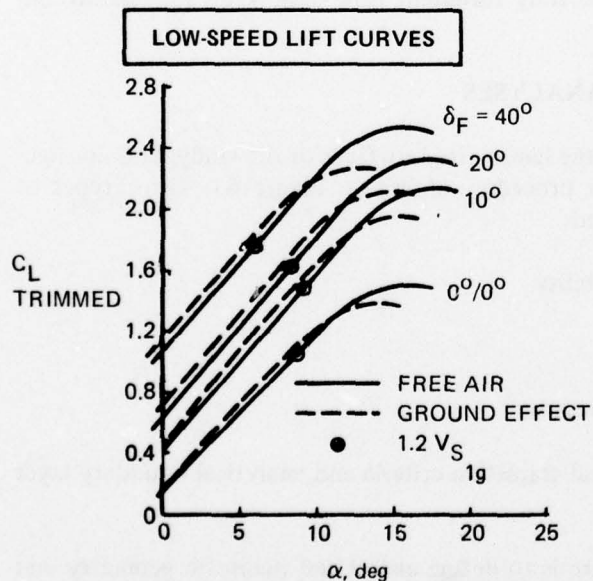
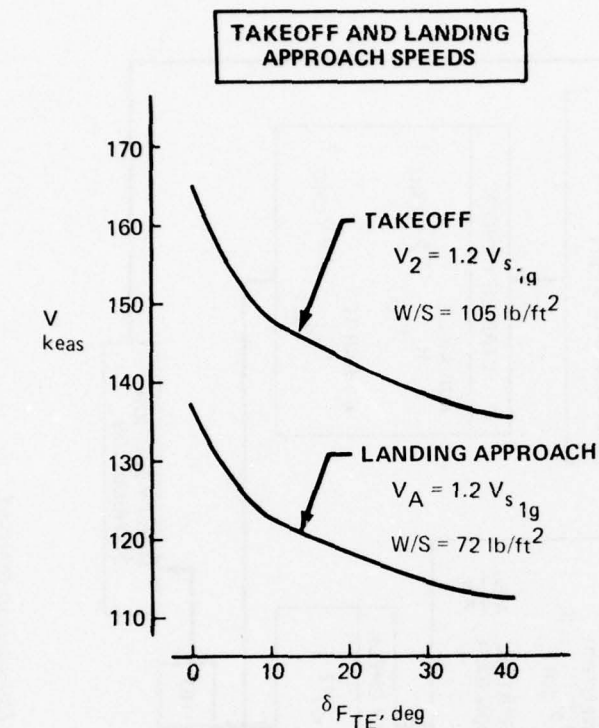


Figure 67 Low-Speed Aerodynamic Data for Turbulent Airplane, Model 767-768



MODEL 767-73

- $S_W = 14,780 \text{ ft}^2$
- $AR = 14$
- $\Lambda_{c/4} = 10^\circ$
- NO LE DEVICES
- SINGLE SLOTTED TE FLAPS
- $b_F/b = 0.683$
- $C_{F/c} = 0.225$
- $C'_{c/c} = 1.08$
- AILERON DROOP $\leq 10^\circ$

MILITARY RULES

(MIL-C-5011A)

- $V_2 \geq 1.2 V_{s1g}$
- $V_A \geq 1.2 V_{s1g}$

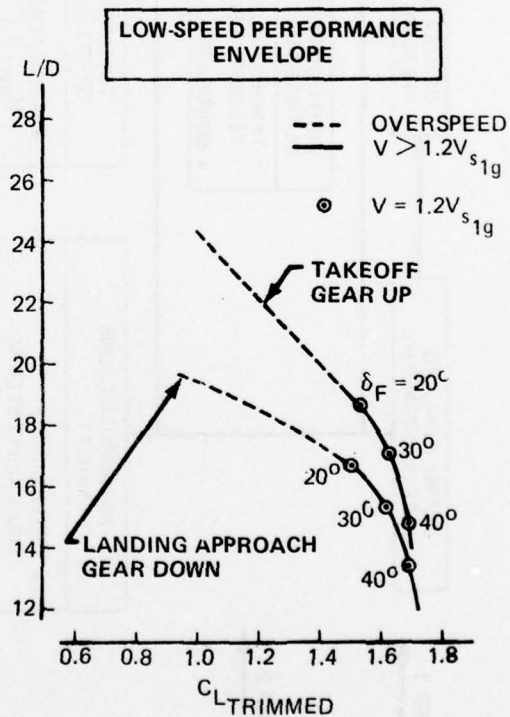
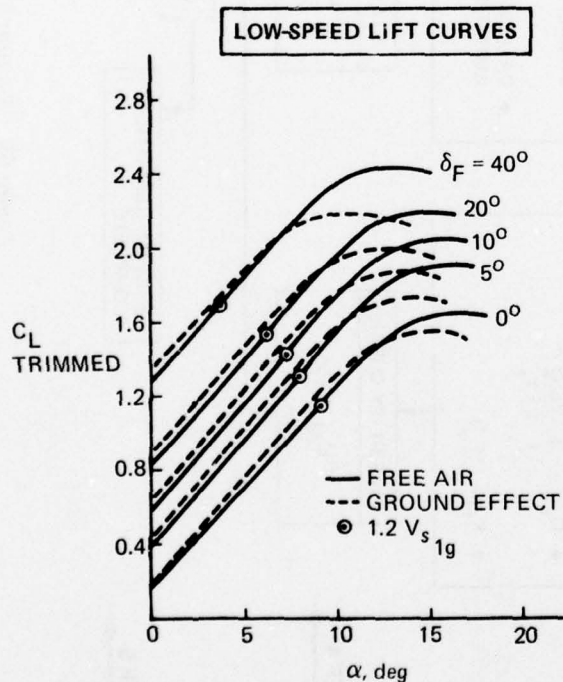


Figure 68 Low-Speed Aerodynamic Data for LFC Airplane, Model 767-773

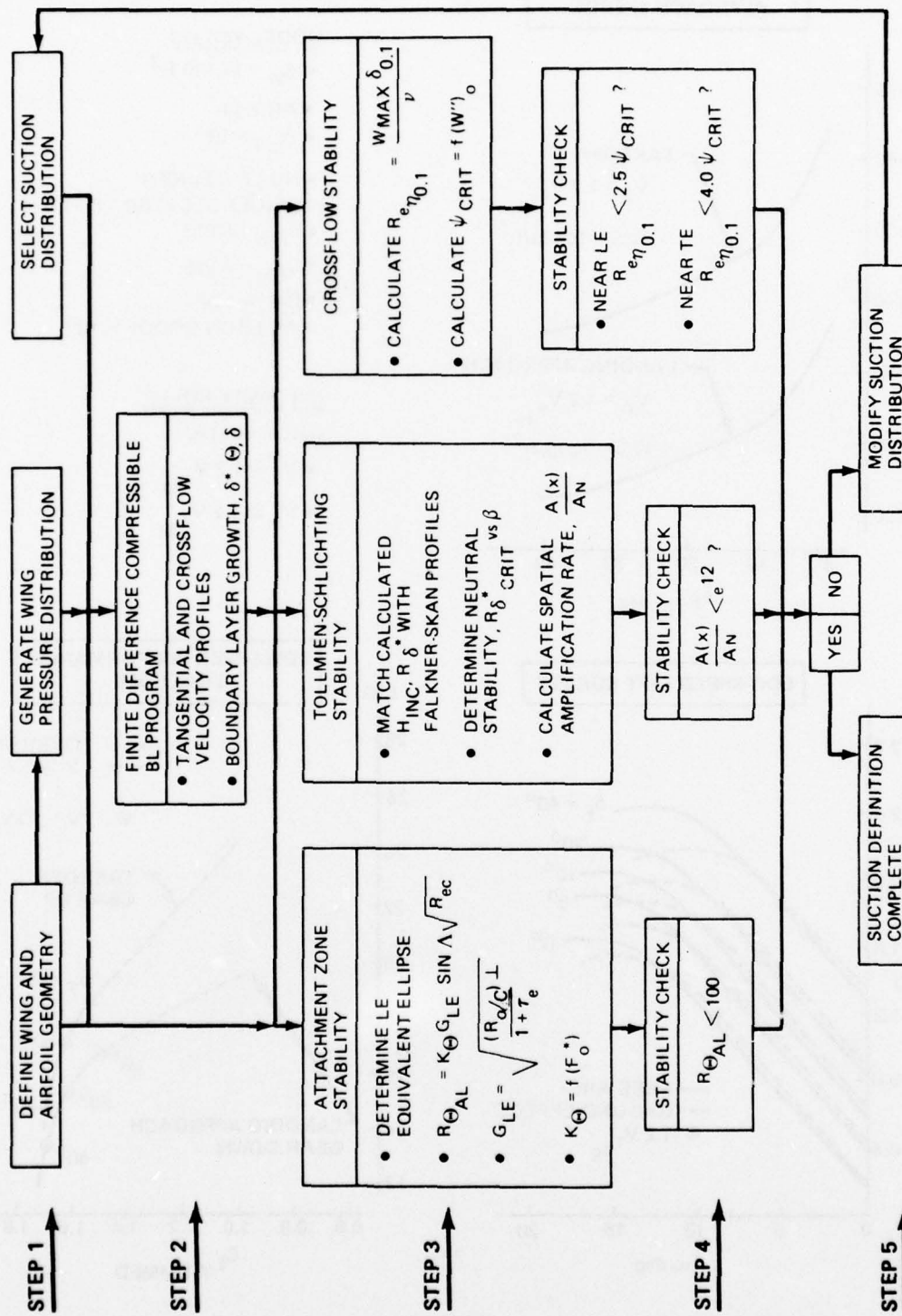


Figure 69 Suction Flow Calculation Method

A finite difference compressible laminar boundary layer program is used to calculate the tangential and crossflow velocity profiles. The displacement thickness, δ^* , momentum thickness, θ , and shape factor also are computed over the surface.

Boundary layer flow over the wing is evaluated for Tollmien-Schlichting stability following the method of Reference 26. The boundary layer program provides the incompressible shape factor, H_{INC} , and the displacement thickness Reynolds number R_{δ^*INC} as a function of arc-length normal to the leading edge. Calculated values of H_{INC} are matched with the Falkner-Skan shape factor, H_S , to obtain the pressure gradient parameter along the surface. The location of the neutral stability point is determined by comparing the computed values of R_{δ^*INC} with critical Reynolds numbers R_{δ^*CRIT} that depend on H_S .

Spatial amplification rate calculations then are started at the neutral stability point. A number of disturbance frequencies are selected. For each of the frequencies considered the amplification rate is determined using the Falkner-Skan profile stability data of Smith⁽²⁷⁾ corresponding to the appropriate value of β_{FS} on the surface. The amplification rate is integrated for each frequency along the surface distance. The disturbance frequency that produces the maximum integrated amplification factor is used. If the amplification factor exceeds e^{12} , transition is assumed to occur.

The crossflow velocity profiles calculated at various stations along the surface are used for crossflow stability calculations. The crossflow Reynolds number, $Re_{\eta_{0.1}}$, based on the maximum crossflow velocity and the boundary-layer thickness to the upper point at which one-tenth the maximum velocity occurs, is calculated along the surface. A minimum critical stability limit Reynolds number, ψ_{CRIT} , is calculated using Brown's⁽²⁸⁾ estimate $\psi_{CRIT} = 57-0.722 N_{ZZ}$ where N_{ZZ} is the nondimensional second derivative of the crossflow velocity profile at the surface and is obtained from the boundary layer calculation program. The criteria used for cross-stability was that $Re_{\eta_{0.1}}$ must be less than $2.5 \psi_{CRIT}$ and less than $4 \psi_{CRIT}$ near the leading and trailing edge, respectively.

To prevent any extensive spanwise contamination at the attachment line in the presence of leading edge disturbances, the attachment line Reynolds number, $R_{\theta_{AL}}$, should be less than 100⁽²⁹⁾. The attachment line momentum thickness Reynolds number was approximated by using a least-squares fit procedure to replace the leading edge region and the front part of the wing or tail surface by an equivalent ellipse of the same leading edge radius and geometry. The values of $R_{\theta_{AL}}$ along the leading edge were then calculated⁽³⁰⁻³¹⁾ in terms of the geometry of the equivalent ellipse, the leading-edge sweep angle, and the leading-edge suction distribution if leading-edge suction was found to be necessary.

26. Jaffe, N. A.; Okamura, T. T.; and Smith, A. M. O., "Determination of Spatial Amplification Factors and Their Application to Predicting Transition," *AIAA Journal*, Feb. 1970, pp301-308.
27. Wazzan, A. R.; Okamura, T. T.; and Smith, A. M. O., *Spatial and Temporal Stability Charts for the Falkner-Skan Boundary-Layer Profiles*, McDonnell Douglas Corp., DAC 67086, Sept. 1, 1968.
28. Brown, W. B., "A Stability Criterion for Three-Dimensional Boundary Layers," Vol. 2, *Boundary Layer and Flow Control*, edited by Lachmann, G. V., Pergamon Press, 1961.

The forementioned stability criteria were based on the recommendations and experimental work by Dr. Pfenninger^(30 31 32). If stability criteria were not satisfied, the selected suction distribution was modified and stability evaluation procedure was repeated until a suitable suction distribution was defined.

An example of the results of this calculation procedure is shown in Figure 70. This figure contains pressure distribution, suction distribution, and boundary layer stability evaluation data for the wing of the final LFC configuration Model 767-773.

7.2 FLIGHT CONTROLS

Flight control tasks included:

- Definition of advanced flight controls technology levels for the study configurations
- Estimation of horizontal and vertical tail sizes and center of gravity (cg) limits that satisfy critical stability and control criteria
- Provision of tail sizing information for airplane sizing, trade, and optimization studies.

7.2.1 FLIGHT CONTROL TECHNOLOGY

The turbulent baseline and the laminar flow airplanes were analyzed assuming 1985 active controls technology. Active control technology (ACT) functions include:

- Augmented stability (AS)
- Maneuver load control (MLC)
- Gust load alleviation (GLA)
- Flutter mode control (FMC)

The projections shown in Figure 71 indicate that large freighter airplanes with long range capability will benefit with increased performance and weight reduction by incorporating ACT into the control system. Use of active controls in conjunction with the application of advanced structural concepts and materials will permit the use of large-span high-aspect-ratio wings that are desirable for long-range airplanes.

29. Nenni, J. P. and Gluyas, G. W., "Aerodynamic Design and Analysis of an LFC Surface," *Astronautics and Aeronautics*, July 1966, pp52-57.
30. Pfenninger, W., "Flow Phenomena at the Leading Edge of Swept Wings," *AGARDograph* 97, May 1965.
31. Pfenninger, W., "Flow Problems of Swept Low-Drag Suction Wings of Practical Construction at High Reynolds Numbers," *Annals of the New York Academy of Sciences*, Vol. 154, Article 2, Nov. 22, 1968, pp672-703.
32. Pfenninger, W., "About the Development of Swept Laminar Suction Wings with Full Chord Laminar Flow," Vol. 2, *Boundary Layer and Flow Control*, edited by Lachmann, G. V., Pergamon Press, 1961.

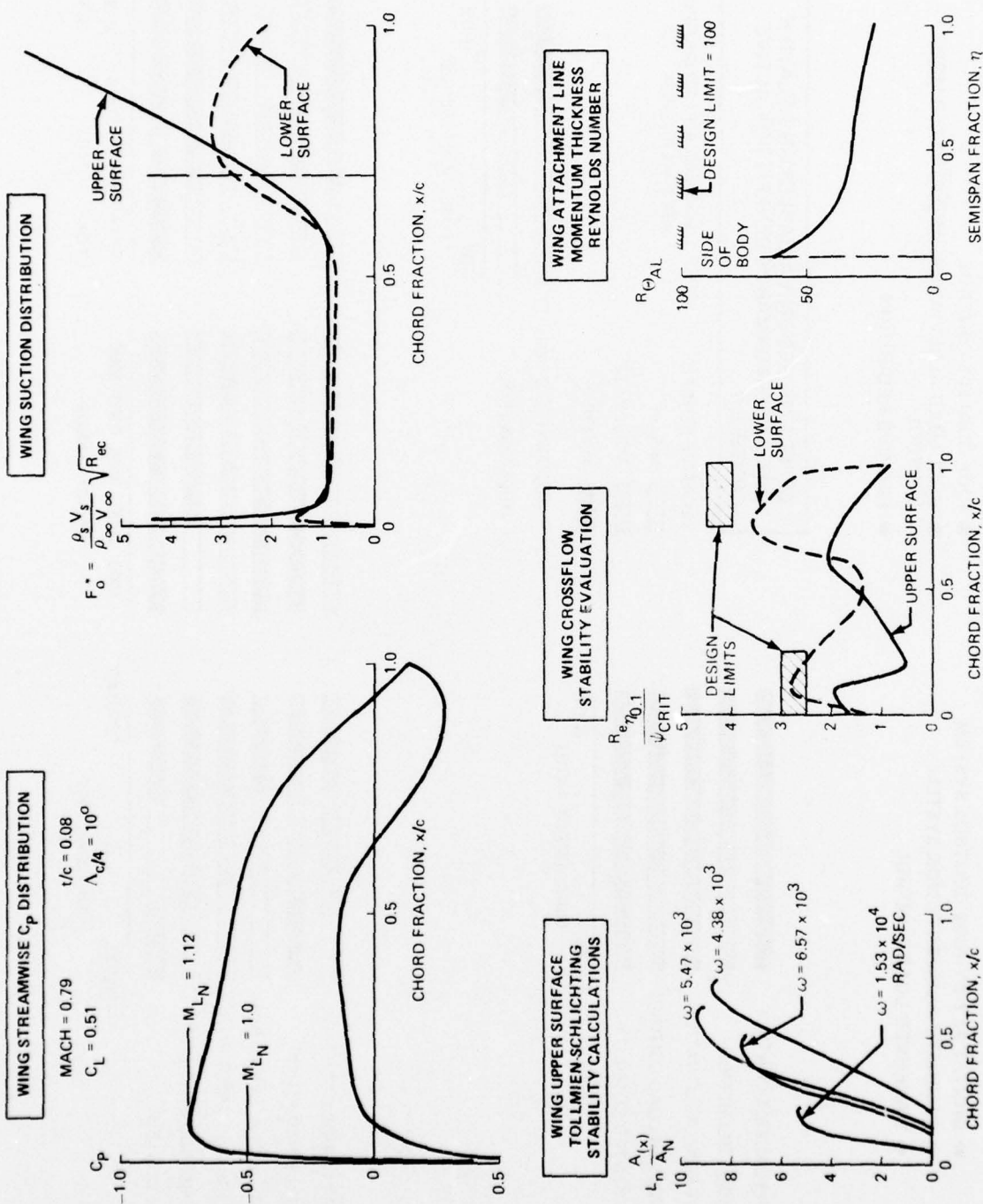
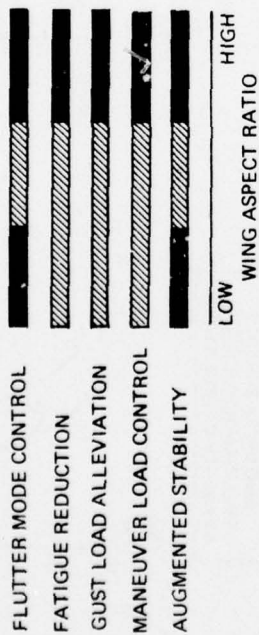


Figure 70 Model 767-773 Wing Suction Distribution and Boundary Layer Stability Evaluation

- DIGITAL FLY-BY-WIRE CONTROL SYSTEM
- STABILITY AUGMENTATION SYSTEM
- MANEUVER LOAD CONTROL

- RIDE QUALITY CONTROL
- GUST LOAD ALLEVIATION AND FLUTTER MODE CONTROL
- FATIGUE REDUCTION

EFFECT OF DESIGN VARIABLES ON RELATIVE DIRECT PERFORMANCE BENEFITS OF ACTIVE CONTROLS



RELATIVE BENEFIT
REF: SCHOENMAN AND SHOMBER
ASE PAPER 751051

- MINOR
- ▨ MODERATE
- MAJOR

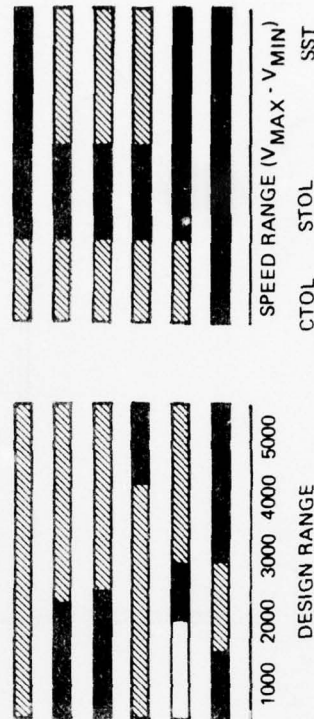
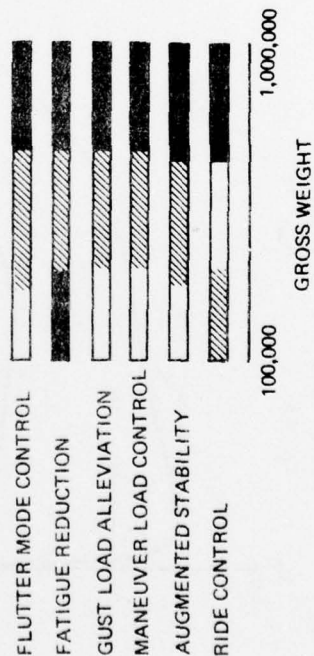
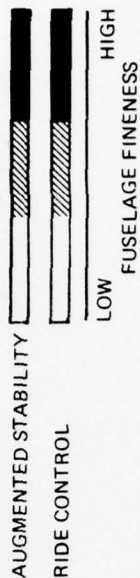


Figure 71 Advanced Flight Control Technology

The ACT functions employ a digital fly-by-wire (FBW) electrical command system with an analog backup and direct electrical link for the primary control system similar to the NASA digital FBW F8C test airplane. Except for flap tabs, all the ACT functions will drive normal airplane control surfaces. The ACT usage of the control surfaces is shown in Table 4.

7.2.2 AIRPLANE BALANCE AND TAIL SIZING

Longitudinal

The study airplanes have a fixed stabilizer with a single hinged elevator for longitudinal trim and control. The airplanes use a "handling qualities" stability augmentation system (SAS) to reduce tail size and trim drag by relaxing the aft flight cg limit. Because the SAS is not a flight-critical aircraft component, airplane stability must meet unaugmented minimum requirements at the aft flight limit. These include:

- Time to double amplitude, $t_2 \approx 6$ seconds at dive
- A 5-percent static margin at cruise and approach

Forward cg control requirements were considered for takeoff rotation and approach trim and flare. The airplane must meet pitch acceleration requirements, $\ddot{\theta}$, 3 deg/sec² for flare and 2 deg/sec² for takeoff rotation. Figure 72 is an example of the horizontal tail sizing procedure for the turbulent baseline and laminar flow airplanes. Only design conditions, dive stability, and takeoff rotation are shown.

Lateral-Directional

Both configurations have a " π " configuration vertical tail with double-hinged rudders.

The turbulent and laminar flow airplanes also have a handling qualities SAS in the lateral-directional axes that is assumed to provide satisfactory flying qualities throughout the flight envelope. The airplane will require an estimated minimum unaugmented static directional stability at least $C_{N\beta} = 0.0015/\text{deg}$ at the aft-most flight limit.

Directional control requirement was calculated using a static engine failure analysis at take-off. From the engine failure speed, $V_{MC\text{GROUND}}$, and the asymmetric thrust balance speed, V_{bal} , the airplanes, with full rudder, are assumed to deviate no more than 30 ft from the runway centerline while accelerating 10 kts; i.e., $V_{\text{bal}} = V_{MC\text{GROUND}} + 10$ kts.

7.3 PROPULSION AND NOISE

Propulsion-related tasks included:

- Definition of propulsion advanced technology levels for the study configuration
- Selection of main propulsion engine cycle characteristics
- Selection of suction engines
- Generation of installed performance data for main engines and suction engines
- Definition and sizing of suction pump compressors

Table 4 Active Control Technology Usage

CONTROL SURFACE	ACTIVE CONTROL TECHNOLOGY USAGE			
	AUGMENTED STABILITY	MANEUVER LOAD CONTROL	GUST LOAD ALLEVIATION	FLUTTER MODE CONTROL
Elevator	X		X	
Outboard aileron				X
Spoilers			X	
Flap tabs		X	X	

- NOTE:
- FIXED STABILIZER
 - $\Delta CG = 62.5$ in.
 - $t_2 = 6$ sec (UNAugMENTED)
 - $V_R = 146$ keas
 - $C_{LH} = -0.86$

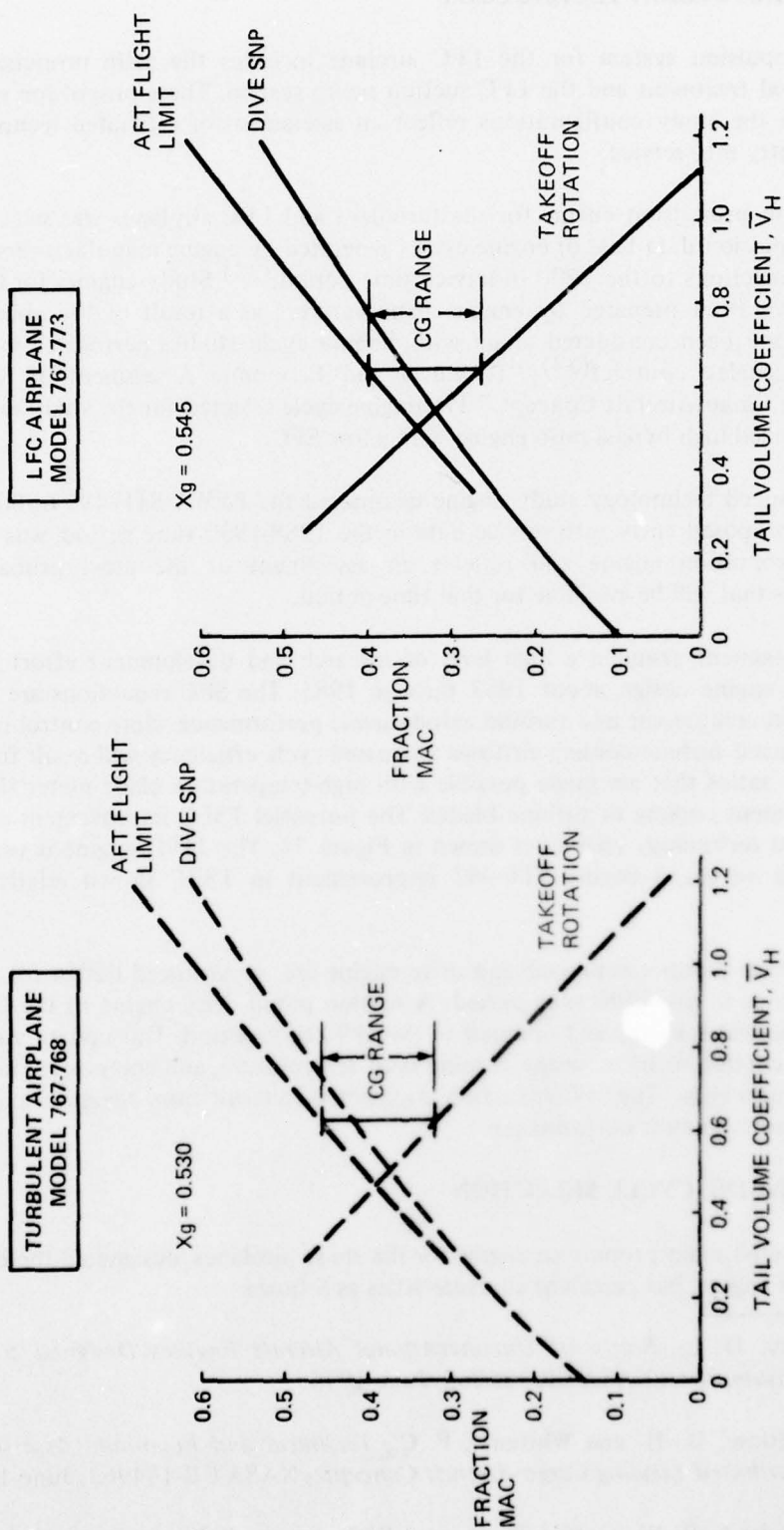


Figure 72 Horizontal Tail Sizing

7.3.1 PROPULSION TECHNOLOGY

The propulsion system for the LFC airplane includes the main propulsion engine with acoustical treatment and the LFC suction pump system. These propulsion systems incorporated in the study configurations reflect an assessment of estimated technology levels for 1990 entry into service.

The main propulsion engine for the turbulent and LFC airplanes was selected by utilizing the propulsion data base of engine cycles generated by engine manufacturers for technology level projections to the 1990 in-service time period.⁽³³⁾ Study engines for that time period that have been prepared by engine manufacturers as a result of the above NASA-Lewis study have been considered along with Boeing cycle studies performed in support of the NASA-Langley contract⁽³⁴⁾ "Technical and Economic Assessment of Span-Distributed Loading Cargo Aircraft Concept." The engine cycle selected for the study reported herein is an advanced high bypass ratio engine with a low SFC.

An advanced technology study engine designated the P&WA STF-482 turbofan engine⁽³⁵⁾, with a proposed entry into service date in the 1988-1990 time period, was selected for the main propulsion engine and reflects an assessment of the most probable technology advances that will be available for that time period.

The assessment assumed a high level of research and development effort from now until start of engine design about 1983 through 1985. The SFC reductions are associated with improved compressor and turbine aerodynamic performance, close control of rotating seals, and reduced turbine cooling airflows. Increased cycle efficiency will result from high overall pressure ratios that are made possible with high-temperature blade materials, and film and impingement cooling of turbine blades. The potential TSFC improvement during cruise for advanced technology engines is shown in Figure 73. The JT9D engine is used as a baseline with the advanced engine STF-482 improvement in TSFC shown relative to the JT9D engine.

The suction pump compressor and drive engine are an advanced design for proposed entry into service in the 1990 time period. A suction pump drive engine of the General Electric T64 type was selected and updated to the 1990 time period. This update assumes advanced turbine cooling to increase the turbine inlet temperature, and composite material to reduce the engine weight. The SFC reduction is expected to result from advances in compressor and turbine aerodynamic performance.

7.3.2 ENGINE CYCLE SELECTION

The selected main propulsion engine for the study airplanes, designated the P&WA STF-482 turbofan engine, has pertinent characteristics as follows:

33. Gray, D. E., *Study of Unconventional Aircraft Engines Designed for Low-Energy Consumption*, NASA CR-135065, June 1976.
34. Whitlow, D. H. and Whitener, P. C., *Technical and Economic Assessment of Span-Distributed Loading Cargo Aircraft Concepts*, NASA CR-144963, June 1976.
35. Goodrich, R. W.; Gaffin, W. O.; and Witherspoon, S. W., *Preliminary Performance and Installation Data for the STF-482 Turbofan Engine*, Pratt & Whitney Aircraft Report CDS-8, Nov. 1975.

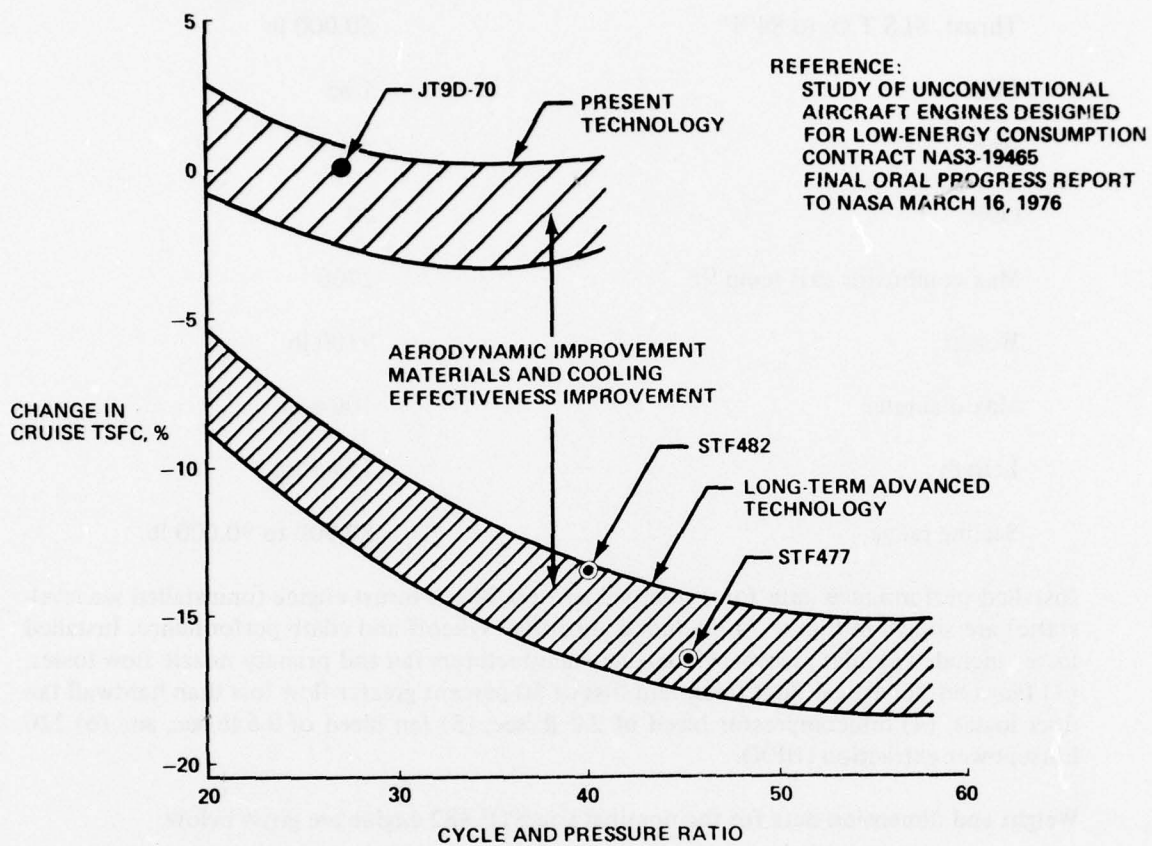


Figure 73 Potential Turbofan Fuel Consumption TSFC Improvement

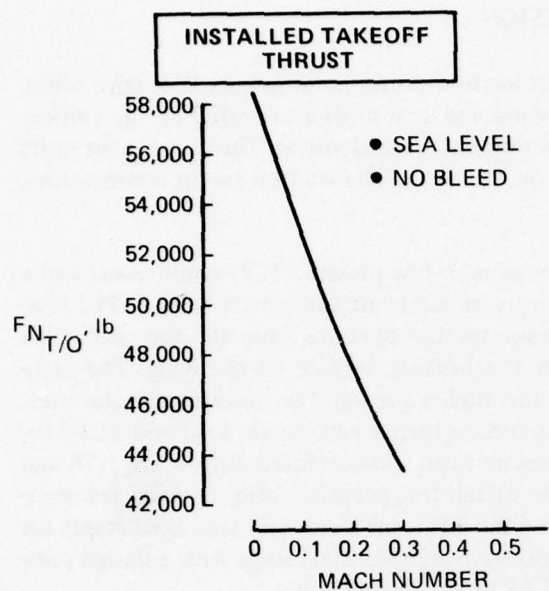
Thrust, SLS T.O. to 84°F	60,000 lb
FPR	1.65
BPR	7.5
OPR	40
Max combustor exit temp °F	2700
Weight	9100 lb
Max diameter	106.8 in.
Length	154.9 in.
Scaling range	50,000 to 90,000 lb

Installed performance data for a nominal size 60,000-lb thrust engine (uninstalled sea level-static) are shown in Figure 74. Included are cruise, takeoff and climb performance. Installed losses include (1) inlet recover, (2) engine manufacturers fan and primary nozzle flow losses, (3) fan duct acoustical duct treatment loss of 50 percent greater flow loss than hardwall fan duct losses, (4) midcompressor bleed of 2.2 lb/sec, (5) fan bleed of 0.6 lb/sec, and (6) 220 horsepower extraction (HPX).

Weight and dimension data for the nominal size STF 482 engine are given below.

	THRUST SIZE	POUNDS
	60,000	Scaling Factor
Bare engine weight (lb)	9,100	(TSF) ^{1.165}
Fan diameter (in.)	106.8	(TSF) ^{0.5}
LP turbine diameter (in.)	58.70	(TSF) ^{0.5}
Engine length (in.)	155.0	(TSF) ^{0.433}

Weight and dimension data for scaled engines from 50,000- to 90,000-lb thrust (uninstalled sea level static) engines can be calculated with the scaling factor from the thrust scale factor (TSF).



- STANDARD DAY
- INSTALLATION LOSSES
 - 220 HPX
 - 2.2 lb/sec MID-COMPRESSOR BLEED
 - 0.6 lb/sec FAN BLEED
 - FAN DUCT ACOUSTICAL TREATMENT LOSSES
 - FAN AND PRIMARY NOZZLE LOSSES

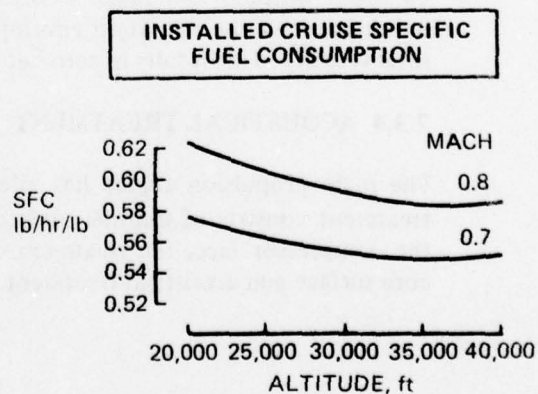
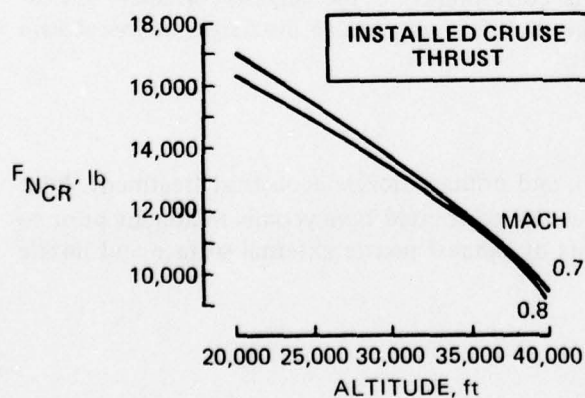
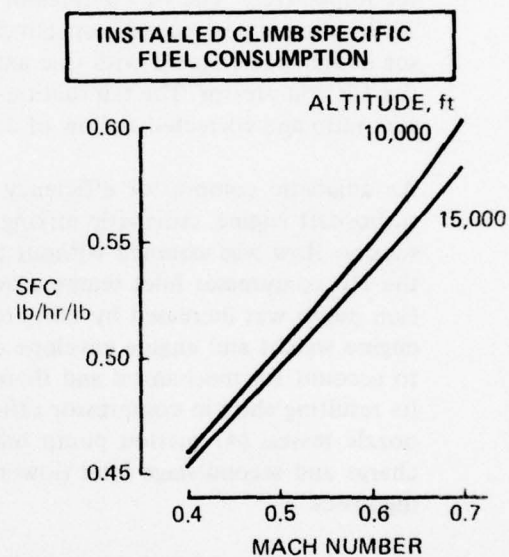
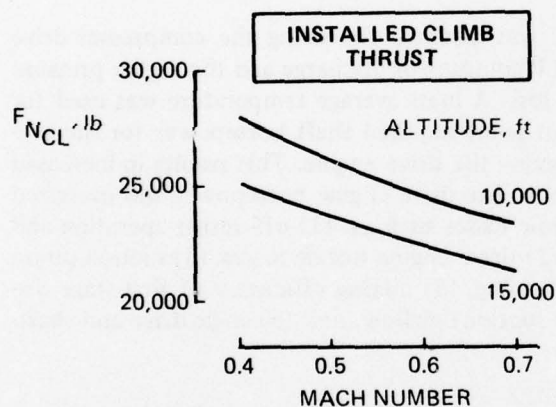


Figure 74 STF 482 Installed Engine Performance, TSLS = 60,000 Pounds

7.3.3 SUCTION ENGINE/COMPRESSOR DESIGN

Each of the study LFC configurations have six suction pump compressors and drive units. Four of the suction units are located on the wing and two units are located on the empennage as shown in Figure 9. The four wing suction units are identical. The empennage units have the same suction drive engines as those on the wing. The suction pump compressors, however, differ from those on the wing.

Each wing suction unit consists of two compressors, a low-pressure (LP) compressor and a high-pressure (HP) compressor that are driven by an adjacent turboshaft engine. The low-pressure compressor is used to increase the lower suction pressure from the top surface of the wing to the higher suction pressure from the bottom surface of the wing. The high-pressure compressor is then used to increase this higher pressure to free-stream total pressure. The LP compressor design pressure ratio and corrected airflow are 1.42 and 51.93 lb/sec respectively. The HP compressor design pressure ratio and corrected airflow are 1.78 and 72.96 pounds per second respectively. Because of the low-pressure ratio, an axial compressor design was selected with one axial stage for the LP compressor and two axial stages for the HP compressor. The tail suction compressors have an additional stage with a design pressure ratio and corrected airflow of 2.39 and 27.88 lb/sec respectively.

An adiabatic compressor efficiency of 0.80 was assumed for sizing the compressor drive turboshaft engine. Adiabatic mixing of the LP compressor discharge and the higher pressure suction flow was assumed without pressure loss. A mass average temperature was used for the HP compressor inlet temperature. Design point required shaft horsepower for the suction pump was increased by 20 percent in sizing the drive engine. This results in increased engine weight and engine envelope dimensions. The drive engine horsepower was oversized to account for mechanical and thermodynamic losses such as: (1) off-design operation and its resulting shift in compressor efficiency, (2) drive engine nozzle losses, (3) suction pump nozzle losses, (4) suction pump inlet face loading, (5) mixing efficiency of first-stage discharge and second-stage inlet (lower surface suction) airflow, and (6) angle drive and shafting losses.

The size and weight of the suction pump units were based on operational design point of 44,000-ft altitude and Mach = 0.79. This corresponds to the largest corrected airflow requirement of the operation envelope. The suction pump nozzle discharges at free-stream total velocity. This results in zero net thrust.

7.3.4 ACOUSTICAL TREATMENT

The main propulsion engine has inlet, fan, and primary nozzle acoustical treatment. Inlet treatment consists of internal surface acoustical perforated honeycomb treatment prior to the compressor face, fan treatment consists of exhaust nozzle external surface and nozzle core surface and acoustical treatment.

7.4 SYSTEMS

Systems-related tasks included:

- Defining slot spacing and geometry characteristics
- Establishing LFC collection duct sizes and internal duct losses
- Defining the airplane systems

Conventional technology levels were assumed for all airplane systems other than the laminar flow control systems.

7.4.1 SUCTION SYSTEM ANALYSIS

The suction system was sized to provide suction requirements determined for each laminarized surface by boundary layer stability calculations described in Section 7.1. Necessary flow requirements for the LFC configuration Model 767-773 are shown in Table 5.

Slot spacing on the laminarized surfaces was obtained by limiting the slot Reynolds number to values less than 100. This should keep the flow viscous through the slots and avoid the possibility that internal duct flow fluctuations will cause boundary layer transition⁽³¹⁾. The maximum slot Reynolds number on the wing of Model 767-773 was approximately 85 at the side of body and decreased outboard to permit continuous slots from root to tip. The wing slot spacing from Model 767-773 is shown in Figure 75.

Calculated slot spacings were used together with airflow characteristics, (including surface pressure, temperature and airflow) to establish collection duct sizes. Collection ducts were then analyzed to determine the internal system losses necessary to size the suction pumps. The procedure used is shown in Figure 76.

7.4.2 ICE PROTECTION

Wing thermal anti-icing represents both an operational and performance consideration. Ice formation on the leading edge can cause transition to turbulent flow and, therefore, must not be allowed to accumulate. In addition, any water runback that could result in ice buildup in the surface flow areas must be prevented. This problem also is related to surface contamination that could build up such that transition would occur. Contamination and erosion problems are being explored for NASA under the current LFC Systems Study contract⁽³⁾ and currently under Boeing IR&D programs. Significant research and development work is required to determine a satisfactory solution to wing thermal anti-icing and surface cleanliness problems.

Table 5 Suction Flow Requirements for Model 767-773 (0 to 70 Percent of Chord)

CONDITION	1 WING			HORIZONTAL STABILIZER		VERTICAL FIN
	OUTBOARD	MIDDLE	INBOARD	OUTBOARD	CENTER	
	1			1	2	
41,000 ft, 0.79 M, std day						
Section airflow, lb/sec						
Upper	8.27	14.59	9.97	5.02	10.99	12.23
Lower	5.57	9.84	6.73			
Suction pressure level, psia						
Upper	1.47	1.47	1.47	1.50	1.43	1.53
Lower	2.07	2.07	2.07			
36,000 ft, 0.79 M, std day						
Section airflow, lb/sec						
Upper	9.37	16.55	11.31	5.65	12.39	13.78
Lower	6.32	11.16	7.63			
Suction pressure level, psia						
Upper	1.83	1.83	1.83	1.90	1.81	1.94
Lower	2.60	2.60	2.60			
44,000 ft, 0.79 M, std day						
Section airflow, lb/sec						
Upper	7.74	13.66	9.34	4.67	10.23	11.37
Lower	5.22	9.22	6.30			
Suction pressure level, psia						
Upper	1.26	1.26	1.26	1.40	1.24	1.32
Lower	1.79	1.79	1.79			

- 1 One side of airplane
2 Full center section
3 One fin

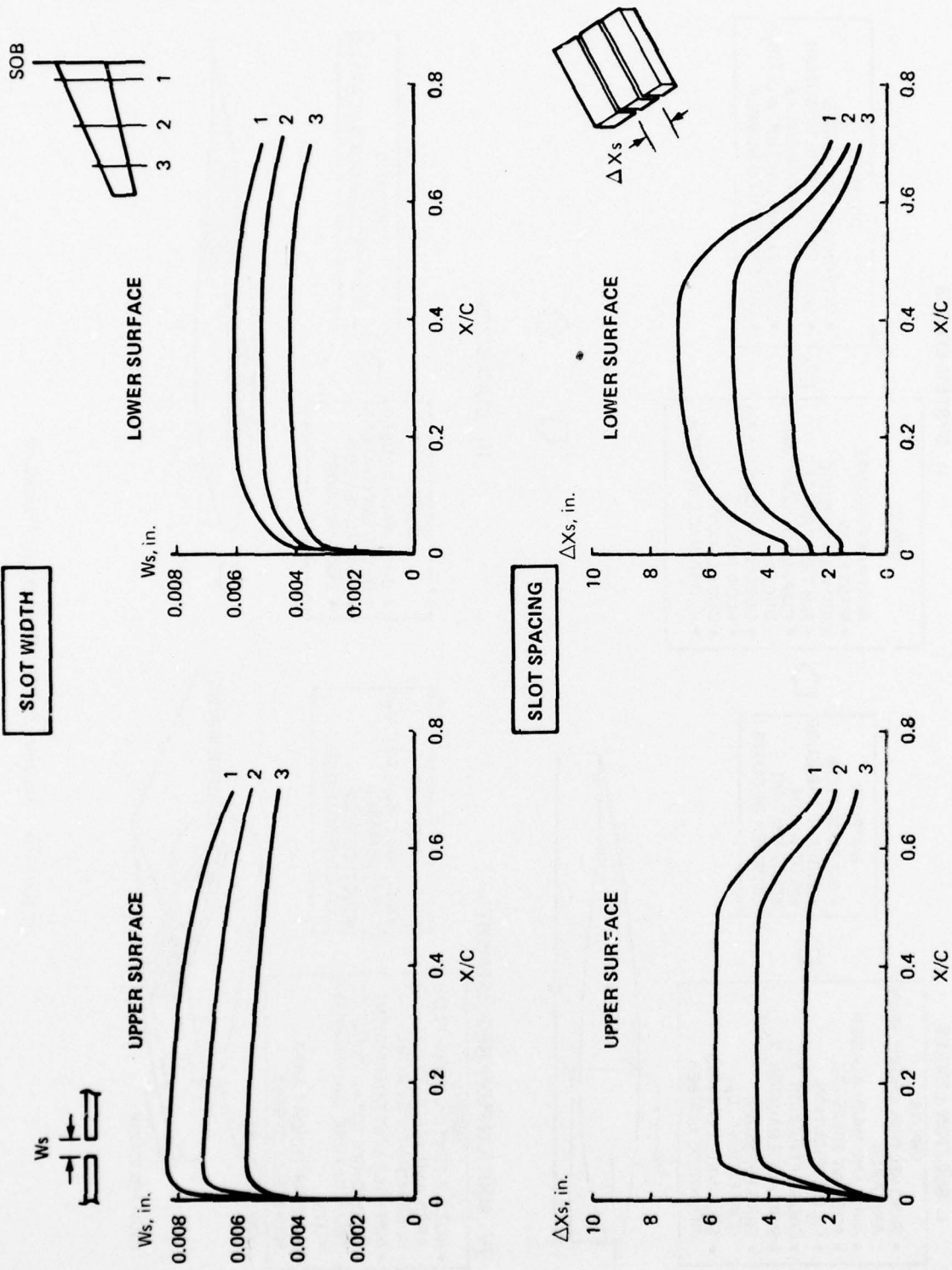


Figure 75 Model 767-773 Wing Slot Geometry and Spacing

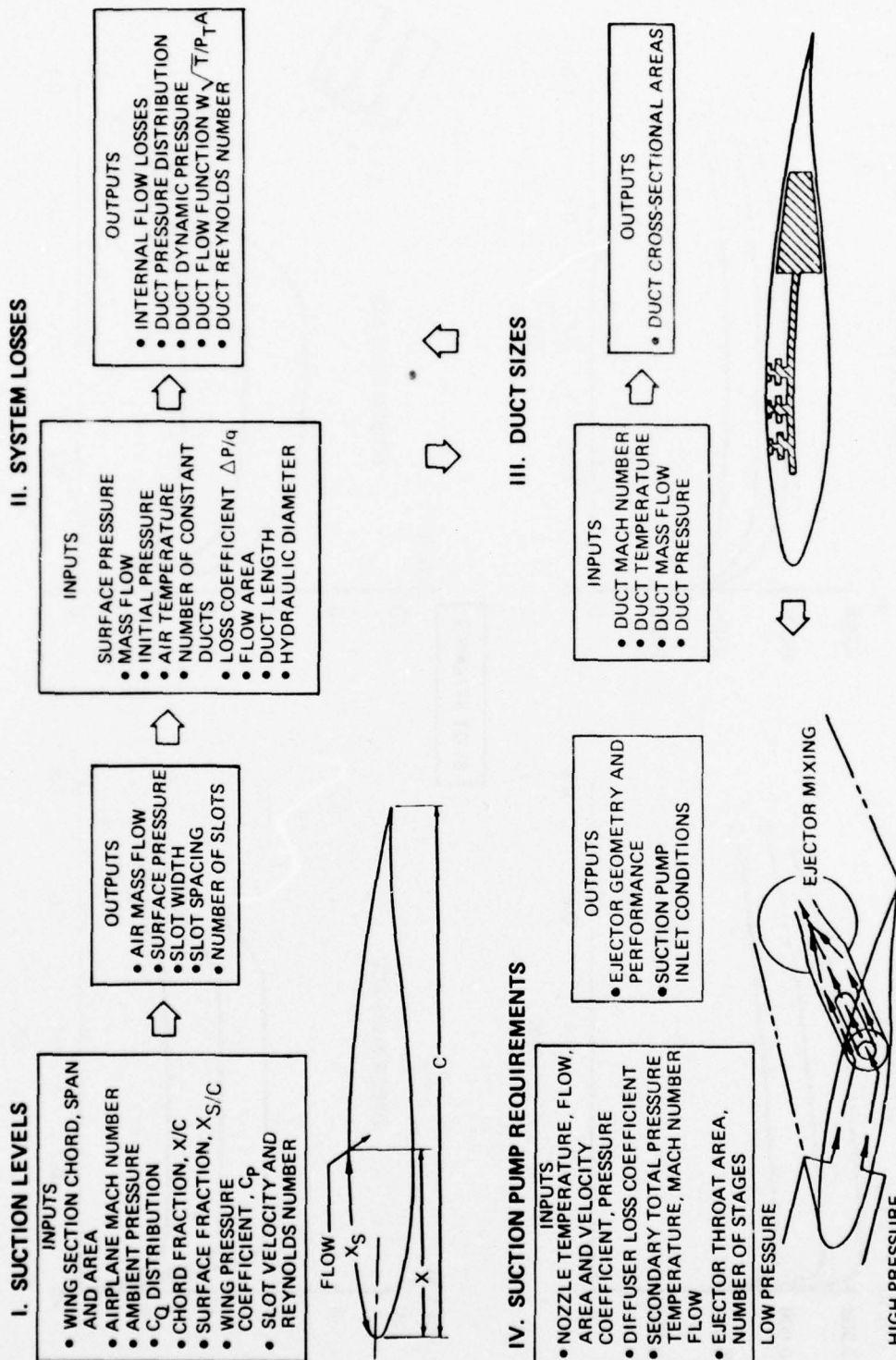


Figure 76 Suction System Calculation Procedure

Wing thermal anti-icing may be accomplished by backflowing hot air through the LE suction system with appropriate valving. Use of buried electrical heating elements, icephobic coatings, or a combination of these methods may be possible for future studies.

7.4.3 LIGHTNING PROTECTION

The problem of lightning protection on advanced composites has been recognized. There are many programs underway to establish the optimum solution. Proposed solutions produce weight penalties ranging from 0.03 to 0.08 lb/ft². This falls within the tolerance band of parametric weight studies used on this program.

Extensive work on defining lightning protection systems has been done under contract by Boeing for the AFFDL/FBC study. ⁽³⁶⁾ This study will provide a basis on which ultimate lightning protection systems can be defined.

7.4.4 INTEGRATED SYSTEMS

The LFC system integration considerations that have been incorporated were limited to those directly related to the study such as wing anti-icing. However, the time/use cycle of LFC is such that consideration should be given to utilizing capability of the LFC engines for added takeoff and/or climb thrust, thus shortening the takeoff distance or allowing potentially smaller engines.

Use of the LFC engines as the source of cabin air for air conditioning was considered. However, the quantity of air and pressure levels required is not compatible with a single design drive unit, and added compressor stages would be needed. In addition, the maximum design power capability of the suction engines is required during cruise. Any power required to meet cabin air pressure and flow demands would be over and above that needed for LFC and would have a significant size effect on the suction engines.

7.5 WEIGHT AND BALANCE

Weight and balance tasks included:

- Defining the weight benefits through application of advanced technology materials and active controls
- Conducting configuration weight analyses to support airplane sizing exercises and the LFC planform optimization study.
- Providing LFC total systems and structural weight data for the sensitivity studies

36. Vulnerability/Survivability of Composite Structures—Lightning Strike. AFFDL/FBC Contract F33615-76-C-5255.

7.5.1 ADVANCED TECHNOLOGY WEIGHT BENEFITS

Advanced technology definitions were identified similar to those of the NASA funded Advanced Transport Technology Studies,⁽³⁷⁾ ATT, with resulting weight improvement that would be available in the 1985-1990 time period. Figure 77 shows estimated weight benefits from using advanced structural materials. The weight benefits are typical for the use of graphite-epoxy honeycomb primary structure and PRD-49 honeycomb secondary structure. The configuration weights also included benefits through the use of the advanced flight controls described in Section 7.2 following the methods of Reference 38.

7.5.2 WEIGHT ANALYSIS APPROACH

Preliminary design type weight and balance analyses were made for evaluations of the turbulent and LFC configurations. Advanced technology effects were applied as percentage benefits to the applicable weight categories.

Weight and balance analyses for the advanced technology turbulent baseline (767-768) configuration were performed by extrapolating known parametric/statistical methods to the higher gross weight and size regimes necessary. Boeing in-house studies of very large freighters were helpful in guiding this extrapolation. Figure 77 shows the degree of extrapolation that was necessary to evaluate the large aircraft of this study.

7.5.3 LFC SYSTEMS AND STRUCTURAL WEIGHT ESTIMATION

Weight evaluations of the initial LFC study configurations were derived from the turbulent airplane analyses by accounting for the LFC systems and structural differences. These differences included:

- Suction engines
- Suction pumps
- Suction engine structural integration
- Distribution ducting
- LFC surface structural integration
- Fuel system aft tank and manifold

In addition, LFC wing weights include a weight reduction to account for removal of leading-edge devices and associated flap controls.

37. NASA Contracts NAS1-1071, NASA-1072, NASA-1073, *Study of the Application of Advanced Technologies to Long-Range Transport Aircraft*.

38. Anderson, R. D., et al., *Development of Weight and Cost Estimates for Lifting Surfaces with Active Controls*, NASA CR-144937, March 1976.

COMPONENT	WEIGHT SAVING, PERCENT
WING	25
HORIZONTAL TAIL	15
VERTICAL TAIL	20
BODY	15
MAIN GEAR	10
NOSE GEAR	10
NACELLE AND STRUT	15

- PERCENT WEIGHT SAVING RELATIVE TO CONVENTIONAL SKIN STRINGER CONSTRUCTION
- ▨ GRAPHITE-EPOXY HONEYCOMB
- ▤ GRAPHITE-EPOXY INTEGRATED ACOUSTICS STRUCTURE
- PRD-49 HONEYCOMB
- ▩ STIFFENED GRAPHITE-EPOXY HONEYCOMB

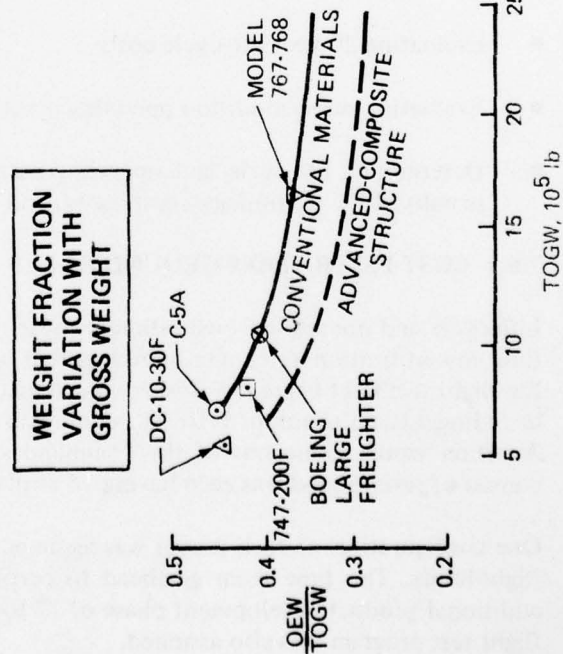
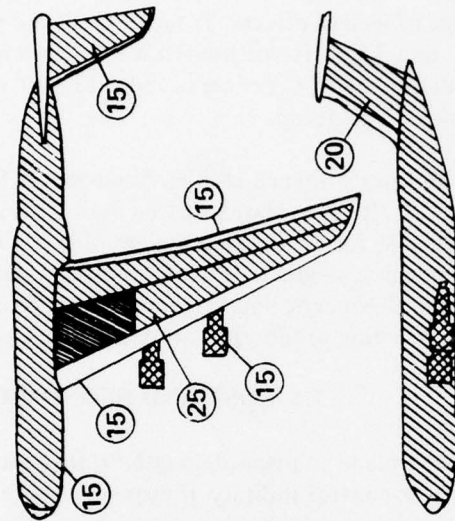


Figure 77 Weight Reduction Due to Advanced Materials

The total LFC systems and structural weight penalty is very dependent on the structural design concept and on the material usage. Development of LFC design integration concepts in the current NASA sponsored LFC systems studies is still proceeding with varying weight effects. Because of the uncertainty of the total LFC weight penalty, the emphasis of the study presented in this report has been to identify the sensitivity of the LFC configuration over a probable range of weight effects. Total LFC system plus structural integration weight penalties of 0, 2.25, and 3.0 lb/ft² of treated wetted area were considered. Ongoing Boeing- and NASA-funded studies of LFC concepts indicate that weight penalties in the lower end of the above range may be achieved.

Many of the trade and performance studies discussed in Section 4.0 assumed a total LFC weight penalty of 2.25 lb/ft² for treated wetted area. This is not a validated weight level but was considered reasonable for conducting the various studies. In order to determine a meaningful LFC weight penalty, a great deal of innovative design effort will be necessary to develop a LFC structural concept and integrated systems design that will minimize weight without unfavorably affecting production or maintenance costs.

7.6 COST AND ECONOMICS

Cost analyses have been made to promote a quantitative measure of the economic characteristics of a laminar flow control military transport relative to a conventional turbulent aircraft developed to a comparable mission design requirement. Economic and cost analyses tasks included:

- Estimating costs of developing, producing and operating the reference turbulent and the LFC aircraft configurations
- Evaluating 20-year life-cycle costs
- Evaluating surge-condition operating costs
- Determining life-cycle and operating cost sensitivities to fuel price, LFC total weight penalty, LFC technology complexity, and maintenance costs.

7.6.1 COST ESTIMATION GROUND RULES

Life-cycle and operational cost estimates were measured in 1976 dollars. Costs reflect peacetime low-utilization rates. One development airplane was assumed, with the remainder of the flight test fleet being refurbished as production articles. A 125-airplane buy was assumed including 112 unit equipped (UE) 12 command support (CS) and one developmental vehicle. Attrition would come out of the command support complement. The 112 UE airplanes consist of seven squadrons each having 16 airplanes.

One configuration of each model was assumed. The flight test program was based on 1500 flight-hours. The time from go-ahead to certification was assumed at 53 months with an additional product development phase of 12 to 24 months preceding go-ahead. A 1500-hour flight test program was also assumed.

Life-cycle costs assumed a peacetime utilization rate of 1080 hours per year. This is less than one-third the utilization of a commercial transport. The surge condition operating cost analyses assumed 10 flying hours per UE per day.

7.6.2 COST ANALYSIS APPROACH

Life-cycle cost estimates include the cost of developing, producing, and operating each fleet of airplanes. Airframe, engine, and avionics costs were estimated using a Boeing cost model. The Air Force CACE model from AFR173-10 was used for operations and support analyses. The C-141 was used as the base for operations and support costs.

Manufacturing costs of the advanced technology turbulent and LFC designs were appraised on a comparative basis, using a conventional wide-body wing design and associated systems as a baseline.

The cost assessment followed the evaluation of Reference 5 in which a number of individuals from different manufacturing areas collectively established manhour complexity factors for each major structural component of the advanced technology turbulent and LFC configurations. The baseline having complexity factors of 1.0 was an equivalent size conventional technology airplane. Overall complexity factors for the advanced technology turbulent wing and empennage, and for the advanced technology LFC wing and empennage, were estimated to be 1.5 and 2.1 respectively.

In addition to the complexity assessment, the cost estimation model as shown in Table 6 requires a description of the airplane, a three-view drawing, airplane weight breakdown, part card estimate, development and production schedule, and commonality assessment. The airplane cost-estimating elements summarized in Table 7 include engineering hours, developmental hours, tooling hours, production hours, production material, purchased material, flight test, engines, labor, and overhead costs. This table also includes a breakdown between recurring and nonrecurring costs.

7.6.3 LFC COST FACTORS

Cost of an LFC airplane differs from the cost of a comparable turbulent airplane because of the design, development, production, and maintenance associated with the suction surfaces, internal ducting, the suction units, and the special LFC systems. Additional cost considerations include differences in airplane weight, engine size, high-lift systems, and fuel requirements.

Many of these cost items are strongly dependent on detailed design features of the LFC structural and systems concepts. These in turn can be quite dependent on the gross characteristics of the airplane dictated by the mission objectives.

Table 6 Airplane Cost Estimating Input Requirements

AIRPLANE DESCRIPTION	THREE-VIEW DRAWING	AIRPLANE WEIGHT
<ul style="list-style-type: none"> • Speed • Materials technology • Systems technology • Engine technology • Unique features <ul style="list-style-type: none"> • Laminar flow control 	<ul style="list-style-type: none"> • Size • Number of landing gear • Number and location of engines • Sweep and aspect ratio • Wing and empennage areas • Unique features <ul style="list-style-type: none"> • Empennage configuration • Fuselage configuration 	<ul style="list-style-type: none"> • Structure section <ul style="list-style-type: none"> • Wing • Fuselage • Empennage • Gear • Propulsion • Systems and equipment <ul style="list-style-type: none"> • By system • Engine thrust • Material type
PART CARD ESTIMATE	DEVELOPMENT/PRODUCTION SCHEDULE	COMMONALITY/COMPLEXITY ASSESSMENT
<ul style="list-style-type: none"> • Structure section <ul style="list-style-type: none"> • Wing • Fuselage • Empennage • Gear • Propulsion • Nonstructure <ul style="list-style-type: none"> • By system 	<ul style="list-style-type: none"> • Development schedule <ul style="list-style-type: none"> • Months from go-ahead to rollout no. 1 airplane • Months from go-ahead to certification • Production schedule <ul style="list-style-type: none"> • Airplane rollouts by month 	<ul style="list-style-type: none"> • Commonality assessment <ul style="list-style-type: none"> • Commonality to existing models • Commonality within configuration • Complexity assessment <ul style="list-style-type: none"> • Material • Speed

Table 7 Airplane Cost-Estimating Elements

ENGINEERING			DEVELOPMENTAL			TOOLING				
PROJECT DESIGN	TECHNICAL STAFF	PROJECT MISC	SERVICE	CUSTOMERS	LABORATORY TEST	MOCKUP	FABRICATION	NATION	Duplicate	CUSTOMERS
• Nonrecurring	• Nonrecurring	• Nonrecurring	• Nonrecurring	• Nonrecurring	• Nonrecurring	• Nonrecurring	• Nonrecurring	• Nonrecurring	• Nonrecurring	• Nonrecurring
Wing Fuselage Empennage Gear Propulsion Systems	Analysis test					Class I Class II Class III Customers	Wing Fuselage Empennage Gear Propulsion Systems			
• Recurring	• Recurring	• Recurring	• Recurring	• Recurring	• Recurring	• Recurring	• Recurring	• Recurring	• Recurring	• Recurring
<u>PRODUCTION LABOR</u>										
• Nonrecurring			• Nonrecurring				<u>PURCHASED EQUIPMENT</u>			
Planning			Castings and forgings				• Nonrecurring			
• Recurring			• Recurring				• Recurring			
Wing Fuselage Empennage Gear Propulsion Systems Final assembly Static and fatigue Planning			Wing Fuselage Empennage Gear Propulsion Systems Static and fatigue			Landing gear items Surface controls Hydraulics Air conditioning Electrical and electronics Flight deck Emergency equipment APU Fuel	Flight test Engines Labor and overhead rates			
							• Nonrecurring			
							• Recurring			
							Flight test Labor and overhead rates			
							• Recurring			
							Flight test Engines Labor and overhead rates			

Hence, a valid cost assessment of an LFC airplane must be preceded by an extensive design, development, and flight test program. This was clearly beyond the scope of this study. However, the ongoing NASA LFC program is directly addressing this task.

Cost estimates of this study strongly relied on engineering judgment supported by existing data. The economic assessments were, therefore, focused on relative costs and on sensitivities of these relative costs to the major LFC uncertainty items. These uncertainty items included the total LFC systems and weight penalty; the LFC technology complexity factor that affects design, development, and production costs; and maintenance costs.

8.0 RECOMMENDED RESEARCH AND DEVELOPMENT

The technical feasibility of LFC has been demonstrated in research carried out by Dr. W. Pfenninger and associates. The Northrop X-21 flight test program succeeded because of the technical knowledge they developed. In addition, a great deal of perseverance, intuition, and careful attention to detail were required. The successful application of LFC to either commercial or military transport aircraft will require similar excellence of effort. To develop an economically viable LFC airplane, one must tread the delicate path of designing with great care without penalizing the airplane weight, or cost of development, production, operation, or maintenance.

As part of the Aircraft Energy Efficient (ACEE) program, NASA is conducting, promoting, and funding extensive LFC studies that will possibly lead to a successful flight test program that will substantiate the operational and economic feasibility of LFC.

The LFC research and development items for this study have been grouped into two main categories:

- General LFC R&D items
- Specific items for large military transport aircraft

The general LFC R&D items will provide necessary information for either commercial or military transport LFC applications. The specific items for large military transport aircraft identify some areas of greatest concern for this type of LFC application.

8.1 GENERAL LFC R&D ITEMS

Many of the general LFC R&D items listed below are now underway or are planned for the immediate future as part of the NASA ACEE program. General R&D items can be grouped into four major categories:

1. Basic LFC technology
2. Configuration/detailed design studies
3. Flight operations
4. Manufacturing/quality control studies

Recommended basic LFC technology items include:

- Aerodynamic LFC design tools
 - Improve potential flow, viscous flow and boundary layer stability methods development
 - Refine and/or establish new empirical stability criteria
 - Improve suction rate prediction/optimization methods
- Aerodynamic design criteria
 - Slot design criteria refinements
 - Over-suction/under-suction limits
 - Aerodynamic smoothness refinements
 - LFC treatment to possibly ease smoothness requirements
 - Interference pressure field disturbance guidelines
- LFC airfoil/wing analytical and experimental studies
- Noise technology
 - Develop external cruise noise prediction techniques
 - Develop internal duct noise prediction techniques
 - Develop noise attenuation technology
- Structure/material technology
 - Develop efficient integrated LFC structural concepts—configuration dependent
 - Select/develop smooth resistant surface materials
 - Develop surface refurbishment procedures
 - Develop structural inspection techniques
 - Understand/minimize aeroelastic effects on suction surfaces and flow rates
- Environmental studies
 - Operational design criteria (e.g., desired climb, cruise altitudes)

Recommended configuration/design studies that are size- and mission-dependent include:

- Propulsion/suction systems optimization studies
 - Engine cycle/cruise altitude studies
 - Engine location studies
- Percent laminar flow design studies
 - Feasibility of laminarizing over control surfaces and rapid descent devices
 - LFC/active control compatibility
- LFC braced wing design studies
- Body drag reduction studies

Recommended flight operation studies include:

- LFC surface maintenance requirements
 - Flight test small suction panels
 - Flight test LFC suction surface
- Develop techniques to prevent icing of slots and leading edges
- Develop efficient and reliable surface cleaning techniques (ground and in-flight)

Manufacturing and Quality Control studies include the development of suction materials and reliable, but cost effective, manufacturing/construction techniques.

8.2 SPECIFIC R&D ITEMS FOR LARGE MILITARY TRANSPORT AIRPLANES

Some specific R&D items were identified during the study as a result of the large size of the airplane configurations. These specific items include the most important general LFC items necessary for the study configurations, and recommendations for some very large airplane detailed design studies.

Airplane balance considerations together with the desire to provide wing-bending-moment relief, dictated the location of the engines on the wing. For this type of LFC configuration, it is essential to validate the design of the engine, and the wing/nacelle/strut that will allow the achievement of laminar flow with minimal suction penalties. Hence, the development of acoustic and aerodynamic-interference LFC design criteria and prediction methods is essential.

The very large wings are a large portion of the OEW. Hence, the wing structural weight and the systems weight associated with LFC must be minimized. Slot design guideline refinements are desirable to minimize the number of slots and provide for slot termination, if necessary.

The large-span wings deflect appreciably in flight. Studies will be necessary to validate suction system effectiveness for large aeroelastic deflections.

The turbulent and LFC configurations, by virtue of their large size, require detailed design studies to validate their characteristics. The large span wings of the study configurations have large ground and flight deflections that might require significant configuration modifications or wing-span limitations.

Recommended system studies related to the current contract configurations include:

- Detailed design studies to determine the LFC structural weight penalty for the most promising concept (S) being developed in the ACEE study
- Engine cycle/cruise altitude optimization studies
- Wing geometry/cruise speed optimization studies for the reference turbulent airplane
- More detailed braced-wing studies for the LFC and turbulent configurations.

9.0 CONCLUSIONS

Purpose of the study was to conduct a preliminary design investigation of a large subsonic military transport to identify the impact of laminar flow control on performance and economics of the airplane. A valid assessment of an LFC airplane must be preceded by an extensive design, development, and flight test program. Consequently, this study focused on relative benefits from applying LFC, and the sensitivities of these relative benefits to major LFC uncertainty items.

Major conclusions of this study that apply specifically to very long-range, high-payload military transport airplanes of relatively low utilization are:

- LFC can provide large reductions in fuel usage (27 to 30 percent).
- LFC also results in lower gross weights (7 to 10 percent). The gross weights are very dependent upon the total LFC structural and systems weight increments ($\Delta(W_T)_{LFC}$).
- Life-cycle costs will probably be higher because of low design utilization rates. Life-cycle costs are very dependent on $\Delta(W_T)_{LFC}$ and on the technology complexity costs associated with the design, development, and production of an LFC surface.
- Sixty-day surge condition operational costs will be less with an LFC airplane (10 to 15 percent) depending on the fuel price and the special LFC maintenance costs.
- Normal military reserves are adequate to meet the mission objectives with reasonable losses in LFC.
- Reserves allow the LFC airplane to fly 2000 nmi or 5 hours with full loss of laminar flow and still achieve the mission range by establishing the design laminarization for the remainder of the flight.
- The LFC wing planform characteristics for optimum performance are compatible with characteristics that ease the task of laminarization. A wing planform having a high aspect ratio, low thickness/chord ratio and low sweep is the optimum arrangement that minimizes both fuel and gross weight, and maximizes productivity. The same geometry results in low chord Reynolds number, low crossflow, and low attachment line Reynolds number.
- Results of the extent of laminarization study suggest the following order for achieving LFC benefits with minimum technical risk:

1. Laminarize the wing back to the TE control surfaces. The nested chord length of the control surfaces should be minimized without compromising the low-speed performance.
 2. Laminarize the empennage back to minimum chord TE controls on the tails.
 3. Conduct the necessary trade and detailed design studies to identify the practical benefits and technical risks of laminarizing over TE surface.
- The fuselage drag on an LFC airplane is a significant drag item. A 25-percent reduction in the body drag of the LFC airplane results in fuel and gross weight reductions of approximately 8 percent and 4 percent respectively.

REFERENCES

1. Kulfan, R. M. and Howard, W. M., *Application of Advanced Aerodynamic Concepts to Large Subsonic Transport Airplanes*, Tech. Report AFFDL-TR-75-112, Nov. 1975.
2. Whites, R. C.; Sudderth, R. W.; and Wheldon, W. G., "Laminar Flow Control on the X-21," *Astronautics and Aeronautics*, July 1966, pp38-43.
3. NASA Contract NAS1-14630, "Evaluation of Laminar Flow Control System for Subsonic Commercial Transport Aircraft," (study underway 1976).
4. Weiss, D. D. and Lindh, D. V., *Development of the Technology for the Fabrication of Reliable Laminar Flow Control Panels*, NASA CR-145124, Feb. 1976.
5. Swinford, G. R., *A Preliminary Design Study of a Laminar Flow Control Wing of Composite Materials for Long Range Transport Aircraft*, NASA CR-144950, April 1976.
6. Sturgeon, R. F., et al, *Study of the Application of Advanced Technologies to Laminar Flow Control Systems for Subsonic Transports*, NASA CR-133949, May 1976.
7. George-Falvy, D., *An Investigation of the Flow Around the Cab of Boeing Jet Transports*, Boeing Document D6-15006, 1966.
8. Wallace, R. E., *Parametric and Optimization Techniques for Airplane Design Synthesis*, Paper No. 7 in AGARD-LS-56, April 1972.
9. Fischer, M. G. and Ash, R. L., *A General Review of Concepts for Reducing Skin Friction, Including Recommendations for Future Studies*, NASA TMS-2894, March 1974.
10. Ash, R. L., *On the Theory of Compliant Wall Drag Reduction in Turbulent Boundary Layers*, NASA CR-2387, April 1974.
11. Howard, F. G. and Hefner, J. N., "Multiple Slot Skin Friction Reduction," *Journal of Aircraft*, Vol. 12, No. 9, Sept. 1975, pp753-754.
12. Pfenninger, W., *Studies of Laminarized Underwater Suction Bodies*, Boeing Document D6-40283, March 1972.
13. Gregory, N., "Research on Suction Surfaces for Laminar Flow," *Boundary Layer and Flow Control*, edited by Lachmann, G. V., Pergamon Press, 1961, pp924-960.
14. Pfenninger, W., *Studies to Verify Laminar Flow at Very High Length Reynolds Numbers by Means of Distributed Suction in the Presence of Minimum Disturbances*, Boeing Document D6-40281, Feb. 1971.

15. Pfenninger, W. and Groth, E., "Low Drag Boundary Layer Suction Experiments in Flight on a Wing Glove of an F-94A Airplane with Suction through a Layer Number of Fine Slots," *Boundary Layer and Flow Control*, edited by Lachmann, G. V., Pergamon Press, 1961, pp961-999.
16. Healy, M. J.; Kawalik, J. S.; and Ramsay, J. W., "Airplane Engine Selection by Optimization on Surface Fit Approximations," *Journal of Aircraft*, Vol. 12, No. 7, July 1975, pp593-599.
17. Wheldon, W. G. and Whites, R. C., *Flight Testing of the X-21A Laminar Flow Control Airplane*, AIAA Paper No. 66-734, Sept. 1966.
18. Kosin, R. E., *Laminar Flow Control by Suction as Applied to the X-21 Airplane*, AIAA Paper No. 64-284, July 1964.
19. Gross, L. W., *Experimental and Theoretical Investigation of a Reichardt Body of Revolution with Low Drag Suction in the NASA Ames 12 ft Pressure Tunnel*, Northrop Report NOR-63-46, BLC-148, July 1963.
20. Gross, L. W., *Investigation of a Reichardt Body of Revolution with Low Drag Suction in the Norair 7 x 10 ft Wind Tunnel*, Northrop Report BLC-143, NOR 62-126, 1962.
21. Pfenninger, W. and Reed, V. D., "Laminar Flow Research and Experiments," *Astrodynamics and Aeronautics*, July 1966, pp44-50.
22. Gaster, M., "On the Flow Along Swept Leading Edges," *The Aeronautical Quarterly*, Vol. XVIII, Part 2, May 1967, pp165-184.
23. Boyd, B. B., et al, *A Comparison of Medium Range Laminar Flow Control and Turbulent Airplane Designs*, Boeing Document D6-E10251-1, May 1974.
24. Smith, A. M. O., "Rapid Laminar Boundary-Layer Calculations by Piecewise Application of Similar Solutions," *Journal of Aeronautical Sciences*, Vol. 23, No. 10, Oct. 1956, pp901-912.
25. R. A. S. Aerodynamic Data Sheets, WINGS 02.04.02, *Profile Drag of Smooth Wings*, May 1969.
26. Jaffe, N. A.; Okamura, T. T.; and Smith, A. M. O., "Determination of Spatial Amplification Factors and Their Application to Predicting Transition," *AIAA Journal*, Feb. 1970, pp301-308.
27. Wazzan, A. R.; Okamura, T. T.; and Smith, A. M. O., *Spatial and Temporal Stability Charts for the Falkner-Skan Boundary-Layer Profiles*, McDonnell Douglas Corp., DAC 67086, Sept. 1, 1968.

28. Brown, W. B., "A Stability Criterion for Three-Dimensional Boundary Layers," Vol. 2, *Boundary Layer and Flow Control*, edited by Lachmann, G. V., Pergamon Press, 1961.
29. Nenni, J. P. and Gluyas, G. W., "Aerodynamic Design and Analysis of an LFC Surface," *Astronautics and Aeronautics*, July 1966, pp52-57.
30. Pfenninger, W., "Flow Phenomena at the Leading Edge of Swept Wings," *AGARDograph* 97, May 1965.
31. Pfenninger, W., "Flow Problems of Swept Low-Drag Suction Wings of Practical Construction at High Reynolds Numbers," *Annals of the New York Academy of Sciences*, Vol. 154, Article 2, Nov. 22, 1968, pp672-703.
32. Pfenninger, W., "About the Development of Swept Laminar Suction Wings with Full Chord Laminar Flow," Vol. 2, *Boundary Layer and Flow Control*, edited by Lachmann, G. V., Pergamon Press, 1961.
33. Gray, D. E., *Study of Unconventional Aircraft Engines Designed for Low-Energy Consumption*, NASA CR-135065, June 1976.
34. Whitlow, D. H. and Whitener, P. C., *Technical and Economic Assessment of Span-Distributed Loading Cargo Aircraft Concepts*, NASA CR-144963, June 1976.
35. Goodrich, R. W.; Gaffin, W. O.; and Witherspoon, S. W., *Preliminary Performance and Installation Data for the STF-482 Turbofan Engine*, Pratt & Whitney Aircraft Report CDS-8, Nov. 1975.
36. Vulnerability/Survivability of Composite Structures—Lightning Strike. AFFDL/FBC Contract F33615-76-C-5255.
37. NASA Contracts NAS1-1071, NASA-1072, NASA-1073, *Study of the Application of Advanced Technologies to Long-Range Transport Aircraft*.
38. Anderson, R. D., et al., *Development of Weight and Cost Estimates for Lifting Surfaces with Active Controls*, NASA CR-144937, March 1976.